



รายงานวิจัยฉบับสมบูรณ์

โครงการ การเตรียมตัวเร่งปฏิกิริยาเคมีไฟฟ้า AuAg/C โดย วิธีการแทนที่กัลวานิคของ Ag/C ด้วย Au สำหรับการใช้งาน ในเซลล์เชื้อเพลิงแลกเปลี่ยนแอนอิออนแบบใช้กลีเซอรอล โดยตรง

โดย ดร. ศรายุทธ ยงประพัฒน์

มิถุนายน 2561

รายงานวิจัยฉบับสมบูรณ์

โครงการ การเตรียมตัวเร่งปฏิกิริยาเคมีไฟฟ้า AuAg/C โดย วิธีการแทนที่กัลวานิคของ Ag/C ด้วย Au สำหรับการใช้งาน ในเซลล์เชื้อเพลิงแลกเปลี่ยนแอนอิออนแบบใช้กลีเซอรอล โดยตรง

ดร. ศรายุทธ ยงประพัฒน์ มหาวิทยาลัยเทคโนโลยีพระจอมเกล้าธนบุรี

สนับสนุนโดยสำนักงานกองทุนสนับสนุนการวิจัยและ มหาวิทยาลัยเทคโนโลยีพระจอมเกล้าธนบุรี

(ความเห็นในรายงานนี้เป็นของผู้วิจัย สกว. และมหาวิทยาลับเทคโนโลยีพระจอมเกล้าชนบุรีไม่ จำเป็นต้องเห็นด้วยเสมอไป)

ABSTRACT

Project Code: TRG5880131

Project Title : Preparation of AuAg/C electrocatalyst by using the galvanic displacement of Ag/C by Au for direct glycerol anion exchange membrane fuel cell application

Investigator: Sarayut Yongprapat, King Mongkut's University of Technology Thonburi

Project Period: 3 years

The activity and stability of AuAg/C electrocatalysts prepared by a galvanic displacement between Au³⁺ and Ag on carbon were investigated. 60 wt% Ag/C was first prepared by using citrate reduction method in alkaline and used as the sacrificed material for Au deposition. The AuAg/C catalysts with different Au loading range from 5 to 30 wt% was prepared by mixing the Au³⁺ with the Ag/C resulting in AuAg/C catalyst with smaller AuAg nanoparticles. The catalyst was inactive at first and require an activation from alcohol electrooxidation by the adsorbate-induced surface segregation in which pull the Au atoms toward the nanoparticle surface. The catalytic activity depends on the molecular weight of the alcohol. Upon interaction with glycerol, the catalyst surface became an Au-rich surface, thereby activating the catalysts. The promotion effects of Ag, such as negative shifts of both an onset potential and a potential at maximum current density, were observed on the catalysts with low Au content but not on those with high Au content. The AuAg/C catalysts with low Au content were more active than the Au/C even though the much larger size of the metal particles on the AuAg nanoparticle. The most active catalysts were 5% AuAg/C and 10% AuAg/C, providing the highest mass normalized current densities in electrolytes containing 0.1 M and 1 M glycerol, respectively. The final current density of 10% AuAg/C in 1 M glycerol electrolyte was at 445 mA mg $_{\mathrm{Au}}^{^{-1}}$, which was about 9 times higher than that of Au/C. The stability of AuAg was also improved by a synergistic effect between Au and Ag. The catalytic activity of AuAg catalyst can be further improved by the addition of Pd.

Keywords : AuAg/C; galvanic displacement; glycerol electrooxidation; anion exchange membrane fuel cell

าเทคัดย่อ

รหัสโครงการ: TRG5880131

ชื่อโครงการ : การเตรียมตัวเร่งปฏิกิริยาเคมีไฟฟ้า AuAg/C โดยวิธีการแทนที่กัลวานิคของ Ag/C ด้วย

Au สำหรับการใช้งานในเซลล์เชื้อเพลิงแลกเปลี่ยนแอนอิออนแบบใช้กลีเซอรอลโดยตรง

ชื่อนักวิจัย: ดร. ศรายุทธ ยงประพัฒน์ มหาวิทยาลัยเทคโนโลยีพระจอมเกล้าธนบุรี

E-mail Address: sarayut.yon@kmutt.ac.th

ระยะเวลาโครงการ: 3 ปี

บทคัดย่อ ตัวเร่งปฏิกิริยา AuAg/C ที่อัตราส่วนของ Au และ Ag ต่างๆ ถูกเตรียมด้วยวิธีการแทนที่กัล วานิคเพื่อใช้เป็นตัวเร่งสำหรับปฏิกิริยากลีเซอรอลอิเลคโทรออกซิเดชันในสภาวะด่าง ในขั้นแรกตัวเร่ง ปฏิกิริยา 60 wt% Ag/C ถูกเตรียมด้วยวิธีซิเทรตรีดักชันในสารละลายด่างเพื่อใช้ในปฏิกิริยาการ แทนที่กัลวานิค เมื่อผสมสารละลาย $\mathrm{Au}^{^{3+}}$ กับ $\mathrm{Ag/C}$ จะทำให้เกิดการแทนที่ของ $\mathrm{Au}^{^{3+}}$ และ Ag และ ได้อนุภาคนาโนของ AuAg ที่มีขนาดเล็กลงกว่าอนุภาค Ag เดิม ตัวเร่งปฏิกิริยาที่เตรียมมีสัดส่วนของ โลหะทองอยู่ในช่วง 5-30 % โดยน้ำหนัก ตัวเร่งปฏิกิริยาที่ได้ไม่ว่องไวต่อปฏิกิริยาแอลกอฮอลอิเลค โทรออกซิเดชันในช่วงแรกแต่จะถูกกระตุ้นให้ว่องไวขึ้นเมื่อทำปฏิกิริยากับแอลกอฮอลจากการเกิด adsorbate-induced surface segregation ซึ่งดึงอะตอมของทองขึ้นมาที่พื้นผิวอนุภาคนาโน โดย ความว่องไวจะขึ้นกับมวลโมเลกุลของแอลกอฮอลที่ใช้ในการทำปฏิกิริยา ในการทำปฏิกิริยากับ กลีเซอรอล กลไกการเสริมปฏิกิริยาของ Ag เช่นการลดลงของศักย์ไฟฟ้าเริ่มต้นและศักย์ไฟฟ้าที่ความ หนาแน่นกระแสสูงสุดสามารถพบได้เฉพาะในตัวเร่งที่มีปริมาณ Au น้อยและจะหายไปเมื่อมีปริมาณ ทองสูงขึ้น ตัวเร่งปฏิกิริยา AuAg/C ที่มีปริมาณ Au น้อยมีความว่องไวสูงกว่าตัวเร่งปฏิกิริยา Au/C แม้ว่าจะมีขนาดอนุภาคใหญ่กว่ามาก โดยความหนาแน่นกระแสสุดท้ายของตัวเร่งปฏิกิริยา 10%AuAg/C ในสารละลาย 1 โมลาร์กลีเซอรอลสูงถึง 445 มิลลิแอมป์ต่อมิลลิกรัมทอง ซึ่งมากกว่าที่ ได้จาก Au/C กว่า 9 เท่า นอกจากนี้ Ag ยังช่วยเพิ่มความเสถียรต่อปฏิกิริยากลีเซอรอลอิเลคโทร ออกซิเดชันด้วยกลไกการเกิดปฏิกิริยาร่วมอีกด้วย การเติม Pd ในปริมาณน้อยเข้าไปในตัวเร่ง AuAg/C สามารถช่วยเพิ่มความหนาแน่นกระแสสูงสุดขึ้นไปได้อีก โดยอาจเกิดจากการส่งเสริมให้ อนุภาคทองขึ้นมาอยู่ที่พื้นผิวโลหะมากขึ้น

คำหลัก : ตัวเร่งปฏิกิริยา AuAg/C; การแทนที่กัลวานิค; กลีเซอรอลอิเลคโทรออกซิเดชัน; เซลล์ เชื้อเพลิงแลกเปลี่ยนแอนไอออน

CONTENTS

TITLE	Page
ABSTRACT	i
บทคัดย่อ	ii
CONTENTS	iii
LIST OF FIGURE	iv
LIST OF TABLE	vi
1. INTRODUCTION	1
2. METHODOLOGY	12
3. RESULTS AND DISCUSSION	15
4. CONCLUSIONS	40
LIST OF REFERENCES	42
RESEARCH OUTPUT	46

LIST OF FIGURES

H	GURE	IIILE	PAGE
	1.1 A c	diagram displaying the five different types of bimetallic	2
		nanoaparticles that can form when Au and Ag constituents	
		are combined.	
	1.2	Glycerol electrooxidation pathway on Au/C catalyst.	4
	1.3	Suggested mechanism of the glycerol electrooxidation on	5
		Au/C, AuAg/C and Ag/C catalysts.	
	3.1	TEM image of Ag/C.	15
	3.2	TEM images of (a) 5%AuAg/C, (b) 10%AuAg/C, (c) 20%AuAg/C	16
		and (d) 30%AuAg/C.	
	3.3	TEM image of Au/C prepared by using the PVA method.	17
	3.4	XRD patterns of (a) 5%AuAg/C, (b) 10%AuAg/C, (c) 20%AuAg/C,	18
		(d) 30%AuAg/C, and (e) Ag/C marked by the main peak	
		positions of AgCl ($ullet$) and Ag $_2$ O ($llet$).	
	3.5	The deconvoluted and XPS data of all the synthesized	18
		catalysts in (a) 4f spectra of Au and (b) 3d spectra of Ag region.	
	3.6	CVs of Ag/C and Au/C in 0.1 M KOH at a scan rate of 20 mV s $^{-1}$.	21
	3.7	CVs of AuAg/C catalysts in 0.1 M KOH at a scan rate of 20	21
		$mV s^{-1}$.	
	3.8	CVs of Ag/C and Au/C in 0.1 M glycerol and 0.1 M KOH at a	22
		scan rate of 20 mV s ⁻¹ .	
	3.9	Au mass normalized CVs of 10%AuAg/C catalysts in (a) 0.1 M	24
		glycerol and 0.1 M KOH and (b) 1 M glycerol and 2 M KOH	
		at a scan rate of 20 mV s ⁻¹ .	
	3.10	CVs of 30%AuAg/C in 1 M glycerol and 2 M KOH (a) fresh	26
		catalyst and (b) the same electrode after deactivated in 2 M	
		KOH at a scan rate of 20mV s ⁻¹ .	
	3.11	CAs of AuAg/C catalysts in 1 M glycerol and 2 M KOH at 0.25 V	27
		after 10 cycle of CV activation in 2 M KOH	

LIST OF FIGURES

-IGURE	IIILE	PAGE
3.12	CVs of 10%AuAg/C and 30%AuAg/C in 1 M ethanol and 1 M	28
	KOH at a scan rate of 20mV s ⁻¹ .	
3.13	CVs of (a) 10%AuAg/C and Au/C, and (b) 30%AuAg/C in 0.1 M	29
	ethylene glycol and 0.1 M KOH at a scan rate of $20 \mathrm{mV \ s}^{-1}$.	
3.14	CVs of (a) 10%AuAg/C and Au/C, and (b) 30%AuAg/C in 1 M	30
	ethylene glycol and 1 M KOH at a scan rate of 20 mV s ⁻¹ .	
3.15	Au mass normalized CVs of Au/C and AuAg/C catalysts in	31
	$0.1~\mathrm{M}$ glycerol and $0.1~\mathrm{M}$ KOH at a scan rate of 20 mV s $^{-1}$.	
3.16	Au mass normalized CVs of Au/C and AuAg/C catalysts in 1 M	33
	glycerol and 2 M KOH at a scan rate of 20 mV s $^{-1}$.	
3.17	CAs of AuAg/C catalysts in (a) 0.1 M glycerol and 0.1 M KOH at	34
	0.25 V after 10 cycles of CV activation in 0.1 M glycerol and	
	0.1 M KOH and (b) 1 M glycerol and 2 M KOH at 0.25 V after 10)
	cycles of CV in 1 M glycerol and 2 M KOH.	
3.18	CVs of glycerol electrooxidation in 1 M Glycerol and 2 M KOH	36
	of fresh AuAg, 1Cl-Pd-AuAg/C, and 10Cl-Pd-AuAg/C at a scan	
	rate of 20 mV s $^{-1}$. Insert: CV of AuAg/C in 0.01 M PdNO3 and	
	0.1 M KCl.	
3.19	CVs of glycerol electrooxidation in 1 M Glycerol and 2 M KOH	38
	at a scan rate of 20 mV s ⁻¹ of 1N-Pd-AuAg/C and 5N-Pd-AuAg/C	
	catalysts. Insert: CV of AuAg/C in 0.01 M PdNO3 and 0.1 M KNO	3.

LIST OF TABLES

TABLE	TITLE	PAGE
2.1	Nomenclature of Pd-AuAg/C catalysts and their	13
	electrodeposition conditions.	
3.1	The peak binding energy of Au and Ag from the	18
	deconvoluted XPS results.	
3.2	The calculated Au and Ag weight ratios from EDX results.	20
3.3	Potential and current density at maximum current density.	37

CHAPTER 1: INTRODUCTION

1.1 Rational

Au-based catalysts has been recently received great attention in academic research for theirs application as an alcohol electrooxidation in alkaline [1-8]. Au is active for a number of alcohols i.e. ethanol, ethylene glycol, glycerol and glucose, especially with glycerol [1, 2, 6]. The electrooxidation reaction rate of glycerol was remarkably high on Au. In half cell study, the catalytic activity and stability were much greater than that of the Pt-based catalysts [6]. For fuel cell application, glycerol in KOH aqueous electrolyte can be fed directly to an anode of an alkaline anion exchange membrane fuel cells (AAEMFC) without any pre-reformer step.

The AAEMFC is a new class of fuel cells that has been extensively developed in recent years [9, 10]. The Nafion membrane used in proton exchange membrane fuel cells (PEMFCs) is replaced by an anion exchange membrane to transport hydroxide ions from the cathode to the anode. Thus, the fuel cell reactions are carried out in an alkaline environment. This alkaline system offers several advantages over the acid environment. The cathode reaction in alkaline is faster than in acid and materials such as MnO_2 [11] and Ag [12, 13] become very active and can be used in place of Pt. The fuel crossover from anode to cathode is minimized due to the reverse direction of ion transport. Many cheaper fuel cell materials can be used to fabricate the cells and this will enable the commercialization of these fuel cells in a future.

Due to global warming, the needs to replace an unsustainable and non-ecofriendly fossil fuel with an alternative energy source become more significant. At present, several sustainable energy sources such as biodiesel and bioethanol are utilized. The annual production rate of these renewable energy sources are significantly increasing. Along with the main biodiesel product, glycerol is also produced in great amount. Glycerol was an inevitable co-product from the trans-esterification of vegetable oils. With no real demand, the glycerol oversupply leads to constantly low price and sometimes considered as a waste [14]. Finding the techniques to fully utilize glycerol would provide

more sustainable way forward. Fortunately, glycerol possesses many advantages including non-flammable, non-toxic and non-volatile properties which make it safe and well-matched for wide scale uses.

In addition to the potential of glycerol used as a fuel based on anion exchange fuel cell, the selective oxidation of glycerol at anode can also be used to co-generate the valuable chemicals beside the electricity. A number of chemicals was found as the products from glycerol electrooxidation on Au such as formic acid, glycolic acid, oxalic acid, glyceric acid, tartronic acid and mesoxalic acid. Among these chemicals, tartronic and mesoxalic acid was reported to be synthesized with high selectivity upon the fuel cell condition [3-4].

The development of Au-based catalysts for alcohol electrooxidation in alkaline was in early state. Several metals and metal oxides were found to improve the catalytic properties toward alcohol electrooxidation of Au. An inexpensive Ag was found to be one of the most suitable promoters of Au. Addition of Ag improves the stability of Au based catalyst for alcohol and glucose electrooxidation [15-21]. Ag lies directly above Au in the periodic table in group XI. Both Au and Ag have a face centered cubic (fcc) unit cell with very close lattice parameter. As a result, Au and Ag were formed as indistinct alloy phases over the entire composition range. Au or Ag can be easily grown on other particle to form a core-shell structure due to absence of lattice mismatch between these two materials. There are 5 possible Au-Ag bimetallic nanoparticle systems, as shown in Fig. 1.1. Moreover, replacing the core of Au nanoparticle with Ag may also increase the mass normalized activity of Au.

However, the synthesis of AuAg nanoparticles with controlled composition was quite difficult due to the precipitation of Ag^{+} in presence of Cl^{-} from the most widely used Au precursor, HAuCl₄. Ag was inactive for alcohol electrooxidation in fuel cell operation potential [15]. Hence, having too much Ag covering Au surface can diminish the catalytic activity of AuAg-based catalyst. This research aims to prepare the highly active Ag_{core} -Au_{shell}/C (I of Fig. 1.1) or Au-rich shell (V of Fig. 1.1) catalysts via galvanic displacement of Au^{+} and Ag/C.

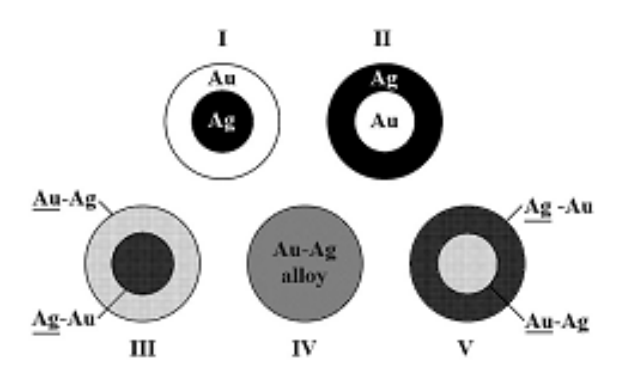


Figure 1.1 A diagram displaying the five different types of bimetallic nanoaparticles that can form when Au and Ag constituents are combined. Type $I = Ag_{core}-Au_{shell}$, type $II = Au_{core}-Ag_{shell}$, type $III = Ag_{core}-Au_{shell}$, type $III = Ag_{$

1.2 Literature review

The electrooxidation of alcohols on Au-based catalysts was faster in alkaline than in neutral or acid electrolyte [23, 24]. The rate determining step was the adsorption of alcohol on Au surface. This process was initiated by the adsorption of alkoxide (R-Ō) group on alcohol molecule [1] or the induced adsorption of alcohol by the pre-adsorbed hydroxide on Au surface [23]. The alcohols with lower pK_a, normally have a high molecular weight, tend to react better than the alcohols with high pK_a. Thus, glycerol was the alcohol that shows a remarkably better performance than the other alcohol such as methanol, ethanol and ethylene glycol [1, 2, 6]. The onset potential displayed for glycerol electrooxidation was also the lowest.

Recently, we studied the preparation of Au/C catalysts by using the polyvinyl alcohol (PVA) protection method [6]. In brief, the Au nanoparticles were formed by reducing of HAuCl₄ precursor using NaBH₄ in presence of PVA. Next, the carbon support was added into the resulting Au sol from the prior step to immobilize Au nanoparticles for 3 hour. Finally, the catalyst was washed and dried. The well dispersed Au/C with average particle size of around 3.8 nm was obtained. The activity and stability of the Au/C were

better than PtRu/C for ethylene glycol and glycerol electrooxidation even though the reaction on Au heavily involves the C-C bond dissociation.

The general reaction pathway of glycerol electrooxidation on Au/C catalyst was displayed in Fig. 1.2. The first step of the reaction was the oxidation of glycerol to glyceric acid. Without C-C bond dissociation, further oxidation produces tartronic or mesoxalic acid as a final product. Another pathway involves C-C dissociation which results in glycolic acid, oxalic acid and formic acid as the possible products. The distribution of products can be controlled by the reaction conditions [3, 4, 7].

Figure 1.2 Glycerol electrooxidation pathway on Au/C catalyst [7].

The prolonged electrolysis at controlled potential with low pH and low glycerol concentration (0.1 M KOH and 0.1 M glycerol) proceeds mainly through the C-C dissociation route. The main electrooxidation product was formic acid at higher than 60% selectivity following by glycolic acid at around 20%. The potential applied has only small effects on the product distribution in this condition [7].

The looped electrolysis study using the AAEMFC single cell at higher glycerol and KOH concentration (> 1 M) pointed out the more selective oxidation of glycerol into tartronic [4] and mesoxalic acid [3]. The parameters involve in controlling the type of products includes type of membrane, glycerol electrolyte flow rate, oxygen flow rate, KOH concentration and temperature. The controlled reaction with low anode and cathode flow rate with high KOH concentration provides the highest tartronic selectivity of 69.3 % at glycerol conversion of 89.2 %. The high value product such as lactic acid, which is an indirect glycerol electrooxidation product from glyceric acid dehydration, was

observed along with glyceric acid, oxalic acid, mesoxalic acid and glyceric acid [4]. Mesoxalic acid was a deepest electrooxidation product of glycerol. All of the hydroxide groups on glycerol molecule must be oxidized without C-C bond breaking. This considerably high selectivity of mesoxalic (46 %) with 22.7 mW cm⁻² power density can be achieved by using low anode overpotential. The C-C bond dissociative products including glycolic acid and oxalic acid become major products at higher potential [3].

The presence of foreign metal in binary- and ternary- catalyst may change the glycerol electrooxidation pathway in alkaline. Addition of Ag to Au-based catalysts increase the ability of the catalysts to break the C-C bond on glycerol molecule [25n]. From the mechanism as shown in Fig. 1.3, AuAg tends to produce mainly 1-carbon atom product. This is interesting for fuel cell application since it leading to improved electron yield extracted from glycerol molecule, however, lower the chance of producing a move valuable products.

Figure 1.3 Suggested mechanism of the glycerol electrooxidation on Au/C, AuAg/C and Ag/C catalysts [25].

The electrocatalytic properties of Au towards alcohols electrooxidation were improved by a number of promoters such as Ce_2O_3 [8], RuO_2 [7], MnO_2 [26] and Ag [15]. The addition of metal oxide promoters gives small effects on the activity of Au catalyst [7, 8, 15]. The main benefit of metal oxide was the stability improvement especially in a reaction heavily involving C-C bond dissociation. The role of metal oxides was to balance

the oxygen-containing species on Au surface. The alcohol electrooxidation activity of Aubased catalyst can be halted by the strongly adsorbed reaction intermediates and the formed Au oxide film which occurred at around alcohol electrooxidation potential. By optimizing the oxide formation on Au surface, the catalyst becomes more stable. However, the metal oxides do not promote the adsorption of alcohol on Au surface as the onset potential was similar to that without metal oxide.

Conversely, the onset potential or mass specific current density of glycerol [15] or glucose [16-21] electrooxidation can be improved by adding Ag. Garcia et al. [15] studied the preparation of AuAg/C catalyst by a co-reduction of AuCl₃ and AgNO₃ employing glycerol as a reducing agent in presence of polyvinylpyrrolidone (PVP) for glycerol electrooxidation in alkaline. The synthesized AuAg/C has an average size of around 15 nm. The Au active surface area of the AuAg/C catalyst was very low because of the segregation of Ag film at particle surface. They suggested that the Ag-rich shell was due to the higher adsorption energy of oxygenated species on Ag over Au. Thus, Ag was pulled to the surface. Another possible explanation was from a slow formation of Ag nanoparticle. Au³⁺ was instantly reduced after introducing the reducing agent while Ag⁺ requires more time before the reduction can be observed. In the system with Au³⁺ and Ag⁺, the Au nucleus should be formed first then followed by the co-deposition of Au and Ag onto the formed Au nucleus. The resulting particle of this process was Au-rich core covered by an Ag-rich shell. The glycerol electrooxidation activity on AuAg/C was much lower than that of Au/C. However, the onset potential was lowered by 120 mV which indicates the electronic properties modification of Au by Ag. Their XANES results pointed out the reduction of the Au 5d band density in presence of Ag which tunes the adsorption strength of adsorbates on Au surface [15].

The promotion effects of Ag on Au were intensively studied on glucose electrooxidation [16-21]. The presence of Ag, even in the form of ad-atom on Au surface was found to improve the activity toward sugar electrooxidation [20]. A number of metals including Cu, Co, Ru, Cd, Ir, Ag and Pt, was decorated on Au(111) by using the under potential deposition (UPD) method. Ag was found to be the best promoter for electrooxidation of most aldose type monosaccharide and disaccharide on Au(111). The

Ag-decorated catalyst provides higher maximum glucose electrooxidation current density with around 100 mV lower onset potential than that of Au (111). The role of Ag on lowering the Au-OH formation potential was proposed to be the possible explanation.

Recently, our group studied the effects of surface Ag on the glucose electrooxidation of Au/C [16]. The introduction of Ag onto Au nanoparticle surface was performed by physical mixing of Ag sol with Au/C or vice versa. The introduction of Ag was occurred via Oswald ripening process. With a short mixing period (15 min), the presence of Ag should had taken placed only at the Au surface, not deep into Au particles. All of the Ag-containing catalysts showed lower maximum current density for glucose oxidation than Au/C. However, the electrooxidation stability of the catalysts was greatly improved.

The AuAg alloy prepared by various methods such as dealloying process [17], Schiffrin's two phase synthesis protocol [18] and impregnation using tetra-octyl-ammonium (TOAB) as a phase transfer agent [21] were used for glucose electrooxidation and similar finding was reported. The AuAg alloy catalysts showed a higher catalytic activity with lower onset potential than that on pure Au catalyst. Ag in AuAg alloy promotes the reaction by facilitating the adsorption of OH onto Au surface.

From all the aforementioned studies regarding the AuAg-based catalysts, Ag plays an essential role in promoting the alcohol and sugar electrooxidation on Au. However, since Ag was inactive for alcohol electrooxidation, the amount of Ag on metal nanoparticle surface should be properly controlled. One of the possible methods to produce the Au-rich shell catalyst was called galvanic displacement.

Galvanic displacement is an electrochemical process that involves the dissolution of the solid electrode with the deposition of higher reduction potential ion in an electrolyte. The overall displacement reaction is given by

$$M_1 + M_r^{z+} \longrightarrow M_1^{z+} + M_r \tag{1.1}$$

 M_l is the metal that is oxidized and dissolved into an electrolyte. M_r is the metal to be deposited. The reaction is driven by the potential difference between M_l and M_r . The

source of electrons for deposition was from the M_l substrate. The kinetics and the growth mechanisms of the deposit differ in each system.

For an Au and Ag system, the $AuCl_4$ /Au has a standard reduction potential of 0.99 V which is higher than that of Ag/Ag^{\dagger} at 0.80 V. This implied that $AuCl_4$ will be reduced in presence of metallic Ag. The reaction bath comprising of $AuCl_4$ and Ag yields the deposit Au and the Ag^{\dagger} as a dissolution product as followed

$$3Ag + AuCl_4 \longrightarrow 3Ag^+ + Au + 4Cl^- \tag{1.2}$$

This reaction is similar to the corrosion of Ag where Ag is oxidized as the anode reaction. The electron was moved to particle surface and then Au was reduced and deposited at cathode. From the equation, 3 moles of Ag was need for 1 mole of Au. As a result, this process leads to the shrinkage or pore formation of metal particles [27-29].

The first step of displacement reaction was the hole formation on the Ag particles [27, 28]. The formation of the hole indicates that the dissolution reaction was initiates at some certain sites on Ag particle. This formed site was the active site for further dissolution reaction rather than the spontaneous dissolution reaction over the entire surface. This process occurs along with the deposition of Au onto Ag surface forming a very thin Au or AuAg alloy phase. The formed Au or AuAg film was more stable than an intact Ag phase. Thus, the hole continued to act as an active dissolution site and grew larger while the deposition of Au continued to deposit on the outer surface of particle.

With high enough concentration of Au, the void inside the structure will be enlarged until the entire structure is filled leaving the shell structure of homogeneous AuAg alloy phase. Further reaction involves dealloying process in which the residual Ag leaches from the alloy leaving pure Au particle. Since the total solid volume was reduced by around 3 fold, the remaining particle will be shrunk. This process may take place along with the surface reconstruction via Ostwald ripening to reduce its surface energy.

The galvanic displacement process can be controlled by a number of parameters such as temperature, Au concentration, active Au species and type of substrate. The effect of temperature was directly on the atomic fraction of Au in the alloy film. The

interdiffusion coefficient which governs the atomic fraction was increased with increasing temperature. Higher temperature provides higher interdiffusion coefficient which yields lower concentration of Au near the surface. For the reaction involving AgCl, the higher solubility of AgCl at higher temperature also offers smoother AuAg nanoparticles as observed by Transmission electron microscopy (TEM) [27].

The effects of the active Au species were observed by Lee $et\ al.$ [28]. The species of Au was controlled by varying the pH of the displacement bath. The AuCl₄ complex was changed into various OH substituted complexes at higher pH. The OH forms of Au precursor have a lower standard potential i.e. E^0 of AuCl₄ is + 1.004 V while that of Au(OH)₄ (pH 10) is + 0.602 V. At pH of 3, the displacement reaction was rapid and causes a collapse of structure. The yielding particle has a dense structure with very high Au:Ag atomic ratio at 94.46:5.54. At pH of 7, the porous particles were obtained with lower Au portion at 73.45:26.55. The use of less active Au forms results in slower displacement reaction.

The preparation of AuAg/C with small metal particle sizes by using galvanic displacement was reported [29]. Firstly, the Ag nanoparticles on multi wall carbon nanotube (MWCNT) were prepared by using chemical reduction of Ag⁺ by polyol in presence of PVP. The Ag nanoparticle on CNT with particle size lower than 10 nm was formed. After that, the Ag/C was placed into 1 mM AuCl₄ solution for galvanic replacement. The short immersion time of 1 to 3 min at 4 °C yielded small AuAg nanoparticles with average size of around 3 nm, while longer immersion time provided larger AuAg particles. Unfortunately, the synthesized nanocomposites have not been tested by any applications; hence, the questions on the activity and stability of such material were remained.

In order to obtain the well dispersed AuAg/C catalyst, the Ag/C which is used as a sacrificed material should be properly synthesized. The Ag/C used should have the well dispersed Ag nanoparticles with narrow size distribution on carbon support. There were several methods that can be used to prepare the Ag nanoparticle with such a requirement. Citrate protection is a facile method that was capable in preparation of Ag nanoparticle with well size distribution [12, 13, 30]. The Ag/C with average particle size

lower than 10 nm was prepared by reduction of $AgNO_3$ by using $NaBH_4$ in presence of citrate to form a Ag sol. Loading of Ag on carbon support can be easily controlled by adjust the amount of carbon used in an Ag sol immobilization step [12].

Citrate reduction method was another possible method that can be used to synthesize nanoparticles with controlled particle size. This method was simple. Citrate was used as both reducing agent and protecting agent. The reduction of metal precursor was carried out by refluxing the metal precursor in presence of citrate solution until the Ag sol was formed. The particle size of metal was controlled by varying the concentration of metal precursor used.

Au-based catalyst was very active for glycerol electrooxidation in alkaline medium. Along with its high activity, a number of chemicals can also be selective synthesized. Ag was found to promote the activity of Au-catalyst for glycerol electrooxidation. However, the composition of bimetallic AuAg/C catalyst must be properly controlled. Galvanic displacement was selected to be used in this study in order to prepare the highly active AuAg/C catalyst for glycerol electrooxidation in alkaline medium.

1.3 Objectives

- To study the effects of preparation parameters of the galvanic displacement of Ag/C by Au ion on the activity and stability for glycerol electrooxidation of AuAg/C catalyst.
- 2. To study the effects of Ag on the catalytic activity and stability of AuAg/C catalyst.

1.4 Scope of research

- 1 Au was base catalyst and Ag was used as a promoter.
- 2 The Ag/C catalysts was prepared by using the citrate reduction or citrate protection method.

- 3 The AuAg/C catalysts was prepared by varying the preparation parameter on galvanic displacement of Ag.
- 4 The electrocatalytic activity and stability of prepared catalyst toward glycerol electrooxidation was measured by cyclic voltammetry and chronoamperometry, respectively.

CHAPTER 2: METHODOLOGY

2.1 Catalyst preparation

2.1.1 Ag/C preparation

The 60% wt Ag/C catalyst was prepared by the citrate reduction method. First, the required amount of AgNO₃, potassium citrate and carbon support (Vulcan XC-72) were dissolved in DI-water. After well mixed, KOH solution was added into the above solution to initiate the reduction reaction. The solution turns olive green as the Ag sol was formed. The reaction bath was kept stirring for 30 min under stirring to immobilize the Ag nanoparticle on the support. Finally, the catalyst was filtered, washed and dried.

2.1.2 Galvanic displacement of Au³⁺ and Ag/C

The synthesized Ag/C was used as a sacrificed material for deposition of Au via galvanic displacement. The Ag/C was dispersed in the DI-water by stirring for 30 min. Then, the required amount of HAuCl₄ solution was added into the above solution in one portion under vigorous stirring. The formation of AuAg nanoparticle occurred along with the formation of white participate of AgCl. The suspended AuAg/C was filter and then washed several time with concentrate NaCl to remove the AgCl and DI-water until Cl was absent from the filtrate. Finally, the catalyst was dried in vacuum oven at 70 °C. Four AuAg/C catalysts were prepared by using this method designated as 5%AuAg/C, 10%AuAg/C, 20%AuAg/C and 30%AuAg/C for 5, 10, 20 and 30wt% Au, respectively.

2.1.3 Au/C preparation

Au/C was prepared by using the PVA protection method. $HAuCl_4$ was dissolved in DI-water in presence of PVA. $NaBH_4$ solution was added drop by drop under vigorous stirring to form a ruby red sol. After 30 minutes of stirring, Vulcan XC-72 was added to

immobilize the Au sol. The catalyst was washed with Di-water and ethanol and finally dried in vacuum oven.

2.1.4 Pd electrodeposition

The role of electrodeposited Pd on the glycerol electrooxidation properties of AuAg/C was carried out on 10%AuAg/C catalyst. The electrodeposition of Pd was performed by using a cyclic voltammetric method. First, the catalyst ink of 10%AuAg/C composed of 10%AuAg/C, nafion ionomer and isopropanol was dropped on the glassy carbon electrode to yield a very thin film of 50 ug cm⁻²_{Au}. After dried in ambient air, the electrode was dipped into the electrodeposition bath containing PdNO₃ and supporting electrolyte. The electrodeposition was performed by cyclic voltammogram mode between -0.8 V-0.8 V vs. Mercury/Mercury oxide (MMO) reference electrode. The effects of supporting electrolyte and number of electrodeposition cycle was studied. The nomenclature of 4 Pd-AuAg/C catalysts presented in this work is shown in Table 2.1.

Table 2.1 Nomenclature of Pd-AuAg/C catalysts and their electrodeposition conditions.

Catalyst	Electrodeposition bath Solution	No. of electrodeposition cycle
1Cl-Pd-AuAg/C	1 mM PdNO $_3$ + 0.1 M KCl	1
10Cl-Pd-AuAg/C	0.01 mM PdNO ₃ + 0.1 M KCl	10
1N-Pd-AuAg/C	$0.01 \text{ mM PdNO}_3 + 0.1 \text{ M KNO}_3$	1
5N-Pd-AuAg/C	$0.01 \text{ mM PdNO}_3 + 0.1 \text{ M KNO}_3$	5

2.2 Physical characterization

The prepared catalysts including Ag/C and Au/C was subjected to physical characterization by using the following techniques:

2.2.1 Transmission electron microscope (TEM) images were taken by using the JOEL JEM 2010 at a voltage of 200 kV. The average particle size was of the catalyst was calculated from approximately 100 particles.

2.2.2 The structure and composition were characterized by using an X-ray diffractometer (XRD) Bruker AXS: D8DISCOVER with Goebel mirror Cu K α radiation (λ = 0.1540 nm) using 40 mA filament current and 40 kV tube voltage.

2.2.3 The energy dispersive spectroscopy (EDX) equipped with scanning electron microscopy (SEM) was used to estimate the metal loading and Au:Ag ratio. The EDX mapping and component analysis were performed at a working distance of 8.5 μ m with an aperture of 30 μ m. The overall composition was analyzed at 200 kV whilst the surface composition was detected using a lower potential at 10 kV. The average element composition was calculated from three points of the collected data.

2.3 Electrochemical characterization

The electrochemical study were carried out by using a 3-electrode cells. The catalyst ink was prepared by mixing a certain amount of catalyst with 5 %wt Nafion solution in isopropanol and then homogenized by using ultrasonic bath. The well mixed ink was dropping onto glassy carbon electrode to form a working electrode. Mercury/mercury oxide (MMO) was used as a reference electrode. A 1 cm² Au gauze was utilized as a counter electrode. All electrolyte used was pre-purged by using Ar gas for at least 30 min before any measurement.

Cyclic voltammetry was used to study the glycerol electrooxidation activity of the catalysts. Chronoamperometry was be used to observe the stability of the catalysts in glycerol electrooxidation.

CHAPTER 3: RESULTS AND DISCUSSION

3.1 Physical characterization

Fig. 3.1 shows the TEM image of the Ag/C catalyst that prepared by using the citrate reduction method, which used as a sacrificed material in the AuAg/C preparation. The Ag nanoparticles appeared as the large agglomerates in various shape with a wide size range. The average particle size of these particle was around 200 nm with most of the particle have a diameter between 130-275 nm.

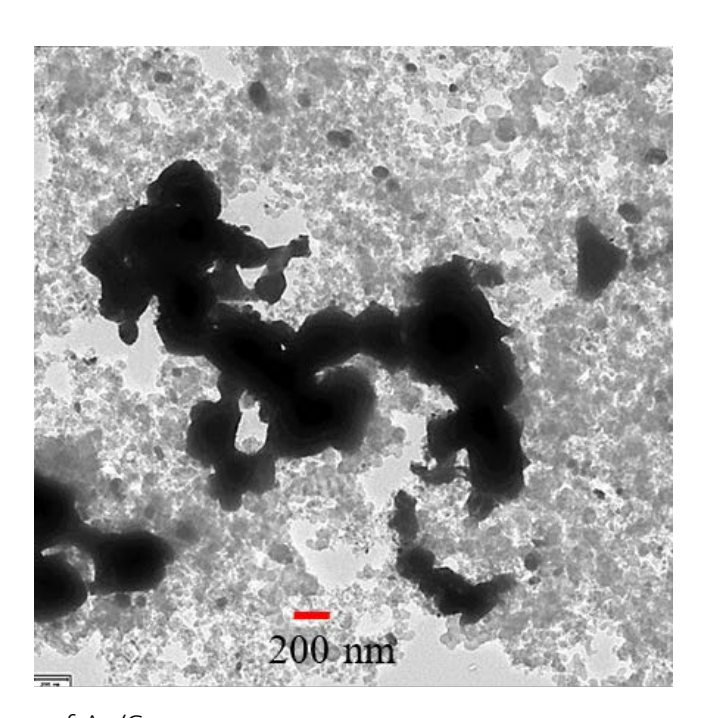


Figure 3.1 TEM image of Ag/C.

Upon displacement reaction with Au³⁺, three moles of metallic Ag on Ag/C were oxidized into the solution along with deposition of one mole of Au on the nanoparticle surface. This process leads to shrinkage of Ag particle. As a result, numbers of smaller

AuAg fragment were generated depends upon the amount of added Au, as shown in Fig. 3.2 (a) to (d). For the low Au loading catalysts such as 5%AuAg/C and 10%AuAg/C, the displacement degree was low, then, the formed AuAg nanoparticles were in both form of large porous particle and smaller fragment. As the displacement degree was higher, as in 20%AuAg/C and 30%AuAg/C, only the small AuAg fragments with the average size around 20 nm were observed.

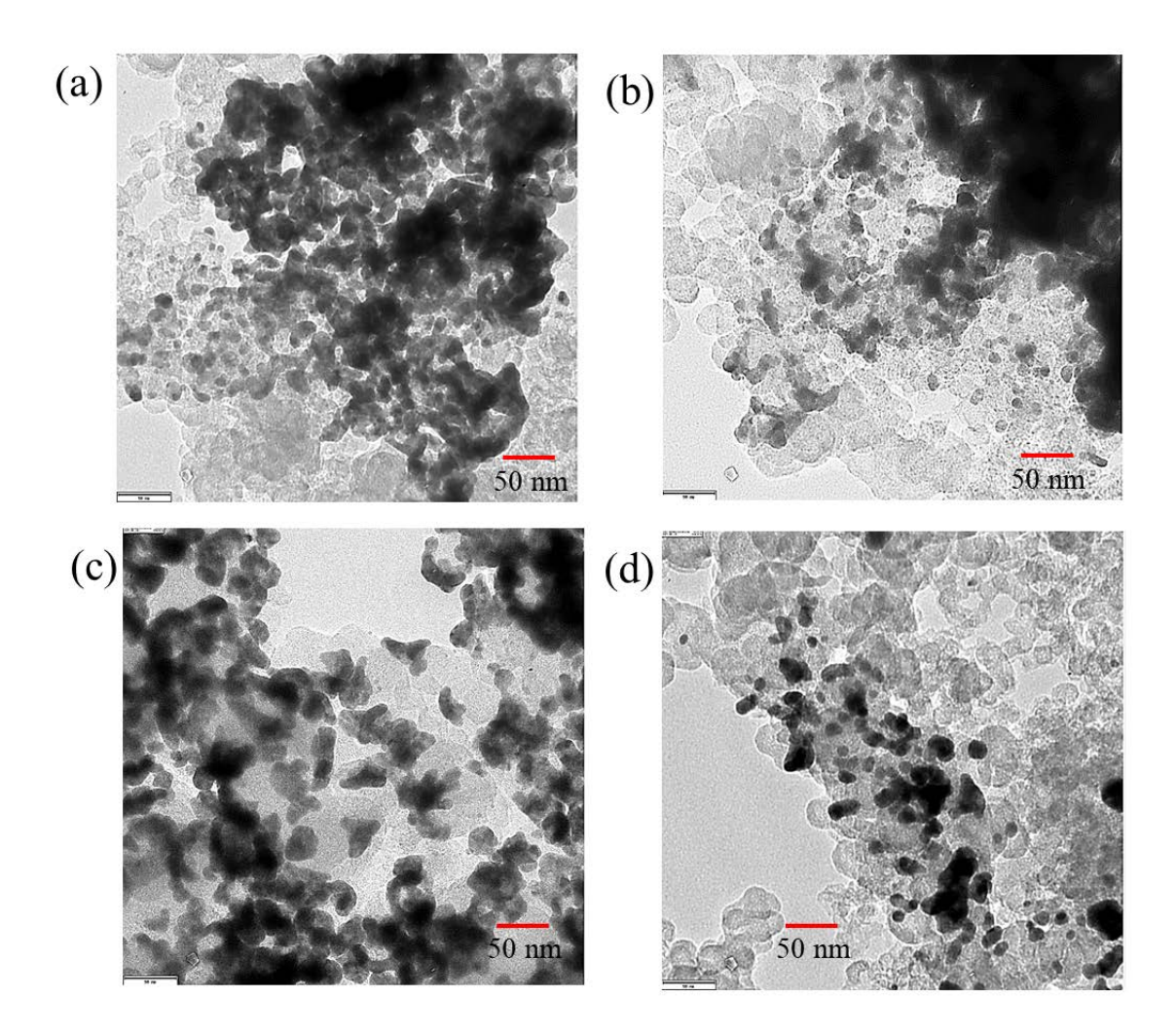


Figure 3.2 TEM images of (a) 5%AuAg/C, (b) 10%AuAg/C, (c) 20%AuAg/C and (d) 30%AuAg/C.

The TEM image of Au/C is shown in Fig. 3.3. The Au nanoparticle were decorated uniformly on the carbon, unlike the formed AuAg nanoparticle prepared via the galvanic

displacement method. The average metal particle size was about 4.12 ± 0.98 nm, which is much smaller than that of the AuAg/C catalysts.

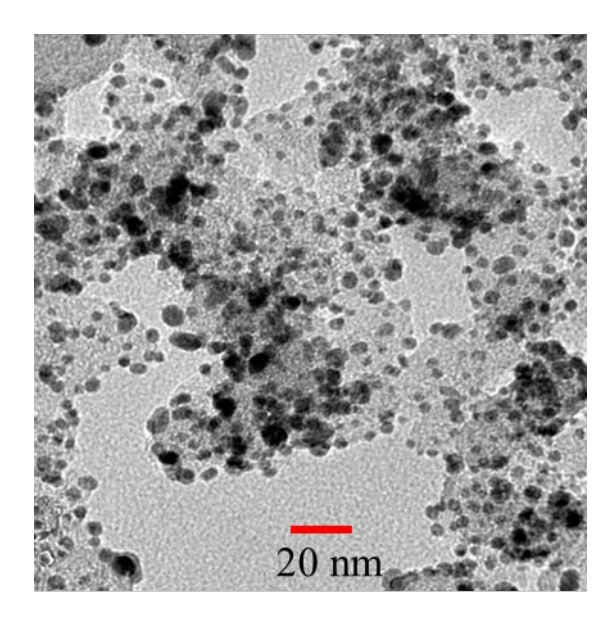


Figure 3.3 TEM image of Au/C prepared by using the PVA method.

Fig. 3.4 presents the XRD patterns of all the prepared catalysts. All the peaks related to Au and Ag appear at the same 2Θ value at 38.2, 44.3, 64.5 and 77.6 degrees (JCPDS NO. 04-0783 for Ag and JCPDS NO. 04-0784), since both Au and Ag have similar lattice constants. On the Ag/C catalyst, a small amount of Ag₂O was observed from the main peaks at 33.1 degrees (JCPDS NO. 41-1104). Small amount of AgCl formed during the galvanic displacement was remained on all the AuAg/C catalysts since four additional peaks corresponding to AgCl (JCPDS NO. 31-1238), were observed.

The deconvoluted XPS spectra of the Ag/C, Au/C, and AuAg/C catalysts in the Au 4f and Ag 3d regions were shown in Fig. 3.5. The peak binding energies of the deconvoluted peaks are summarized in Table 3.1. In the Au 4f region, as shown in Fig. 3.5(a), the peaks of metallic Au $4f_{7/2}$ and $4f_{5/2}$ are observed at 84.7 and 88.4 eV, respectively. The binding energy of the Au peak to lower energy were observed for all the AuAg/C catalysts.

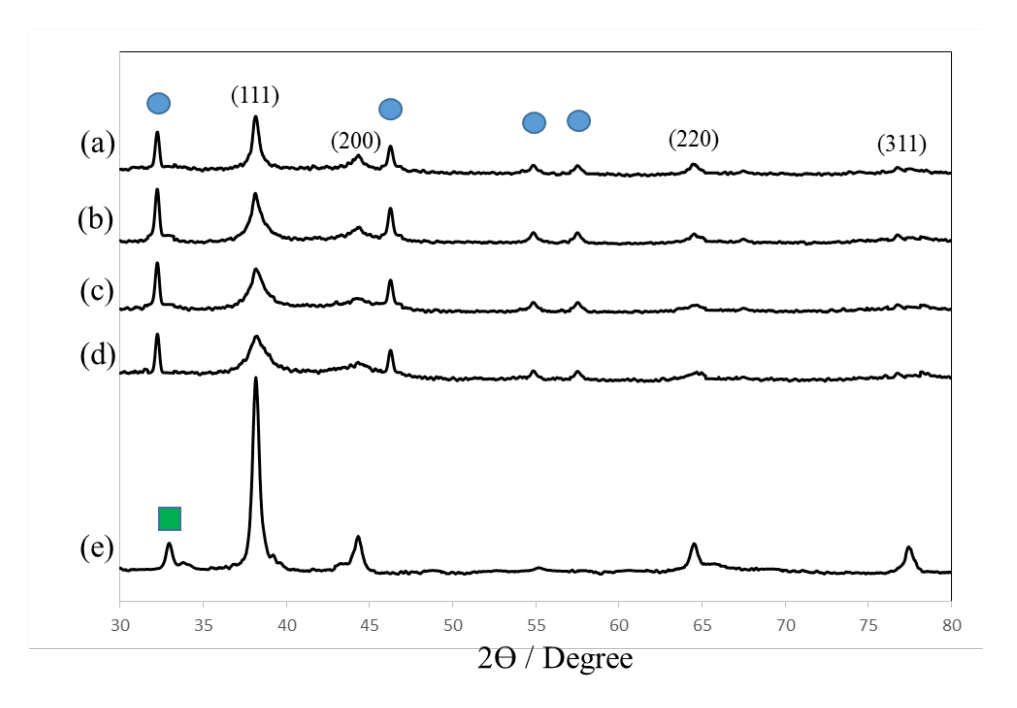


Figure 3.4 XRD patterns of (a) 5%AuAg/C, (b) 10%AuAg/C, (c) 20%AuAg/C, (d) 30%AuAg/C, and (e) Ag/C marked by the main peak positions of AgCl (\bullet) and Ag₂O (\blacksquare).

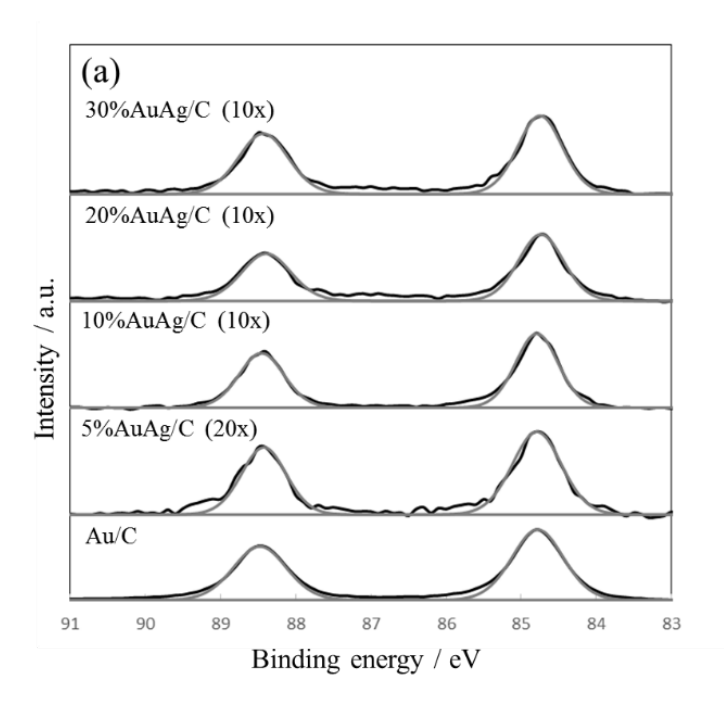


Figure 3.5 The deconvoluted and XPS data of all the synthesized catalysts in (a) 4f spectra of Au and (b) 3d spectra of Ag region.

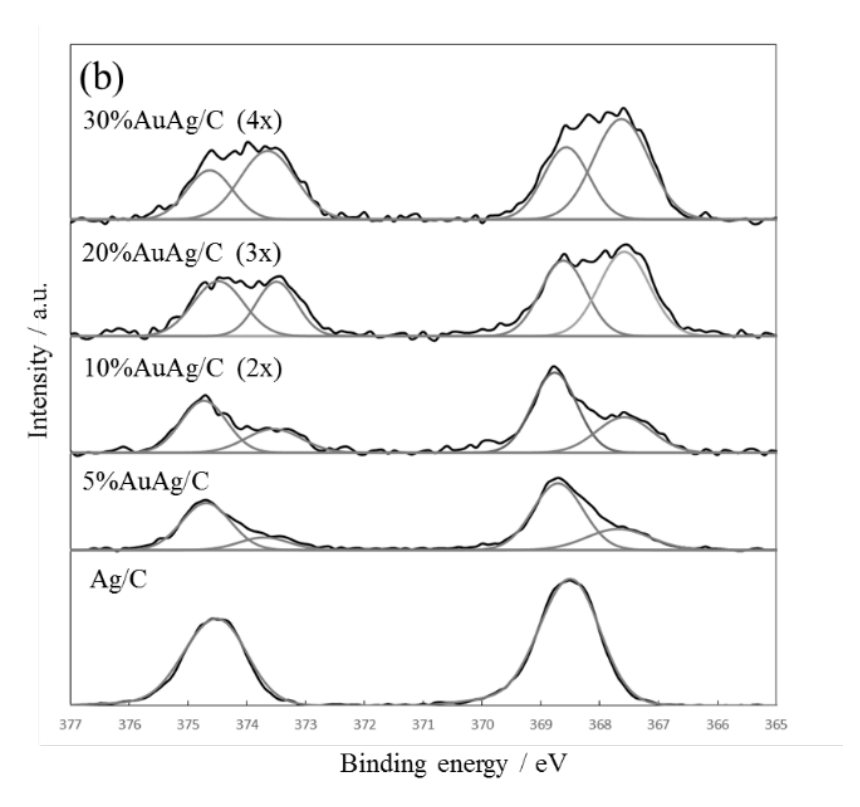


Figure 3.5 Cont. The deconvoluted and XPS data of all the synthesized catalysts in (a) 4f spectra of Au and (b) 3d spectra of Ag region.

Table 3.1 The peak binding energy of Au and Ag from the deconvoluted XPS results.

Electrocatalysts	Binding Energy (eV)			
_	Au		А	vg
	4f _{7/2}	4f _{5/2}	3d _{5/2}	3d _{3/2}
Au/C	84.8	88.5	-	-
5%AuAg/C	84.8	88.4	368.7	374.7
10%AuAg/C	84.8	88.5	368.8	374.7
20%AuAg/C	84.7	88.4	368.6	374.6
30%AuAg/C	84.7	88.4	368.6	374.6
Ag/C	-	-	368.5	374.5

The XPS spectra in the Ag region showed two species of Ag: ionic and metallic. In 3d region of Ag, the peak of ionic Ag appears at lower energy than that of its metallic

form [19]. The Ag/C catalysts used as a sacrifice material contained only the metallic peak at the binding energy of 368.5 and 374.5 eV. For AuAg/C catalysts, the peaks of Ag⁺, from the remaining AgCl formed during the galvanic displacement were observed at around 373.6 and 367.8 eV. The binding energy of metallic Ag were shifted to higher values, indicating that the electrons had transferred from Ag to Au to form an AuAg alloy. This electron transfer is normally observed in an AuAg bimetallic catalyst [15].

The actual Au loading and the calculated Au:Ag weight ratio from the EDX results of all the AuAg/C catalysts were collected in Table 3.2. The metal loading and the weight ratio of all the AuAg/C catalysts, except for 5%AuAg/C, were close to the intended ratio. This indicates the complete displacement reaction under the preparation used.

Table 3.2 The calculated Au and Ag weight ratios from EDX results.

	Average Au	Au:Ag weight ratio	
Catalysts	loading (%wt)	Actual	Intended
5%AuAg/C	2.01 ± 1.86	0.046 ± 0.043	0.096
10%AuAg/C	9.16 ± 1.72	0.206 ± 0.154	0.230
20%AuAg/C	18.28 ± 2.86	0.841 ± 0.349	0.737
30%AuAg/C	32.23 ± 5.28	3.048 ± 0.233	2.801

3.2 Electrochemical activity

The typical CVs of Ag/C and Au/C in alkaline solution are shown in Fig. 3.6. Both Ag/C and Au/C exhibit the oxidation and reduction peaks related to oxide formation and reduction, respectively, on their surfaces. For Ag/C, two oxide formation peaks correspond to the formation of Ag₂O (0.25 V), and the mixed phases of Ag₂O and AgO (0.7 V) [31-32]. The oxidation peak in the forward scan of Au/C relates to oxide formation on the Au surface. In the reverse scan, two states of Au oxide were reduced at two potentials: the quasi-2D oxide at about 0.3 V and the quasi-3D oxide at about 0.0 V.

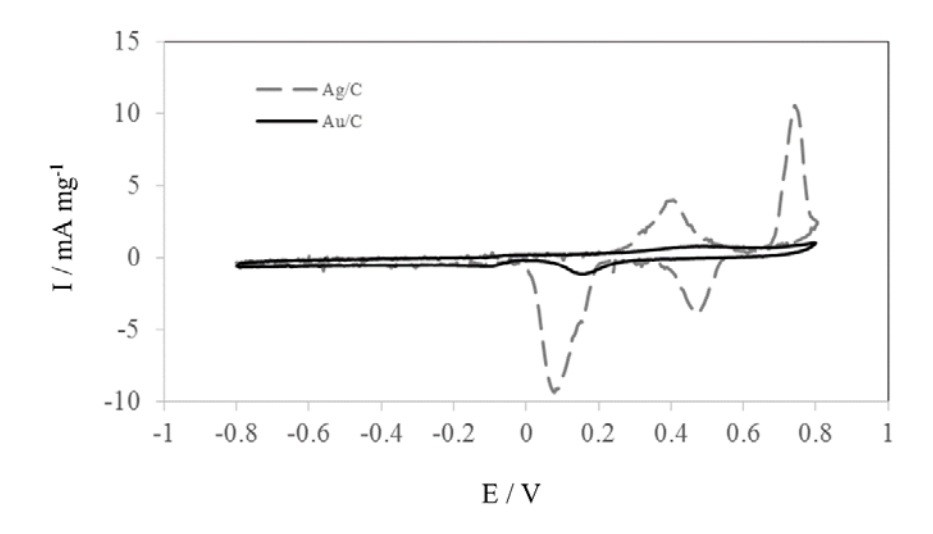


Figure 3.6 CVs of Ag/C and Au/C in 0.1 M KOH at a scan rate of 20 mV $\rm s^{-1}$.

The CVs of the AuAg/C catalysts with different Au loadings are shown in Fig. 3.7. These CVs were quite similar to that of Ag/C, with a shift in the peak potential even when the catalyst, such as 30%AuAg/C, had a very low content of Ag. In addition, the onsets of the oxide formation and reduction peaks of all the AuAg/C catalysts, except for 30%AuAg/C, were similar to those of Ag/C. For 30%AuAg/C, the anodic shift was observed with all the peaks, indicating higher metal oxide stability.

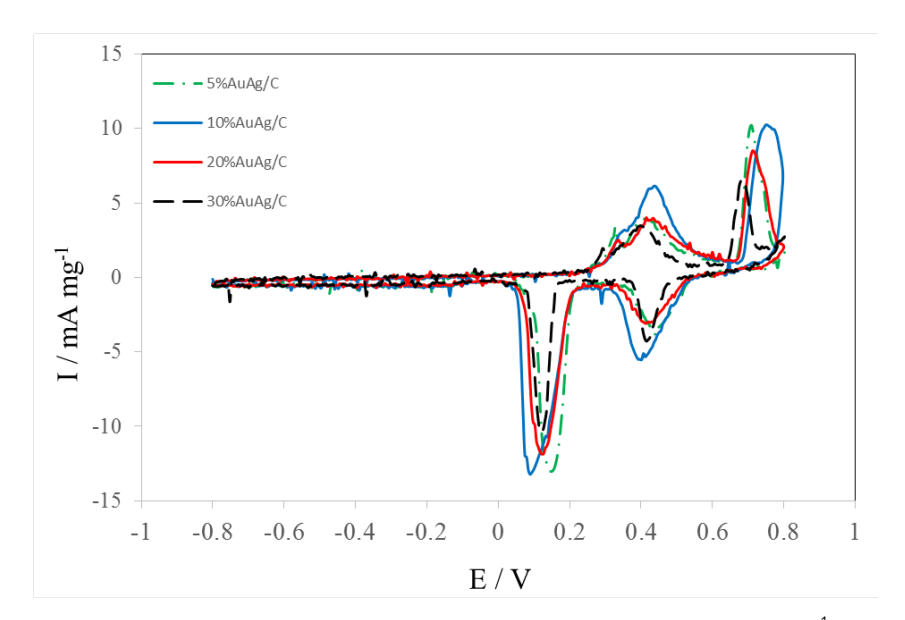


Figure 3.7 CVs of AuAg/C catalysts in 0.1 M KOH at a scan rate of 20 mV s⁻¹.

Both Ag/C and Au/C were active for glycerol electrooxidation under the condition of the experiment, as shown in Fig. 3.8. By comparing the CVs of the Ag/C catalyst in Figs. 3.6 and 3.8, the glycerol electrooxidation peak occurs at 0.2 V, which is more positive than the first peak of AgO formation. It is anticipated that the alcohol electrooxidation on Ag takes place on its oxide surface, which is different from other metals, such as Au and Pt [33]. This catalytic active surface was not recovered by the cycling of the potential, since the activity gradually declined as the number of cycles increased.

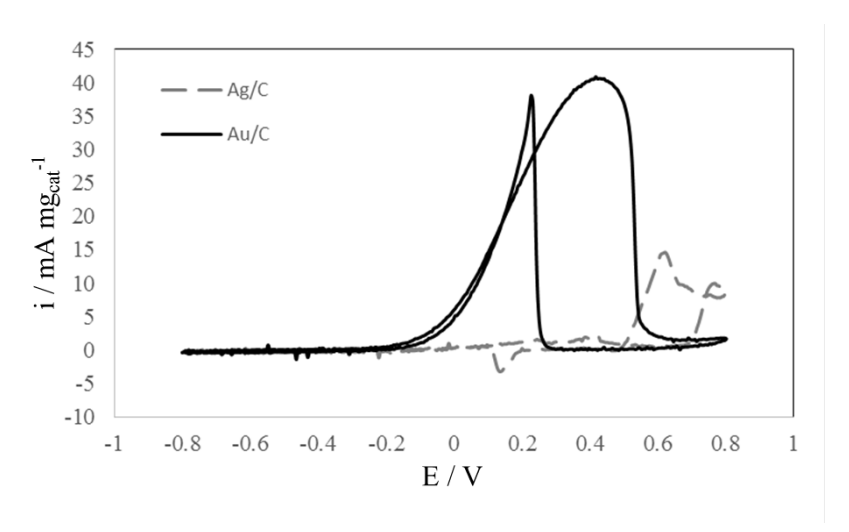


Figure 3.8 CVs of Ag/C and Au/C in 0.1 M glycerol and 0.1 M KOH at a scan rate of 20 mV $_{\rm S}^{\rm -1}$.

For Au/C, the glycerol electrooxidation took place on the bare Au surface and was inhibited by the surface oxide formation. The onset of the reaction was observed at about -0.2 V. The current density rapidly increased and reached the maximum current density at 0.4 V. After this point, the surface oxide formed and the reaction was inhibited. In the reverse scan, the oxide was removed from the Au surface at 0.25 V and the catalyst activity was recovered, resulting once again in the oxidative current of glycerol electrooxidation.

3.3 Surface activation of the AuAg/C catalyst

All the AuAg/C catalysts in this work require an activation by cycling the potential in alcohol-containing electrolyte before they were in an active form, for example for 10%AuAg/C which were displayed in Fig 3.9(a) and (b). It was noticed that the peak characteristic and current density of the CVs change as the number of cycles increase. This means that the structure of AuAg/C catalyst could be change as the reaction with glycerol proceeded. In the 1st loop (see Fig. 3.9(a)), the CVs of the 10%AuAg/C in 0.1 M glycerol and 0.1 M KOH was guite similar to that of the Ag/C in 0.1 M KOH but with the appearance of the sharp peak of glycerol electrooxidation on the recovered gold surface in the reverse scan. In addition, the oxidation peaks of glycerol on the Au (from -0.2 V to 0.6 V) are very low while the dominant oxidation peak belongs to glycerol electrooxidation on AgO (from 0.7 V onward). As the number of cycle increased, the peak of glycerol electrooxidation on the Au was enhanced whereas that on the AgO was reduced. The Au catalyst activity improved with the advances of the scan and become steady at the 9th loop, in which the glycerol electrooxidation on Au was more pronounced than that on AgO. The potential at maximum current density and the onset of AuO reduction were also shifted closer to those of the Au/C catalyst.

In addition, the surface activation of catalyst surface could be accelerated by increasing glycerol concentration. At higher glycerol concentration, the activation process proceeded much faster, as shown in Fig. 3.9 (b). The glycerol electrooxidation on Au catalyst can be clearly observed and became a main oxidation peak starting since the $1^{\rm st}$ scan. The steady CV was achieved after the $6^{\rm th}$ loop.

This evidence indicates the reconstruction of the AuAg surface. Prior to glycerol electrooxidation test, the working electrode was activated and cleaned by performing cyclic scan in KOH solution at the same concentration. This process may bring the Ag atom to the nanoparticle surface since Ag exhibit a higher affinity to adsorb the oxygenate species (OH) than Au [34]. The catalyst shows a low glycerol electrooxidation activity in this state since Ag was inactive for glycerol electrooxidation at low potential. However, the surface of AuAg nanoparticle was reconstructed and became highly active from the activation by glycerol. The role of glycerol in this surface reconstruction was clear. The activation process proceeded much faster at high glycerol concentration. Hence, the

reconstruction may be led by the strong interaction between surface- or underneath- Au atoms and glycerol which bring the Au atom to the nanoparticle surface since the Au is better at adsorption of alcohol than the Ag.

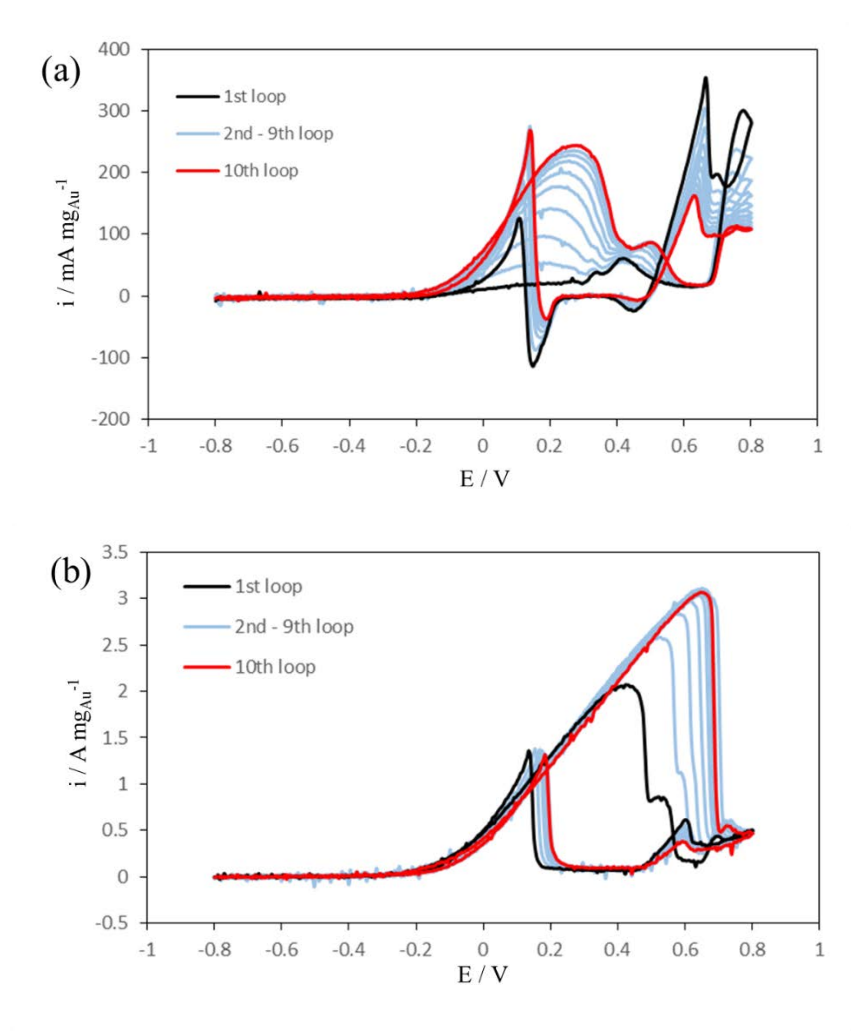


Figure 3.9 Mass normalized CVs of 10%AuAg/C catalysts in (a) 0.1 M glycerol and 0.1 M KOH and (b) 1 M glycerol and 2 M KOH at a scan rate of 20 mV $\rm s^{-1}$.

The surface compositions of the as-prepared 10%AuAg/C and the catalyst activated by glycerol electrooxidation in 1 M electrolyte at a low EDX potential were compared. Au and Ag on all the catalysts were non-uniformly distributed all over the nanoparticles. The Au:Ag ratios of the prepared catalyst and the catalyst cycled in the KOH electrolyte were similar at 0.145 ± 0.017 and 0.142 ± 0.066 , respectively. However,

the catalyst surface became an Au-rich surface after scanning in 1 M glycerol electrolyte, since the Au:Ag ratio increases to 0.366 ± 0.050 , providing evidence of the adsorbate-induced surface segregation of the AuAg surface. The surface segregation of a more reactive component to the adsorbate on the surface of the alloy was well described [35].

Prior to the glycerol electrooxidation test, the working electrode was cleaned by performing a cyclic scan in a KOH solution at the same concentration. This step may bring the Ag atom to the nanoparticle surface, since Ag exhibits a higher affinity for adsorbing the oxygenated species than does the Au atom [34]. The catalyst showed a low glycerol electrooxidation activity in this state, since Ag was inactive for glycerol electrooxidation at low potentials. However, the surface of the AuAg nanoparticles was reconstructed and became highly active after interacting with glycerol. The activation process proceeded much faster at high glycerol concentration. Hence, the surface segregation may have been led by a strong interaction between either the surface or underlying Au atoms and the glycerol, which induced the Au atoms to rise to the nanoparticle surface, since Au is better than Ag at adsorbing alcohol [25]. In other words, the deactivation of the catalyst surface is reversible depending on the electrolyte deployed. The catalyst was easily deactivated by the interaction between Ag and hydroxide ions. The fully activated catalyst was reversed to its inactive form after cycling the potential in the KOH electrolyte, as shown in Fig. 3.10 (a) and 3.10 (b) shows the results of the same electrode as shown in Fig. 3.10 (a) after cycle in 2 M KOH. Even though this electrode was fully activated in the first experiment, the electrode was deactivated by KOH and was inactive. Then, after subjected to the electrolyte with glycerol the AuAg surface was reactivated and the current density raised again. Hence, the surface of AuAg may constantly be changing as the reaction proceeds in the electrolyte containing both glycerol and OH.

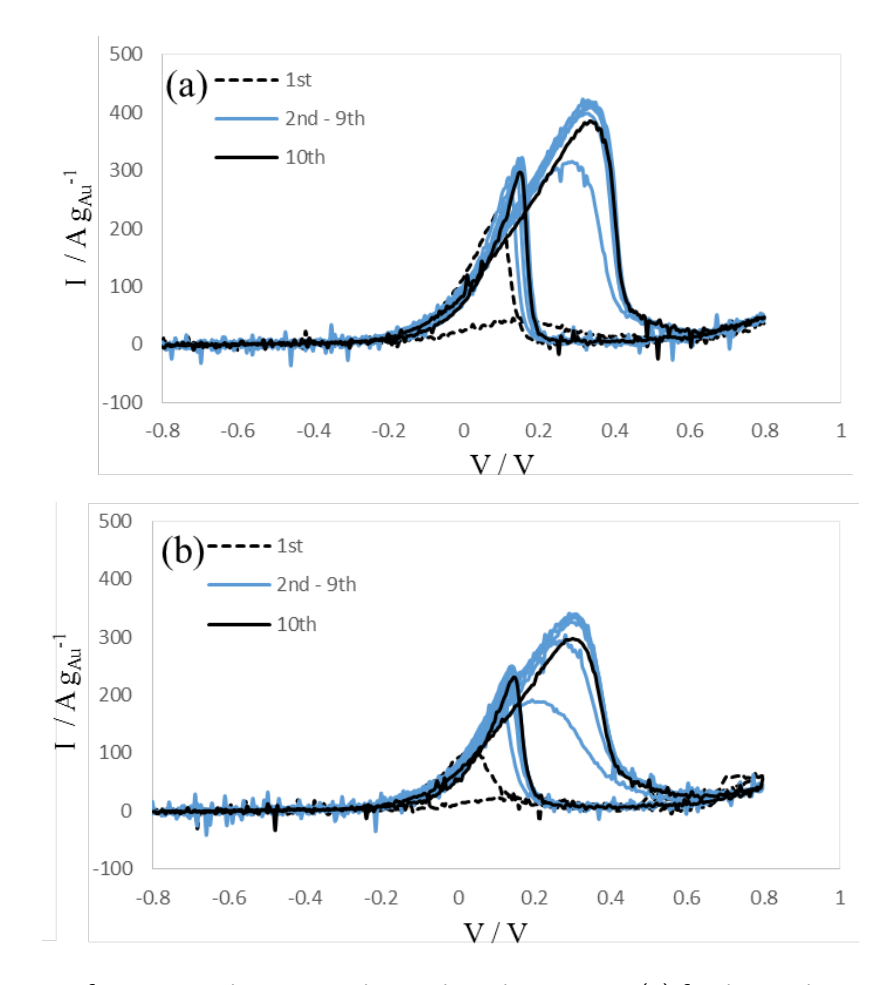


Figure 3.10 CVs of 30%AuAg/C in 1 M glycerol and 2 M KOH (a) fresh catalyst and (b) the same electrode after deactivated in 2 M KOH at a scan rate of 20mV s⁻¹.

The displacement reaction resulted in Au or AuAg alloy phase [27]. AuAg alloy phase was formed at the surface of the particle, yielding the Au rich shell at the beginning of displacement. With the remaining Au³⁺, the displacement reaction continues and the AuAg film expanded as the bulk Ag was sacrificed. Finally, at very high Au content, Ag in AuAg alloy phase was further replaced and yielded an alloy with higher Au content [27]. The large amount of Au at surface or near surface facilitated the process of surface reconstruction to produce an active catalyst. In contrast, this process may not be possible for the case of Ag-rich shell since the interaction between Au and deep underlying Au may not be strong enough. This might be the main difference between catalysts prepared by co-reduction method of AgNO₃ and AuCl₃ and the one fabricated by the galvanic

displacement method. The co-reduction method mainly yields the Ag-rich shell catalyst because of the slow reduction rate of Ag^{+} [15].

The catalysts containing different Au contents show dissimilar behaviors during the activation process. As shown in Fig. 3.11, two distinct activation types were observed as a function of Au content in alloyed catalyst. The current density obtained from the low Au content catalysts, 5% and 10%AuAg/C, was firstly decreased according to the decrease of double layer charging current. Later, the current density was gently increased and become rather steady after about 5 minute. The stable or increase of the current density indicates that the surface activation was continuing in a long time span. For the 20% and 30%AuAg/C, the activation happened in a more acute manner. Owing to a high content of the near surface Au, the current density was immediately raised within few second. After that a generated current was dropped. Unlike the others, the current density obtained from the 30%AuAg/C progressively declined. This indicates a much shorter surface reconstruction required for this catalyst since its Ag content was very low.

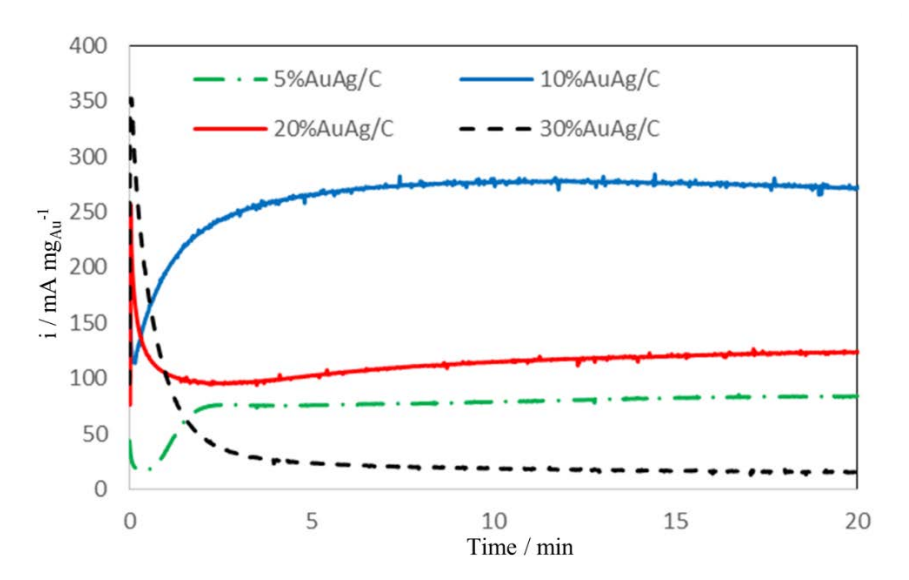


Fig. 3.11 CAs of AuAg/C catalysts in 1 M glycerol and 2 M KOH at 0.25 V after 10 cycle of CV activation in 2 M KOH.

The activity of AuAg/C catalysts also depends on type of the alcohol solutions. Au/C was active for alcohol electrooxidation on most alcohols except methanol.

However, the AuAg/C catalysts were not active for ethanol electrooxidation even in 1 M ethanol electrolyte, as shown in Fig. 3.12. This result was quite astonishing since the AuAg particle of 30%AuAg/C was comprised mainly by Au atoms.

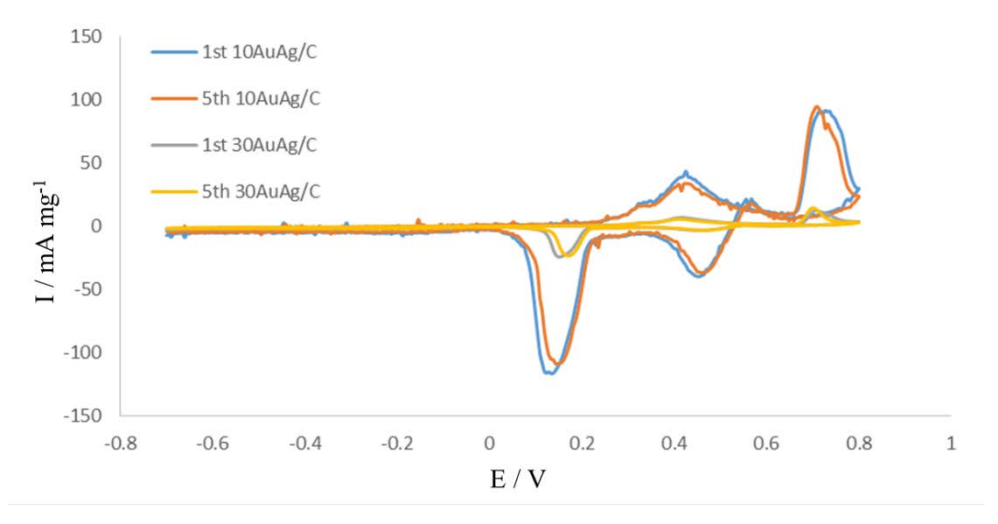


Figure 3.12 CVs of 10%AuAg/C and 30%AuAg/C in 1 M ethanol and 1 M KOH at a scan rate of 20mV s⁻¹.

Fig. 3.13 and 3.14 show the CVs of ethylene glycol electrooxidation on 10%AuAg/C and 30%AuAg/C in 0.1 M and 1 M ethylene glycol electrolyte in comparison with those of Au/C. In 0.1 M electrolyte, 10%AuAg/C was inactive in glycerol electrooxidation in Au region (around -0.1-0.4 V). For 30%AuAg/C, the catalysts was inactive in the first cycle of scan. However, the activity was gradually increased after cycling the potential. The current density at steady state was still much lower than that on the Au/C by at least 10 fold. The main electrooxidation peaks were on Ag_2O surface which occur as the 2 sharp peaks in both forward and reverse scan from about 0.5 V onward.

In 1 M electrolyte, the ethylene glycol electrooxidation activity on both AuAg/C catalysts were clearly observed, as shown in Fig. 3.14. The electrooxidation on Au surface arises in the potential range of -0.2-0.4V. The potential at the maximum current density of AuAg/C was around 0.3 V compared with that at 0.5 V on Au/C, indicate the ease of oxide formation on the AuAg/C catalyst. The current density in this range was very low in the first scan and then increased as the course of scan progress. Despite a much higher

activity at increasing alcohol concentration, the current density was still much lower than that on Au/C. The 30%AuAg/C catalyst was faster activated than 10AuAg/C. The current density in Au region reaches half of the maximum current density in the 2^{nd} loop while that on 10AuAg/C was on the 5^{th} loop.

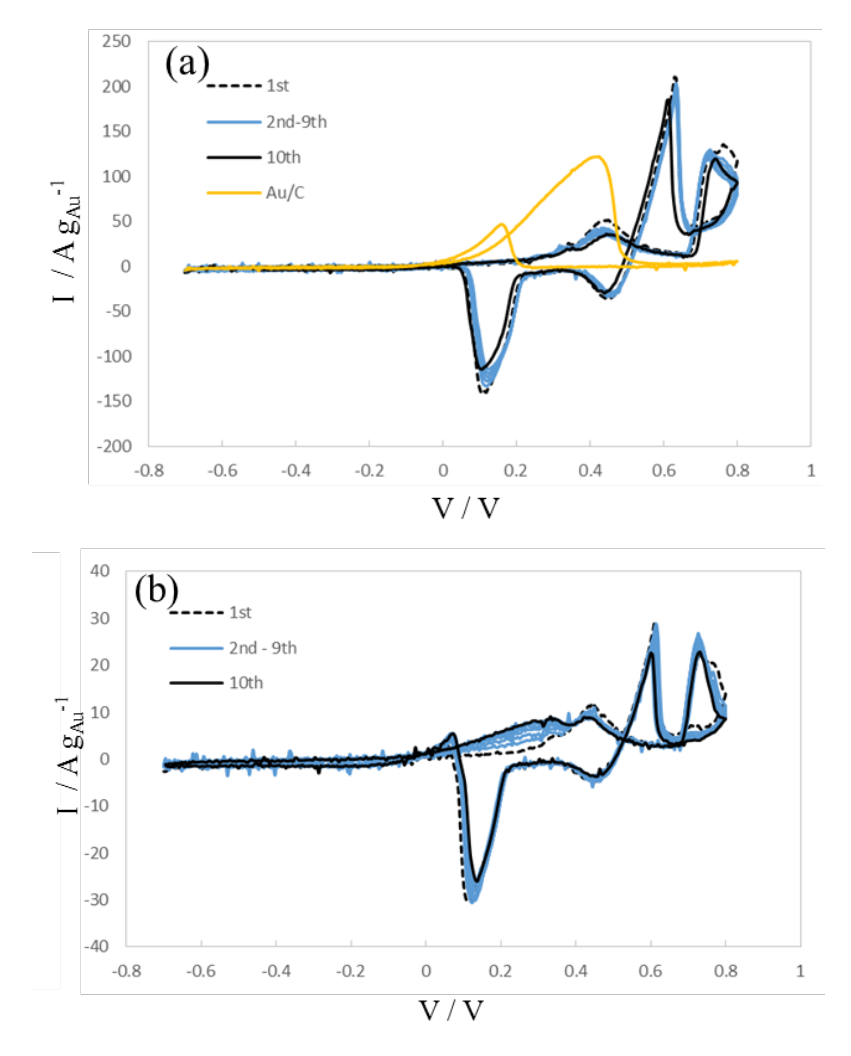


Figure 3.13 CVs of (a) 10%AuAg/C and Au/C, and (b) 30%AuAg/C in 0.1 M ethylene glycol and 0.1 M KOH at a scan rate of 20mV s $^{-1}$.

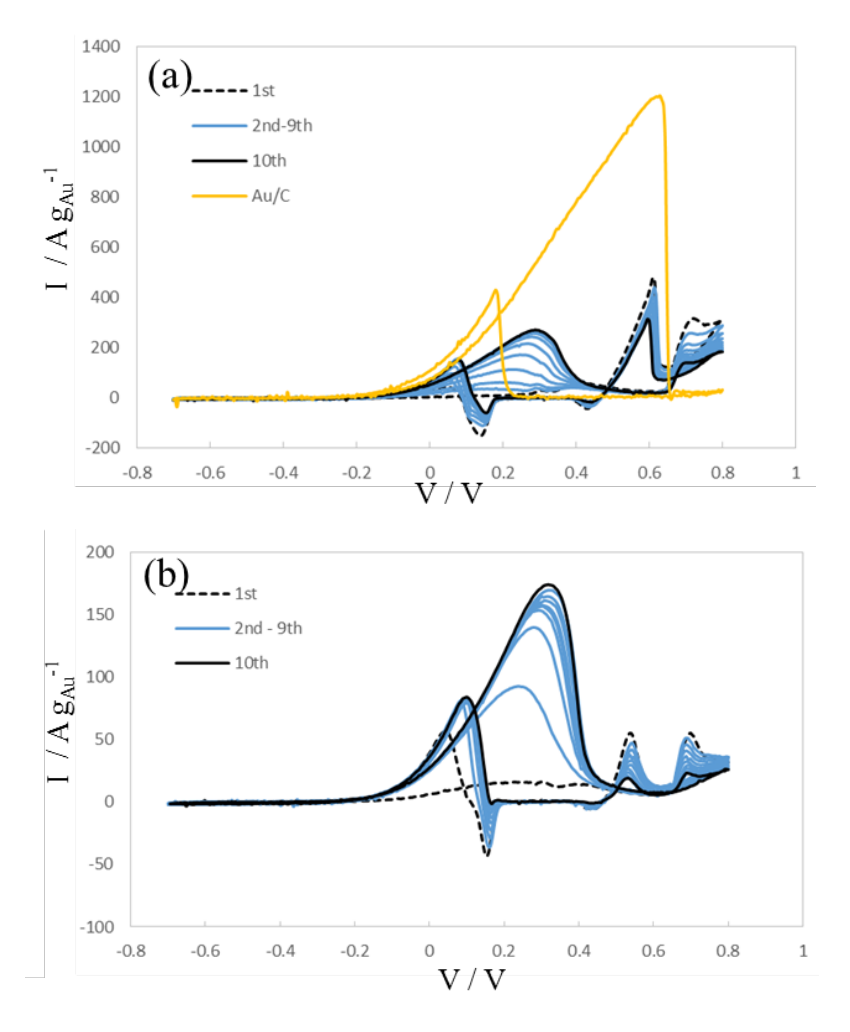


Figure 3.14 CVs of (a) 10%AuAg/C and Au/C, and (b) 30%AuAg/C in 1 M ethylene glycol and 1 M KOH at a scan rate of 20mV s⁻¹.

These results suggested that the surface activation was reversible when the electrolyte was changed. This indicates that the composition of AuAg/C was electrolyte dependent. Ag was the metal with the higher affinity to adsorb the oxygenate species such as hydroxide than Au. However, Ag was inactive toward alcohol electrooxidation in the region of alcohol electrooxidation on Au. As a consequence, Ag atom may be pulled toward the catalyst surface by hydroxide and cover the active Au surface. For Au, however, had better adsorption of alcohol. Since Au was more active for alcohol with high molecular weight, the surface activation which pulls Au atom to the nanoparticle surface progressed better with high molecular weight alcohol such as glycerol. For low molecular weight alcohol such as ethanol and ethylene glycol, however, the AuAg surface

cannot be activated and became inactive. Moreover, the concentration of alcohol and the ratio of Au in nanoparticle also affected the activation process.

3.4 Catalytic activity test

Fig. 3.15 shows the steady and fully activated CVs of AuAg/C in a solution of 0.1 M glycerol and 0.1 M KOH. The glycerol electrooxidation characteristic and activity of the synthesized AuAg/C catalysts depended strongly on the Au:Ag ratio. For the catalysts with low Au:Ag ratios, e.g. 5% and 10% AuAg/C, the promotional roles of Ag such as the negative shifts of both the onset potential and the potential at the maximum current density can be clearly observed. The lower onset potential was caused by the reduction of the 5d band density of Au which altered the adsorption capability of the Au surface [15]. The addition of Ag would also result in a faster self-poisoning by oxide formation. The potential at maximum current density of both 5% and 10%AuAg/C was at around 0.29 V.

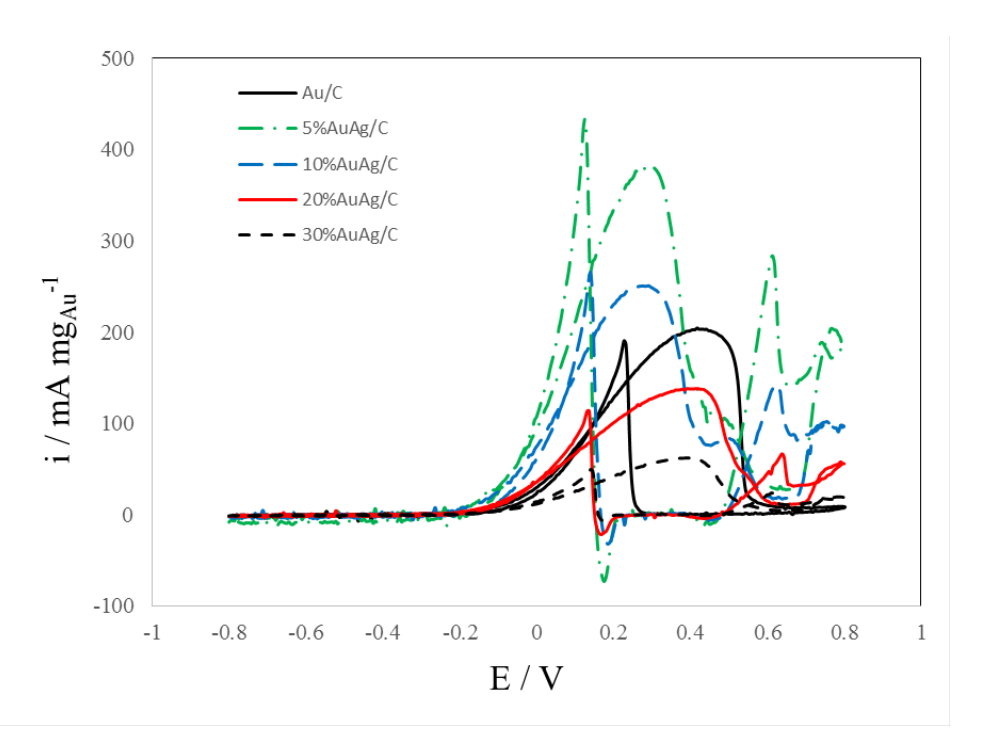


Figure 3.15 Au mass normalized CVs of Au/C and AuAg/C catalysts in 0.1 M Glycerol and 0.1 M KOH at a scan rate of 20 mV s $^{-1}$.

At high Au contents, e.g. 20% and 30%AuAg/C, the promotion effects of Ag were almost vanished. The main glycerol electrooxidation peaks on these two catalysts were similar to that of Au/C. However, the small oxidation peak related to glycerol electrooxidation on Ag surface and the higher stability of oxide reduction were still observed.

Apparently, the peak potential was affected by the Au loading [36, 37]. The drop-off potential was generally increased with increasing Au loading. However, the results shown here did not follow the regular trend. Thus, it was possible that the effects of Ag on the glycerol electrooxidation was more prevailing than the effect of the support [36] or the accumulation of the oxidative species within the catalysts layer [37].

For the electrolyte containing 0.1 M glycerol and 0.1 M KOH, the most active catalyst was the 5%AuAg/C providing mass normalized current density at about 382 mA mg_{Au}⁻¹ which was almost 2-fold higher than that of Au/C at 203 mA mg_{Au}⁻¹. This result contradicted with the Ag-rich shell AuAg/C catalyst prepared by the co-reduction method, which was quite inactive in low glycerol concentration electrolyte [15]. Despite their large particle sizes, both 5% and 10%AuAg/C catalysts benefited by the promotion effect of Ag and the activation of AuAg nanoparticles. The formation of Au-rich shell may compensate for the low surface area of the large particles. For the high Au loading catalysts, however, this promotional effect of Ag was diminished according to the lower content of Ag and the particle size played an important role instead.

Fig. 3.16 depicts the CVs of all the AuAg/C and Au/C catalysts in high concentrations electrolyte, 1 M glycerol and 2 M KOH. The electrooxidation characteristic of Au was obviously dominant in this condition while the reaction on Ag was diminished. The synergistic effect between Au and Ag was still observed under this condition, i.e. the negative onset potential shift for the 5% and 10%AuAg/C catalysts which was the same as in low glycerol and electrolytes concentration. However, no clear trend on the potential at maximum current density can be concluded, although this potential was related to the stability of the surface oxide. The AuAg/C catalyst with faster oxide reduction in the

reverse scan was less deactivated by the oxide formation and tended to oxidize glycerol at higher potentials.

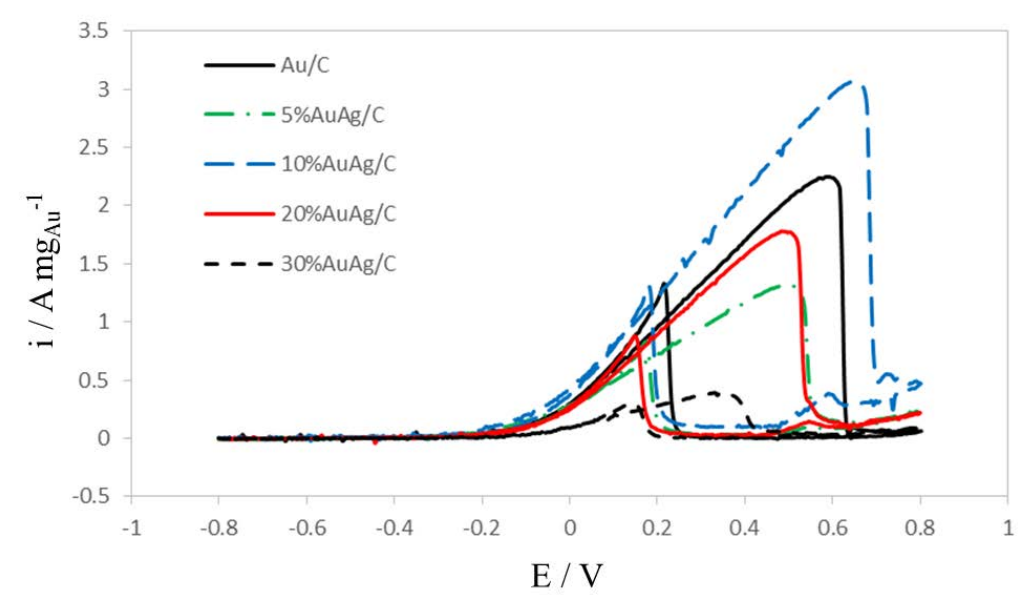


Figure 3.16 Au mass normalized CVs of Au/C and AuAg/C catalysts in 1 M Glycerol and 2 M KOH at a scan rate of 20 mV s $^{-1}$.

From Fig. 3.16, it was found that 10%AuAg/C was the most active catalyst yielding 3.04 A mg_{Au}^{-1} while the Au/C catalyst provided only 2.22 A mg_{Au}^{-1} . The activity of 20% and 30%AuAg/C was still low under this condition according to the reasons given in the prior condition.

3.5 Catalytic stability test

To measure the stability of the AuAg/C catalysts at its fully activated state, the CA experiments were conducted after the catalyst was activated by 10 cycles of CV scan in their respective electrolytes. The resulting CA in low and high glycerol concentration electrolyte are displayed in Fig. 3.17 (a) and 3.17 (b) respectively. After activated by glycerol, the typical CA shape of the AuAg/C was similar to that of the Au/C.

In the low glycerol concentration electrolyte, see Fig. 3.17 (a), most of the AuAg/C catalysts exhibit a slower decay of current density than the Au/C during the initial stage except for the 30%AuAg/C. Unfortunately, the final current density of all the AuAg/C

catalysts was lower than that of the Au/C except the 5%AuAg/C. The final current density at 60^{th} minute of 5%AuAg/C was close to that of Au/C. Moreover, the average current density declined from 20^{th} min to 60^{th} min of 5%AuAg/C and 10%AuAg/C (0.30 and 0.19 mA mg_{Au}⁻¹ min⁻¹) was close or lower than that of Au/C at 0.28 mA mg_{Au}⁻¹ min⁻¹. This indicated that all the AuAg/C catalysts were subjected to the surface deactivation by the other cause rather than the poisoning by the reaction intermediates, which was proposed here as the Ag segregation.

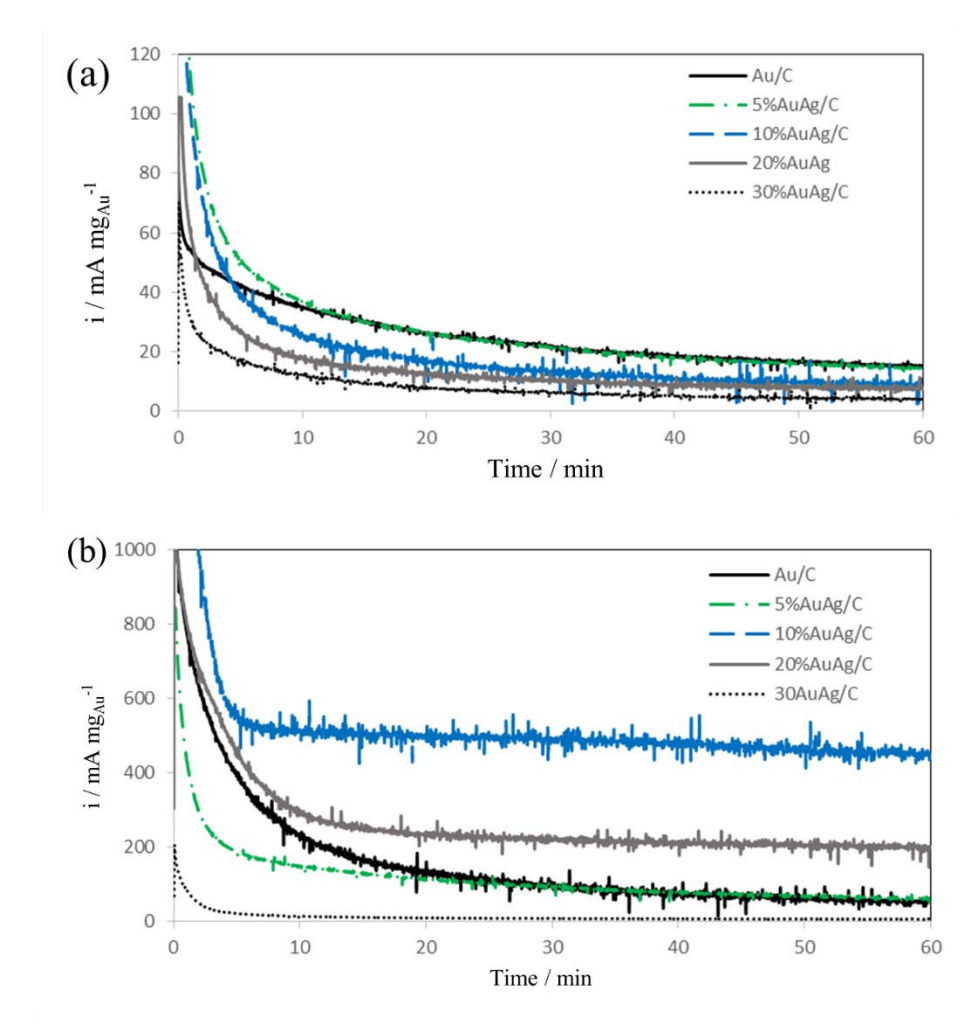


Figure 3.17 CAs of AuAg/C catalysts in (a) 0.1 M glycerol and 0.1 M KOH at 0.25 V after 10 cycles of CV activation in 0.1 M glycerol and 0.1 M KOH and (b) 1 M glycerol and 2 M KOH at 0.25 V after 10 cycles of CV in 1 M glycerol and 2 M KOH.

The use of higher glycerol concentration in electrolyte gave different results. In Fig. 3.17 (b), the current density trend of the CA was similar to that of the CV. The 10%AuAg/C catalyst was the most active catalyst and more stable than Au/C. The average current decay rates of the highly active AuAg/C such as 10%AgAu/C and 20%AuAg/C (1.24 and 0.82 mA mg_{Au}^{-1} min^{-1}) were much lower than that of the Au/C (1.94 mA mg_{Au}^{-1} min^{-1}). Hence, 10%AuAg/C was the best catalyst in this condition.

These results suggested that the activation by using glycerol is an essential step for the AuAg/C catalysts prepared by galvanic displacement method and a certain glycerol concentration was required to maintain catalyst activity and stability during the glycerol electrooxidation reaction since the interaction between glycerol and Au was needed to keep Au on the catalyst surface. The remaining Ag can supply the oxygenate species to the Au atom on surface for the glycerol electrooxidation reaction, thereby improving the stability of the Au catalyst.

3.6 Role of electrodeposited Pd

Fig. 3.18 shows the steady state of glycerol electrooxidation of the AuAg/C and Pd-AuAg/C catalysts prepared via Pd electrodeposition in KCl electrolyte containing 0.01 mM and 1 mM PdNO₃. All the Pd-AuAg/C catalysts require several cycles of reaction to activate from their inactive state, similar to the AuAg/C catalysts. The CV of the Pd electrodeposition process was showed in the insert of Fig. 3.18. The Pd deposition in KCl electrolyte contains only one pair of redox peak associated with AgCl formation and reduction without peak related to the Pd deposition. However, the deposition of Pd was confirmed as the 1Cl-Pd-AuAg/C became a Pd-like surface since the glycerol electrooxidation on Pd took place at more anodic potential than on Au-based catalyst, as shown in Fig. 3.18. The glycerol electrooxidation on Pd surface starts at -0.4 V. After that, the current density sharply increases until reaches the peak potential at around -0.05 V and then declines in a narrow potential range. The following oxidation peak from 0.1 V onward was the glycerol electrooxidation on Au-surface which indicated that Pd was

deposited on the AuAg surface and decrease the glycerol electrooxidation activity in this region.

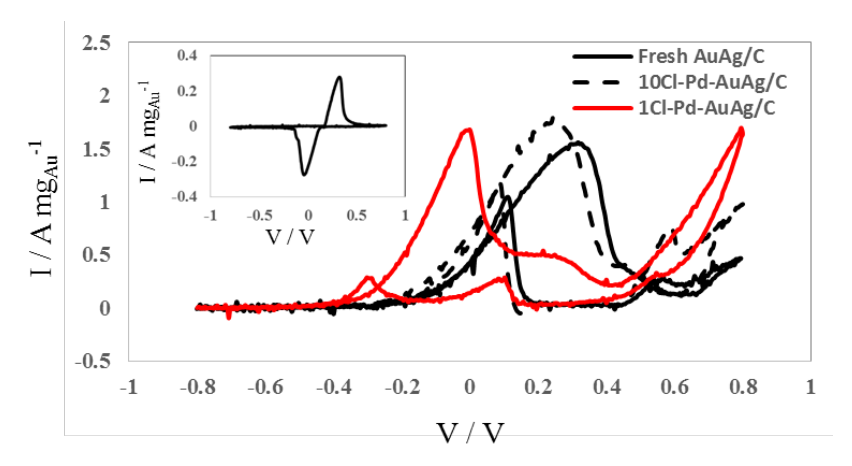


Figure 3.18 CVs of glycerol electrooxidation in 1 M Glycerol and 2 M KOH of fresh AuAg, 1Cl-Pd-AuAg/C, and 10Cl-Pd-AuAg/C at a scan rate of 20 mV s $^{-1}$. Insert: CV of AuAg/C in 0.01 M PdNO₃ and 0.1 M KCl.

The glycerol electrooxidation on AuAg/C begins around -0.3 V where glycerol adsorption on Au occurred. This onset potential was more anodic than that on Au/C due to the promotional effect from Ag [15]. After that, the current density increases until it reaches the maximum current density at around 0.31 V. At this potential, oxide formation on metal surface occurred which prevented further glycerol adsorption. Hence, the current density was lowered and normally diminished on Au-based catalysts as the entire metal surface was covered by the oxide. The two consecutive peaks from 0.45 V onward are corresponding to glycerol electrooxidation on Ag oxide. In the reversed scan, the catalytic activity was regained as a very sharp oxidation peak after the surface metal oxide was reduced at 0.2 V.

For the 10Cl-Pd-AuAg/C, the onset of the glycerol electrooxidation was close to that of the AuAg/C catalyst. However, the potential at maximum current density was shifted to a lower potential. In the reversed scan, the small oxide reduction peak can also be observed at 0.2 V prior to the sharp glycerol electrooxidation peak. These two occurrences indicate that the oxide formation and reduction on this catalyst takes place

at lower potentials than that on AuAg/C catalyst. The maximum current density, as shown in Table 3.3, was higher than that on the AuAg/C catalyst.

Table 3.3 Potential and current density at maximum current density.

Catalyst	Potential (V)	Current density (A mg _{Au} ⁻¹)
AuAg/C	0.31	1.52
1Cl-Pd-AuAg/C	0.00	1.62
10Cl-Pd-AuAg/C	0.26	1.74
1N-Pd-AuAg/C	0.34	1.71
5N-Pd-AuAg/C	0.66	2.83

The change in catalytic activity of this catalyst could be raised from 2 possibilities: the surface modification via the AgCl formation in the electrodeposition process and the deposited Pd. However, the CVs of glycerol electrooxidation on the AuAg/C catalyst preconditioned by using on only KCl electrolyte (without PdNO₃) was similar to that on fresh AuAg/C catalyst. This means that the modification of the catalytic properties might be from the deposited Pd.

The CVs of glycerol electrooxidation on 1N-Pd-AuAg/C and 5N-Pd-AuAg/C are shown in Fig. 3.19. In KNO_3 electrolyte, the main peaks occurred are corresponding to the oxide formation on the Au and Ag surface. The current densities of these peaks were decreased as the number of deposition cycle increased indicating the deposition of Pd on the AuAg surface.

The behavior of glycerol electrooxidation on both 1N-Pd-AuAg/C and 5N-Pd-AuAg/C catalysts were more like Au/C more than that of AuAg/C [6]. The potential at maximum current density and oxide reduction were shifted toward higher potential, as shown in Table 3.3. The potential shift was larger as the number of electrodeposition cycle increased. Moreover, the peak related to Ag was almost disappeared in both catalysts. Despite all these changes, the onset potential was still close to that on the

AuAg/C catalyst. This indicated that the synergistic effect of Ag on Au remained since the promotion effects of Ag was based on the electron transfer between Au and Ag [15].

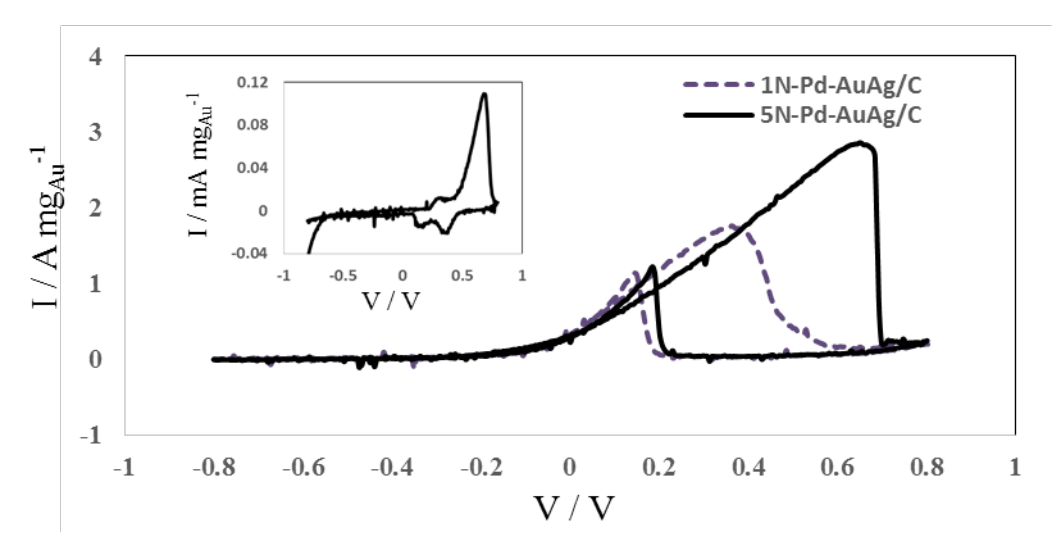


Figure 3.19 CVs of glycerol electrooxidation in 1 M Glycerol and 2 M KOH at a scan rate of 20 mV sec⁻¹ of 1N-Pd-AuAg/C and 5N-Pd-AuAg/C catalysts. Insert: CV of AuAg/C in 0.01 M PdNO₃ and 0.1 M KNO₃.

The maximum current density of both 1N- and 5N-Pd-AuAg/C was increased as the number of electrodeposition cycle increased, as shown in Table 3.3. The glycerol electrooxidation on 5N-Pd-AuAg/C yielded almost 2-fold higher than that on AuAg/C. The higher activity of these two catalysts may be because of the promotional effects of Pd which increased the portion of Au on the electrocatalyst surface via a stable PdAu alloy. Theoretically, the PdAu alloy was formed to lower the overall surface energy of the PdAuAg nanoparticles since PdAu was more stable at the surface than PdAg and the separated Pd-Au form. As a consequence, the surface of AuAg nanoparticles become an Au-rich surface. Thus, the CVs of these catalysts were shift toward Au/C pattern with a high current density while still keeping the synergistic of Ag from the underlying Ag core. However, this finding need further investigation.

The role of supporting electrolyte on the catalytic activity of the electrodeposited Pd-AuAg/C was clearly observed. The properties of Pd-AuAg/C prepared by using KNO_3 as a supporting electrolyte was much different with those using KCl. While KCl was used, the

surface of the metal oxide was changed to a stable and non-electron conduct AgCl. This AgCl-covered surface may make the AuAg surface less active for Pd deposition. Then, only small amount of Pd was deposited on the catalyst surface or Pd may only deposited on the site that was not entirely covered with AgCl, eg. Au-rich area. However, NO_3^- ion cannot form a stable species on AuAg surface. As a consequence, the AuAg surface was more active in KNO_3 than in KCl electrolyte. Larger amount of Pd may possibly deposit on AuAg surface and then make a greater change on the catalytic activity of the catalyst.

CHAPTER 4: CONCLUSIONS

A series of AuAg/C catalysts were prepared by using the galvanic displacement of Ag on carbon with an Au³⁺. The Ag/C used as a sacrifice material prepared by using the citrate reduction methods appeared as a large particle with size around 200 nm. After galvanic displacement with Au³⁺, the morphology of the resulting AuAg nanoparticles depends upon the Au loading. For low displacement degree catalysts e.g. 5%AuAg/C and 10%AuAg/C, large porous structure of AuAg/C or large fragments were observed. At higher Au content, smaller fragment with average size around 15-20 nm were formed. The size of AuAg nanoparticles on all catalysts was much larger that of the Au/C prepared by the PVA protection method. The complete galvanic displacement was confirmed as the ratios of Au:Ag were close to the intended ratio. However, small amount of AgCl was observed from XPS and XRD results. The electronic modification of AuAg alloy was observed which alter the activity of the catalysts.

The catalytic performance of the AuAg/C catalysts greatly depends on type and concentration of alcohol. All the as-prepared AuAg/C catalysts require reaction with alcohol to change into their active form via the adsorbate induce surface segregation. By the reaction with alcohol, Au atoms, which has a higher affinity toward alcohol than Ag, were pulled toward AuAg surface. This process was confirmed by the higher concentration of Au atoms at the AuAg nanoparticle surface after reaction with glycerol molecule.

This surface activation process require a strong interaction between Au and alcohol molecule. Au shows a stronger interaction with the alcohol with higher molecular weight. Hence, AuAg only active for large molecule such as glycerol and ethylene glycol (at high concentration) but not active for ethanol electrooxidation even though Au/C was active for all mentioned alcohols.

In their active form, the promotion effects from Ag such as the anodic shift of onset potential and potential at maximum current density were observed. The oxide

formation on AuAg/C also occurred at a lower potential than the Au/C because Ag induce hydroxide species to adsorb on the metal surface. The AuAg/C catalysts were more active than the Au/C at low Au loading. 5%AuAg/C and 10%AuAg/C were the most active catalyst in the electrolyte of 0.1 M glycerol and 1 M glycerol, respectively.

The stability of the AuAg/C catalyst was also depends on the electrolyte, the high interaction between Au and glycerol was essential to keep the Au atoms at the catalyst surface. As a result, all of the AuAg/C catalysts show a lower stability than Au/C in 0.1 M glycerol electrolyte, while 10%AuAg/C was much more stable than Au/C in 1 M glycerol electrolyte. The high glycerol concentration was demanded to keep the Au atoms on the catalyst surface to maintain the catalytic activity. The reaction was promoted by the small amount of Ag on the surface to induce the hydroxide species to adsorb on the metal surface for glycerol electrooxidation, and thus promote the stability of the catalyst.

The activity of 10%AuAg/C can be further improved by the deposition of Pd on its surface. All of the Pd-electrodeposited AuAg/C catalysts were more active than 10%AuAg/C. For the Pd-AuAg/C prepared in KNO₃ electrolyte, the activity was improved as the number of Pd electrodeposition cycle increase. However, the potential at maximum current density was shift to more positive potential and the CVs of glycerol electrooxidation was more resemble that on Au/C. This results suggested that that the role of Pd in this case was to increase the surface Au portion via the stable PdAu alloy on the catalyst surface. However, this proposed role need further investigation.

LIST OF REFFERENCES

- [1] Kwon, Y.; Lai, S.C.S.; Rodriguez, P.; Koper, M.T.M. (2011), Electrocatalytic oxidation of alcohols on gold in alkaline media: base or gold catalysis?, J. Am. Chem. Soc., 133, pp. 6914-6917.
- [2] Zhang, J.H.; Liang, Y.J.; Li, N.; Li, Z.Y.; Xu, C.W.; Jiang, S.P. (2012), A remarkable activity of glycerol electrooxidation on gold in alkaline medium, Electrochim. Acta, 59, pp. 156-159.
- [3] Xin, L.; Zhange, Z.; Wang, Z.; Li, W. (2012), Simultaneous generation of mesoxalic acid and electricity from glycerol on a gold anode catalyst in anion-exchange membrane fuel cells, ChemCatChem, 4, pp. 1105-1114.
- [4] Qi, J.; Xin, L.; Chadderdon, D.J.; Qiu, Y.; Jiang, Y.; Benipal, N.; Liang, C.; Li, W. (2014), Electrocatalytic selective oxidation of glycerol to tartronate on Au/C anode catalysts in anion exchange membrane fuel cells with electricity cogeneration, Appl. Catal. B, 154-155, pp. 360-368.
- [5] Padayachee, D.; Golovko, V.; Ingham, B.; Marshall, A.T. (2014), Influence of particle size on the electrocatalytic oxidation of glycerol over carbon-supported gold nanoparticles, Electrochim. Acta, 120, pp. 398-407.
- [6] Yongprapat, S.; Therdthianwong, A.; Therdthianwong, S. (2012), Au/C catalyst prepared by polyvinyl alcohol protection method for direct alcohol alkaline exchange membrane fuel cell application, J. Appl. Electrochem., 42, pp. 483-490.
- [7] Yongprapat, S.; Therdthianwong, S.; Therdthianwong, A. (2012), RuO₂ promoted Au/C catalysts for alkaline direct alcohol fuel cells, Electrochim. Acta, 83, pp. 87-93.
- [8] Yongprapat, S.; Therdthianwong, A.; Therdthianwong, S. (2013), Au/C catalysts promoted with metal oxides for ethylene glycol electro-oxidation in alkaline solution, J. Electroanal., Chem., 697, pp. 46-52.
- [9] Merle, G.; Wessling, M.; Nijmeijer, K. (2011), Anion exchange membranes for alkaline fuel cells: A review, J. Membr. Sci., 377, pp. 1-35.

- [10] Hickner, M.A.; Herring, A.M.; Coughlin, E.B. (2013), Anion exchange membranes: Current status and moving forward, J. Polym. Sci., 51, pp. 1727-1735.
- [11] Lima, F.H.B.; Calegaro, M.L.; Ticianelli, E.A. (2006), Investigations of the catalytic properties of manganese oxides for the oxygen reduction reaction in alkaline media, J. Electroanal. Chem., 590, pp. 152-160.
- [12] Guo, J.; Hsu, A.; Chu, D.; Chen, R. (2010), Improving oxygen reduction activities on carbon-supported Ag nanoparticles in alkaline solutions, J. Phys. Chem. C, 114, pp. 4324-4330.
- [13] Cheng, Y.; Li, W.; Fan, X.; Liu, J.; Xu, W.; Yan, C. (2013), Modified multi-walled carbon nanotube/Ag nanoparticle composite catalyst for the oxygen reduction reaction in alkaline solution, Electrochim. Acta, 111, pp. 635-641.
- [14] Ciriminna, R.; Pina, C.D.; Rossi, M.; Pagliaro, M. (2014), Understanding the glycerol market, Eur. J. Lipid Sci. Technol., 116, DOI: 10.1002/ejlt.201400229
- [15] Garcia, A.G.; Lopes, P.P.; Gomes, J.H.; Pires, C.; Ferreira, E.B.; Lucena, R.G.M.; Gasparotto, L.H.S.; Tremiliosi-Filho, G. (2014), Eco-friendly synthesis of bimetallic AuAg nanoparticles, New J. Chem., 38, pp. 2865-2873.
- [16] Yongprapat, S.; Therdthianwong, S.; Therdthianwong, A. (2013) AuAg/C catalysts preparation for glucose electrooxidation in alkaline media, The 39th congress on Science and Technology of Thailand (STT 39), Bangkok, Thailand.
- [17] Liu, Z.; Huang, L.; Zhang, L.; Ma, H.; Ding, Y. (2009), Electrocatalytic oxidation of D-glucose at nanoporous Au and Au-Ag Alloy electrodes in alkaline aqueous solutions, Electrochimica Acta, 54, pp. 7286-7293
- [18] Toninaga, M.; Shimazoe, T.; Nagashima, M.; Kusuda, H.; Kubo, A.; Kuwahara, Y.; Taniguchi, I. (2006), Electrocatalytic oxidation of glucose at gold-silver alloy, silver and gold nanoparticles in an alkaline solution, Journal of Electroanalytical Chemistry, 590, pp. 37-46
- [19] Aoun, S.M.; Bang, G.S.; Koya, T.; Nonaka, Y.; Sotomura, T.; Taniguchi, I. (2003) Electrocatalytic oxidation of sugars on silver-UPD single crystal gold electrodes in alkaline solutions, Electrochemistry communications, 5, pp. 317-320

- [20] Cuevas-Muniz, F.M.; Guerra-Balcazar, M.; Castaneda, F.; Ledesma-Garcia, J.; Arriaga, L.G. (2011), Performance of Au and AuAg nanoparticles supported on Vulcan in a glucose laminar membraneless micro fuel cell, Journal of Power Sources, 14, pp. 5853-5857.
- [21] Aoun, S.B.; Dursun, Z.; Koga, T.; Bang, G.S.; Sotomura, T.; Taniguchi, I. (2004) Effect of metal ad-layers on Au (1 1 1) electrodes on electrocatalytic oxidation of glucose in an alkaline solution, Journal of Electroanalytical Chemistry, 567, pp. 175-183
- [22] Uppal, M.A.; Ewing, M.B.; Parkin, I.V. (2011) One-pot synthesis of core-shell silver-gold nanoparticle solutions and their interaction with methylene blue dye, Eur. J. Inorg. Chem., 29, pp. 4534-4544.
- [23] Betowska-brzezinska, M.; Uczak, T.; Holze, R. (1997), Electrocatalytic oxidation of mono- and polyhydric alcohols on gold and platinum, J. App. Electrochem., 27, pp. 999-1011.
- [24] Change, S.; Ho, Y.; Weaver, M.J. (1991), Applications of real-time FTIR spectroscopy to the elucidation of complex electroorganic pathways: electrooxidation of ethylene glycol on gold, platinum and nickel in alkaline solution, J. Am. Chem. Soc., 113, pp. 9506-9513.
- [25] Gomes, J.F., Garcia, A.C., Gasparotto, L.H.S., de Souza, N.E., Ferreira, E.B., Pires, C. (2014), Influence of silver on the glycerol electro-oxidation over AuAg/C catalysts in alkaline medium: a cyclic voltammetry and in situ FTIR spectroscopy study, Electrochim Acta, 144, pp. 361–368.
- [26] Padayachee, D.; Golovko, V.; Marshall, A.T. (2013), The effect of MnO₂ loading on the glycerol electrooxidation activity of Au/MnO₂/C catalysts, Electrochim. Acta, 98, pp. 208-217.
- [27] Sun, Y.; Xia, Y. (2004), Mechanistic study on the replacement reaction between silver nanostructures and chloroauric acid in aqueous medium, J. Am. Chem. Soc., 126, pp. 3892-3901.
- [28] Lee, K.J.; Lee, Y.I.; Lee, J.; Myung, N.V.; Cjoa, Y.H. (2012), Structural evolution of Ag-Au nanoplates by pH controlled galvanic displacement, Curr. Appl. Phys., 12, pp. 553-558.
- [29] Obliosca, J.M.; Wu, Y.S.; Hsieh, H.Y.; Chang, C.J.; Wang, P.C.; Tseng, F.G. (2012), Synthesis and optical properties of gold/silver nanocomposites prepared on multi-

- walled carbon nanotubes via galvanic replacement of silver nanoparticles, J. Nanopart. Res., 14, pp. 834
- [30] Zhange, Y.; Yang, P.; Zhang, L. (2013) Size- and shape-tunable silver nanoparticles created through facile aqueous synthesis, J. Nanopart. Res., 15, pp. 1329.
- [31] Mayer, S.T., Muller, R.H. (1988), Nucleation of silver (I) oxide investigated by spectroscopic ellipsometry, J. Electrochem. Soc., 135(9), pp. 2133–2142.
- [32] Hecht, D., Frahm, R., Strehblow, H.H. (1996), Quick-scanning EXAFS in the reflection mode as a probe for structural information of electrode surfaces with time resolution: an in situ study of anodic silver oxide. J. Phys. Chem., 100 pp. 10831–10833.
- [33] Avramov-Ivić, M., Jovanović, V., Vlajnić, G., Popić, J. (1997), The electrocatalytic properties of the oxides of noble metals in the electro-oxidation of some organic molecules. J. Electroanal. Chem. 423, pp. 119–124.
- [34] Yang, C., Huang, B., Xiao, L., Ren, Z., Liu, Z., Lu, J. (2013), Activating Ag by even more inert Au: a pericular effect on electrocatalysis toward oxygen reduction in alkaline media. Chem. Commun., 49, pp. 11023–11025.
- [35] Liao, H., Fisher, A., Xu, Z.J. (2015), surface segregation in bimetallic nanoparticles: a critical issue in electrocatalyst engineering. Small, 11 (27) pp. 3221.
- [36] Gomes, J.F., Gasparotto, L.M.S., Tremiliosi-Filho, G. (2013), Glycerol Electro-oxidation over glassy-carbon-supported Au nanoparticles: direct influence of the carbon support on the electrode catalytic activity. Phys. Chem. Chem. Phys., 15, pp. 10339–10349.
- [37] Marshall, A.T., Golovko, V., Padayachee, D. (2015), Influence of gold nanoparticle loading in Au/C on the activity towards electrocatalytic glycerol oxidation. Electrochim. Acta, 153, pp. 370–378.

RESEACRH OUTPUT

1. ผลงานตีพิมพ์ในวารสารวิชาการระดับนานาชาติ

1.1 Yongprapat, S*.; Therdthianwong, A.; Therdthianwong, S. (2018) Improvement of catalytic performance of AuAg/C catalysts prepared by galvanic displacement technique for glycerol electrooxidation in alkaline medium, *J. Appl. Electrochem.*, **48** (3) pp. 317-328.

2. ผลงานการเสนอผลงานในที่ประชุมระดับนานาชาติ

- 2.1 Yongprapat, S.*; Therdthianwong, A.; Therdthianwong, S., The activity of AuAg/C prepared by galvanic displacement of Ag on carbon by Au³⁺ towards alcohol electrooxidation, SEE 2016 in conjunction with ICGSI 2016 and CTI 2016 On "energy & climate change: innovating for a sustainable future. November 28-30, 2016, Bangkok, Thailand.
- 2.2 **Yongprapat, S.***; Therdthianwong, A.; Therdthianwong, S., Roles of electrodeposited Pd on glycerol electrooxidation activity of AuAg/C catalyst, The 7th international TIChE conference (ITIChE 2017). October 18-20, 2017, Bangkok, Thailand.

RESEARCH ARTICLE



Improvement of catalytic performance of AuAg/C catalysts prepared by galvanic displacement technique for glycerol electrooxidation in alkaline medium

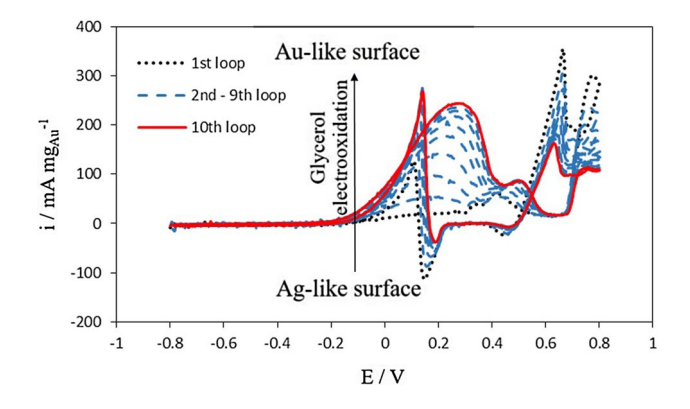
S. Yongprapat 10 · A. Therdthianwong 1 · S. Therdthianwong 2

Received: 27 September 2017 / Accepted: 27 January 2018 / Published online: 8 February 2018 © Springer Science+Business Media B.V., part of Springer Nature 2018

Abstract

The activity and stability of AuAg/C electrocatalysts prepared by a galvanic displacement between Au³⁺ and Ag on carbon were investigated. First, Ag/C was prepared by citrate reduction in alkaline and used as the displaced material. The addition of Au³⁺ into the Ag/C resulted in smaller fragments of AuAg nanoparticles. These AuAg/C catalysts were prepared at four Au loadings ranging from 5 to 30%wt Au. Upon interaction with glycerol, the catalyst surface became an Au-rich surface, thereby activating the catalysts. The promotion effects of Ag, such as negative shifts of both an onset potential and a potential at maximum current density, were observed on the catalysts with low Au content but not on those with high Au content. The AuAg/C catalysts with low Au content were more active than the Au/C one despite the very much larger size of the metal particles on the AuAg/C catalysts. The most active catalysts were 5%AuAg/C and 10%AuAg/C, providing much higher mass normalized current densities in electrolytes containing 0.1 and 1 M glycerol, respectively. The final current density of 10%AuAg/C after 60 min in 1 M glycerol electrolyte was 445 mA mg_{Au}⁻¹, which was about 9 times higher than that of Au/C. A synergistic effect between Au and Ag improved the stability of the AuAg/C catalysts.

Graphical Abstract



Keywords AuAg/C catalyst · Glycerol electrooxidation · Galvanic displacement · Bimetallic · Alkaline fuel cell

Extended author information available on the last page of the article

1 Introduction

An alkaline anion exchange membrane fuel cell (AAEMFC) fed with alcohols has received much interest in recent years due to its several advantages. This low-temperature fuel cell is fed by liquid fuel and is capable of being utilized as an alternative power source for mobile and portable devices.



S. Yongprapat sarayut.yon@kmutt.ac.th

A number of alcohols, such as ethanol, ethylene glycol, glycerol, and xylitol, can be fed directly to the anode [1–6]. Among these fuels, glycerol has been wildly studied, since it is a non-toxic, non-flammable, low volatile, and low-cost fuel that is suitable for large-scale usage. Glycerol can be produced in large volumes as a byproduct of the trans-esterification of vegetable oils. The current production rate of glycerol exceeds its demand, so a new approach to utilizing glycerol is necessary [7].

The potential of using Au as an anode catalyst for direct glycerol fuel cells has been demonstrated by many studies [1–3, 8–13]. Au shows a remarkably higher activity in glycerol electrooxidation than do other noble metals, such as Pt and Pd [1–3]. Moreover, in studies of half cells, Au has exhibited better stability than a Pt-based catalyst [3]. However, the electrooxidation potential onset of glycerol on Au occurs at a considerably high potential, because the oxygenated species is required to form on the surface [1, 2].

The electrocatalytic properties of Au in alcohol electrooxidation are improved by several promoters, such as Ce_2O_3 [8], RuO_2 [9], MnO_2 [10], and Ag [11]. The addition of these metal oxides affects the activity slightly [8, 9, 11] and improves the stability of Au catalysts. However, these metal oxides do not promote the adsorption of alcohol on the Au surfaces, since their onset potentials are about the same as that of the catalysts without the metal oxides.

The onset potential or mass-specific current density of glycerol [11–13] or glucose [14–18] electrooxidation on the Au catalyst can be improved by the addition of Ag. For glucose [14–17], Au catalysts decorated by Ag generate a higher maximum current density and have a lower onset potential than do undecorated ones, possibly due to Ag's lowering of the formation potential of Au-OH.

A series of AuAg/C catalysts prepared by the co-reduction of AuCl₃ and AgNO₃ with glycerol as a reducing agent was tested for glycerol electrooxidation in an alkaline solution [11–13]. In these studies, the active surface area of Au on AuAg/C was low because of the segregation of the Ag film on the catalyst's surface. The reduction of the Au³⁺ species proceeded much faster than that of Ag⁺, yielding an Au-rich core with an Ag-rich shell. Therefore, the glycerol electrooxidation activity on AuAg/C was much lower than that on Au/C. However, the onset potential of glycerol electrooxidation on AuAg/C was lower than that on Au/C, indicating that the electronic properties of Au had been modified by Ag with the magnification of the adsorption strength of the adsorbates on the Au surface [11]. Moreover, the presence of Ag promoted C-C bond cleavage and yielded more electrons [13].

Glycerol electrooxidation on an AuAg catalyst consists of several pathways and yields a variety of products ranging from 3-C to 1-C-atom products. The very first electrooxidation step involves a reaction with the C-O bond to yield the

3-C-atom products, such as dihydroxyacetone, glyceraldehyde, and glyceric acid. The C–C bond cleavage takes place when the glyceric acid is further oxidized to yield glycolic and oxalic acids (2-C-atom products) along with formic acid (1-C-atom product) [13].

The synthesis of the AuAg nanoparticles with a specific controlled composition was quite difficult because of the uncontrollable precipitation of Ag⁺ in the presence of Cl⁻ contained in the Au precursor (HAuCl₄). Ag was inactive for alcohol electrooxidation at the normal operating potential of direct alcohol fuel cells [11]. Hence, too much Ag covering the Au surface can diminish the catalytic activity of the AuAg-based catalyst. Both Au and Ag have the same face-centered cubic (fcc) structure with very similar lattice parameters. As a result, Au and Ag can form indistinct alloy phases over the entire composition range. With the absence of a lattice mismatch between Au and Ag, the crystals can easily grow on top of each other to form a core-shell structure. Therefore, the aim of this research was to prepare highly active Ag_core-Au_shell/C-type or Au-rich shell-type catalysts via the galvanic displacement of Au³⁺ on the prefabricated Ag/C. The catalytic activity of the synthesized AuAg/C catalysts toward glycerol electrooxidation was measured.

Galvanic displacement is an electrochemical process that involves the dissolution of less noble metals from a solid electrode into the solution followed by the deposition of more noble metals onto the solid electrode. Electrons produced from the former reaction are used by the latter reaction, which is a reduction reaction. For AuAg, AuCl₄⁻/Au has a standard reduction potential of 0.99 V, which is higher than that of Ag/Ag⁺ at 0.80 V, implying that AuCl₄⁻ can be reduced in the presence of metallic Ag. The reaction system, which is composed of AuCl₄⁻ and Ag, yields the deposited Au and the dissolved Ag⁺, as described by the following reaction:

$$3Ag_{(s)} + AuCl_{4(aq)}^{-} \rightarrow 3Ag_{(aq)}^{+} + Au_{(s)} + 4Cl_{(aq)}^{-}$$
 (1)

Three moles of Ag were consumed for every mole of Au deposited, causing the shrinkage or formation of pores inside the metal particles [19–21].

The first step of the displacement reaction is the dissolution of Ag, which creates holes on the Ag particles [19, 20]. The dissolution reaction is indicated at certain active sites for a further dissolution reaction rather than the reaction's occurrence over the entire surface. Simultaneously, the Au ions deposit onto the Au surface and form a very thin Au film in the AuAg alloy phase.

In this work, a highly active AuAg alloy catalyst supported on carbon was synthesized by the galvanic displacement of Ag with Au. The Ag/C catalyst was first prepared by using the citrate reduction method in an alkaline solution.



After that, Au was deposited onto Ag by the galvanic displacement method to form AuAg/C at various Au loadings. The electrocatalytic activities and stability of the synthesized catalysts toward glycerol electrooxidation were studied by cyclic voltammetry and chronoamperometry, respectively. The effects of the %Au ratio and electrolyte concentration on the catalyst's performance and stability were investigated. A conceptual diagram of Ag/C before and AuAg/C after galvanic displacement is shown in Fig. 1. An Au/C catalyst prepared by the polyvinyl alcohol protection method (PVA method) [3] was used for comparison.

2 Experimental procedure

2.1 Electrocatalyst preparation

To prepare an AuAg/C catalyst by the galvanic displacement method, Ag nanoparticles were first deposited onto a carbon support to obtain Ag/C, which was then used as a sacrificial substrate for depositing Au to synthesize AuAg/C. 60 wt% Ag/C was prepared by the citrate reduction method while AgNO₃ and tripotassium citrate were dissolved in de-ionized water at concentrations of 200 μg cm⁻³ and 0.1 M, respectively. A Vulcan XC-72 was added to the above solution, which was mixed by using a magnetic stirrer for at least 30 min. After that, 2 M KOH solution was added to the mixture to initiate the reduction reaction, quickly turning the solution's color olive green, which indicated the formation of Ag nanoparticles. The mixture was stirred for another 30 min to immobilize the Ag sol on the carbon support. Finally, the catalyst was filtered, washed with de-ionized water and ethanol, and then dried in a vacuum oven at 70 °C.

The AuAg/C catalysts at different Au loadings were prepared by dispersing the 60%Ag/C from the previous step in de-ionized water for 30 min. Then, the calculated amount of HAuCl₄ was added to the mixture under vigorous stirring to obtain an Au³⁺ solution at a concentration of 0.1 mg cm⁻³. Simultaneously, the white precipitate of AgCl of

the displacement reaction was observed. After stirring for 30 min, the suspended catalyst was filtered, then washed with an adequate amount of NaCl solution to dissolve and remove AgCl from the solid residue followed by de-ionized water and alcohol. Then, the residue was dried in a vacuum oven at 70 °C. The samples on the Ag/C catalysts were designated as 5AuAg/C, 10AuAg/C, 20AuAg/C, and 30AuAg/C for 5, 10, 20, and 30 wt% Au, respectively.

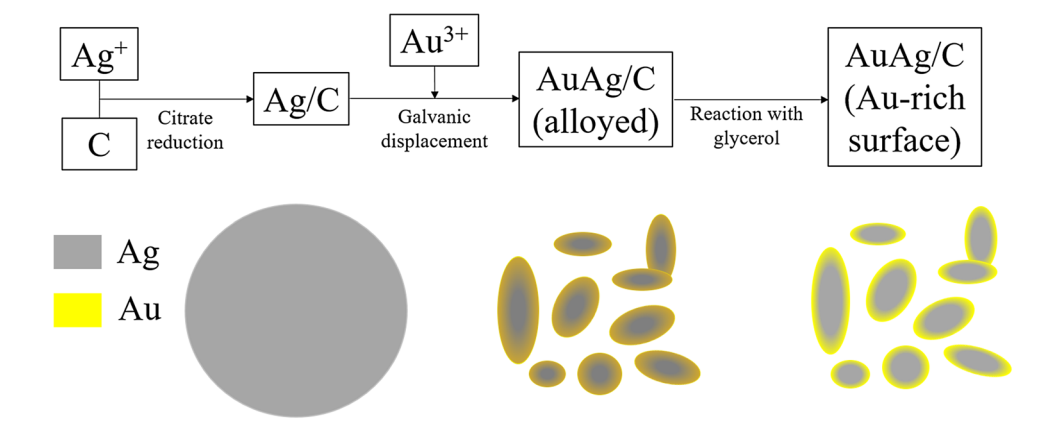
20 wt% Au/C prepared by the PVA protection method [3] with a slight modification was used as a reference catalyst in the activity and stability tests. In brief, the $\mathrm{Au^{3+}}$ precursor at a metal concentration of $200~\mu\mathrm{g}~\mathrm{cm}^{-3}$ in the presence of PVA was reduced by using $0.1~\mathrm{M}~\mathrm{NaBH_4}$ solution. The dropwise adding of this solution under vigorous stirring yielded a ruby red Au sol, which was immobilized on the Vulcan XC-72. Finally, the suspended catalyst was filtered, washed, and dried.

2.2 Catalyst characterization

The Transmission Electron Microscopy (TEM) images and electron diffraction rings were taken by a JOEL JEM 2010 at a voltage of 200 kV. The rough average size of the catalyst was calculated from approximately 100 particles. The structure and composition of the as-prepared catalysts were characterized by an X-ray diffractometer (XRD) Bruker AXS: D8DISCOVER with Goebel mirror Cu K α radiation (λ = 0.1540 nm) using 40 mA filament current and 40 kV tube voltage. Using an AXIS Ultra DLD (Kratos Analytical) with Al K-alpha monochromatic X-ray radiation (1486.68 eV) at 150 W, X-ray photoelectron spectroscopy (XPS) was used to observe the electronic states of Au and Ag.

Energy dispersive spectroscopy (EDX) equipped with scanning electron microscopy (SEM) was used to estimate the Au loading and Au:Ag ratio. The sample was prepared by dispersing a small amount of the catalyst onto a copper tape. In addition, the samples of the catalysts activated by KOH and glycerol were also tested for comparison. These

Fig. 1 A proposed conceptual diagram of the Ag and AuAg/C catalysts during the preparation step and after reaction with glycerol. (Color figure online)





samples were prepared by wiping the dry-well washed catalyst on the electrode onto the carbon tape. The EDX mapping and component analysis were performed at a working distance of 8.5 μm with an aperture of 30 μm . The overall composition was analyzed at 200 kV while the surface composition was detected using a lower potential at 10 kV. The average element composition was calculated from three points of the collected data.

All the electrochemical measurements were conducted by using the Bipotentiostat AFCBP1 (Pine Research Instruments). The working electrode with a catalyst loading of 50 µg cm⁻² was formed by the drop casting of the well-mixed catalyst ink containing the catalyst, Nafion solution, and isopropanol onto the glassy carbon electrode. A mercury/mercury oxide (1 M NaOH MMO) electrode (BAS Inc.) was used as a reference electrode. All the potentials reported in this work were taken versus the MMO. A 1-cm² Au gauze (Alfa Aesar) was employed as a counter-electrode. A large volume of the electrolyte was used to keep the glycerol utilization low.

3 Results and discussion

3.1 Physicochemical characterization

Figure 2a shows a TEM image of the Ag/C that was used as the material sacrificed to prepare the AuAg/C catalysts. The Ag particles appeared as many large agglomerates in various shapes. Most of these particles have diameters in the range of 130–275 nm with an average particle size of about 200 nm. Some small particles with diameters lower than 50 nm were also observed.

By the displacement with Au³⁺, Ag was oxidized into the solution. As a result, large numbers of smaller fragments were produced according to the amount of added Au, as illustrated in Fig. 2b–e. For the 5 and 10 wt%AuAg/C catalysts, parts of the fragments were still attached together as a large nano-network along with the smaller separated particles. These two shapes of the metal particles may be formed by the same mechanism but with different displacement degrees. For the 20 and 30%AuAg/C catalysts, as shown in Fig. 2d–e, a higher amount of Ag was replaced and the cluster of particles was torn apart, yielding many small fragments of AuAg nanoparticles, of which the average particle

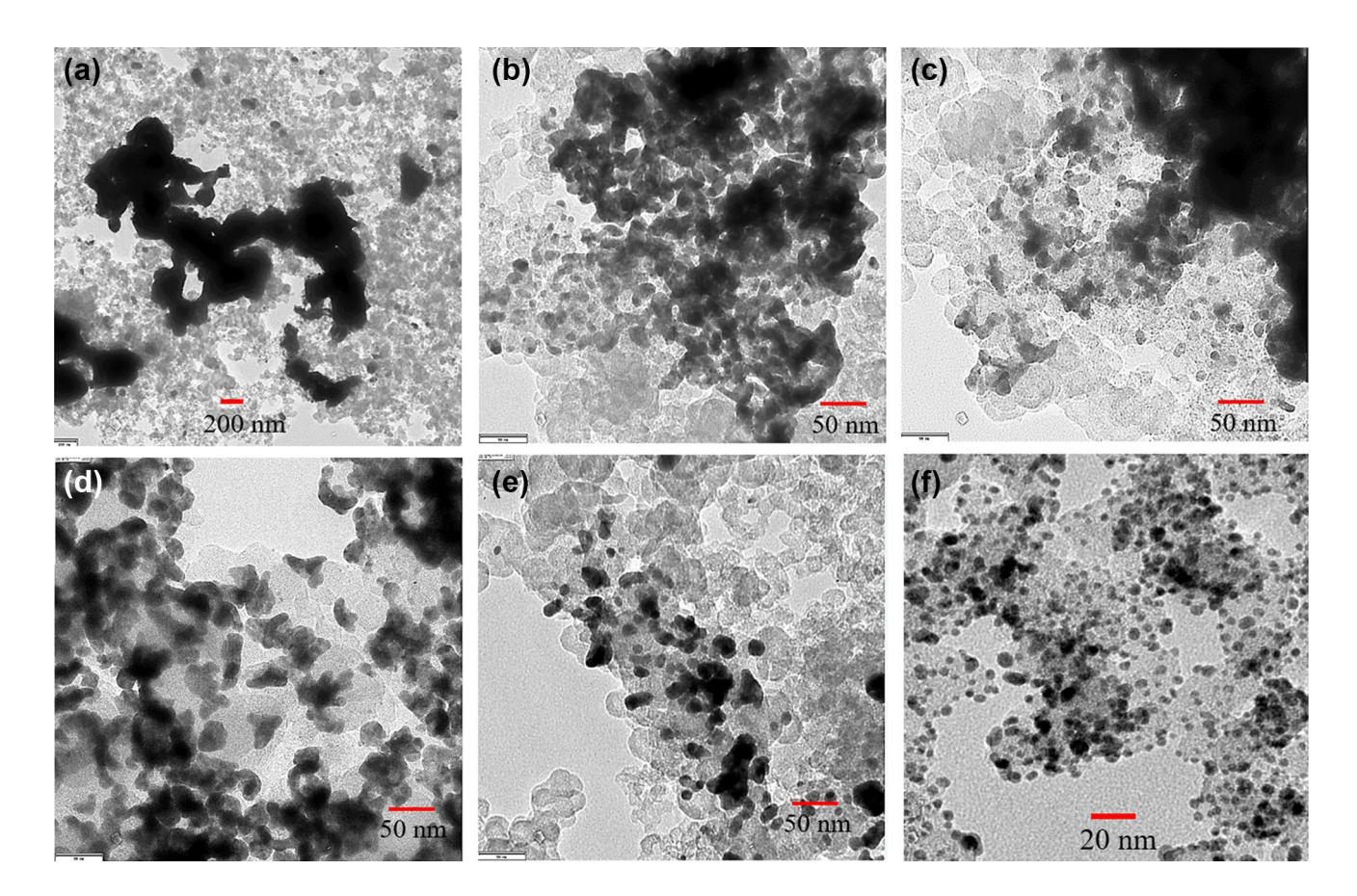


Fig. 2 TEM images of (a) Ag/C, (b) 5%AuAg/C, (c) 10%AuAg/C, (d) 20%AuAg/C, (e) 30%AuAg/C, and (f) Au/C



sizes on all particles were in the range of 15–20 nm. The AuAg nanoparticles were not decorated uniformly on the carbon. These AuAg nanoparticles may land simultaneously after having been detached from the sacrificed Ag nanoparticles, then positioned close to the other particles produced from the same Ag particle.

The TEM image of Au/C is shown in Fig. 2f. The average metal particle size was about 4.12 ± 0.98 nm, which is much smaller than that of the AuAg/C catalysts.

Figure 3 presents the XRD patterns of all the prepared catalysts. As both Au and Ag have similar lattice constants, all the peaks related to Au and Ag appear at the same 2Θ

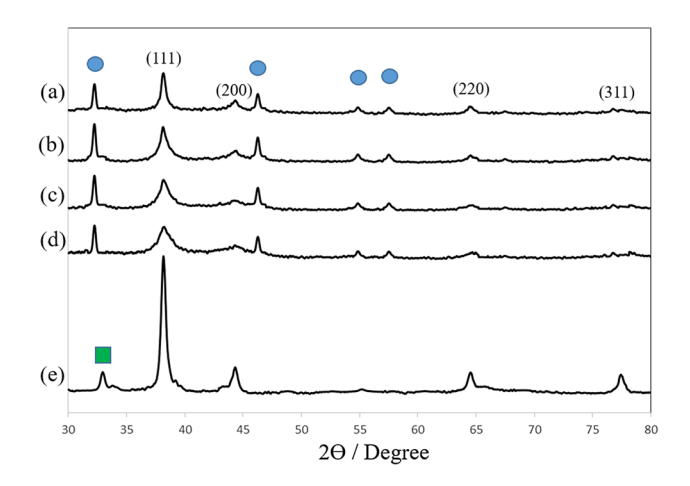


Fig. 3 XRD patterns of (a) 5%AuAg/C, (b) 10%AuAg/C, (c) 20%AuAg/C, (d) 30%AuAg/C, and (e) Ag/C marked by the main peak positions of AgCl (\bullet) and Ag₂O (\blacksquare)

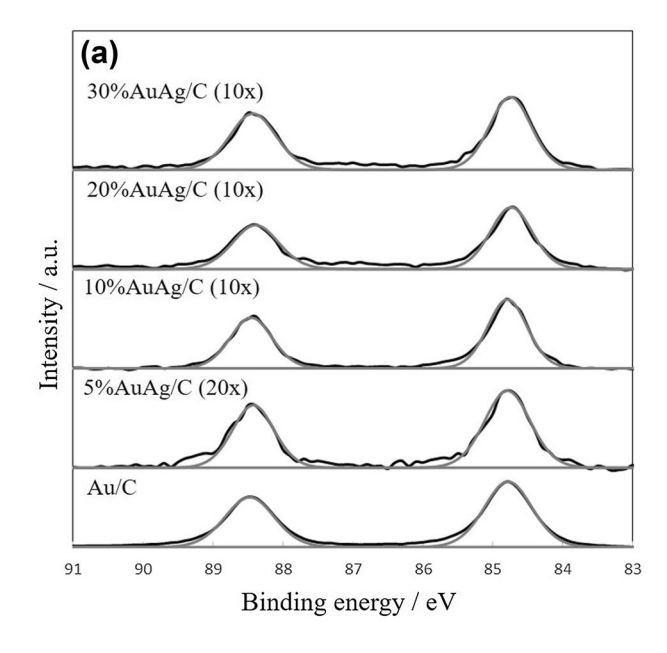
value at 38.2, 44.3, 64.5, and 77.6 degrees (JCPDS NO. 04-0783 for Ag and JCPDS NO. 04-0784). On the Ag/C catalyst, a small amount of Ag₂O was observed from the main peaks at 33.1° (JCPDS NO. 41-1104). For all the AuAg/C catalysts, four additional peaks corresponding to AgCl (JCPDS NO. 31-1238), which was formed during the galvanic displacement method, were observed.

Figure 4 shows the XPS spectra of the Ag/C, Au/C, and AuAg/C catalysts in the Au 4f and Ag 3d regions. The peak binding energies of all the deconvoluted peaks are summarized in Table 1. In the Au region, as shown in Fig. 4a, the metallic Au $4f_{7/2}$ and $4f_{5/2}$ peaks are visible at 84.7 and 88.4 eV, respectively. The slight shifts of the Au peak binding energy to a lower energy level were also observed for all the prepared AuAg/C catalysts.

The deconvoluted XPS spectra in the Ag region showed two species of Ag: ionic and metallic. The 3d peaks of the

Table 1 The peak binding energy of Au and Ag from the deconvoluted XPS results

Electrocatalysts	Binding energy (eV)			
	Au		Ag	
	4f _{7/2}	4f _{5/2}	3d _{5/2}	3d _{3/2}
Au/C	84.8	88.5	_	
5%AuAg/C	84.8	88.4	368.7	374.7
10%AuAg/C	84.8	88.5	368.8	374.7
20%AuAg/C	84.7	88.4	368.6	374.6
30%AuAg/C	84.7	88.4	368.6	374.6
Ag/C	-	-	368.5	374.5



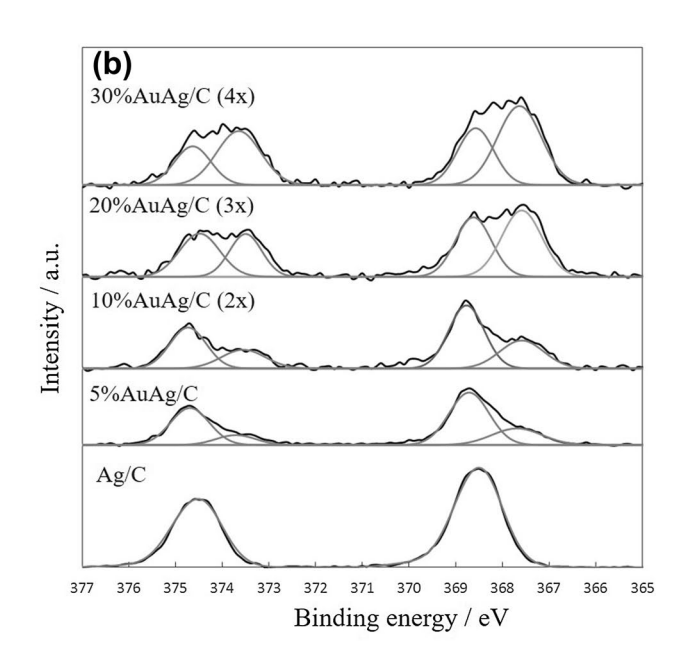


Fig. 4 The deconvoluted and XPS data of all synthesized catalysts in a 4f spectra of Au region and b 3d spectra of Ag region

ionic Ag appear at a binding energy lower than that of the metallic Ag [22]. The as-prepared Ag/C contained only the metallic Ag with the binding energies of 368.5 and 374.5 eV. After galvanic displacement, part of the displaced Ag formed suspended AgCl with the Cl⁻ from the Au precursor and remained in the catalyst, even though most of the AgCl had been removed during the cleaning process. The binding energies corresponding to Ag⁺ were observed at around 373.6 and 367.8 eV.

For the AuAg/C catalysts, the binding energy of Ag shifted to higher values, indicating that the electrons had transferred from Ag to Au to form an AuAg alloy. This electron transfer is normally observed in an AuAg bimetallic catalyst [11].

The actual Au loading and Au:Ag weight ratio from the EDX results of all the AuAg/C catalysts, along with their intended weight ratios, are exhibited in Table 2. The Au loadings on all the catalysts, except for 5%AuAg/C, were close to the intended Au loadings, indicating a completed displacement reaction under the conditions of the catalyst preparation employed in this work. For the case of 5%AuAg/C, the actual Au:Ag weight ratio was about half of the intended value. This result may be attributed to the non-uniform metal distribution of low Au loading on the catalyst support, as noticed from the high value of the standard deviation as compared to the average value of Au loading.

3.2 Electrochemical activity

The typical CVs of Ag/C and Au/C in alkaline solution are shown in Fig. 5. Both Ag/C and Au/C exhibit the oxidation and reduction peaks related to oxide formation and reduction, respectively, on their surfaces. For Ag/C, two oxide formation peaks correspond to the formation of Ag₂O (0.25 V), and the mixed phases of Ag₂O and AgO (0.7 V) [23, 24]. The oxidation peak in the forward scan of Au/C relates to oxide formation on the Au surface. In the reverse scan, two states of Au oxide were reduced at two potentials: the quasi-2D oxide at about 0.3 V and the quasi-3D oxide at about 0.0 V.

The CVs of the AuAg/C catalysts with different Au loadings are shown in Fig. 6. These CVs were quite similar to that of Ag/C, with a shift in the peak potential even when

Table 2 The calculated Au and Ag weight ratios from EDX results

Catalysts	Average Au	Au:Ag weight ra	tio
	loading (wt%)	Actual	Intended
5%AuAg/C	2.01 ± 1.86	0.046 ± 0.043	0.096
10%AuAg/C	9.16 ± 1.72	0.206 ± 0.154	0.230
20%AuAg/C	18.28 ± 2.86	0.841 ± 0.349	0.737
30%AuAg/C	32.23 ± 5.28	3.048 ± 0.233	2.801

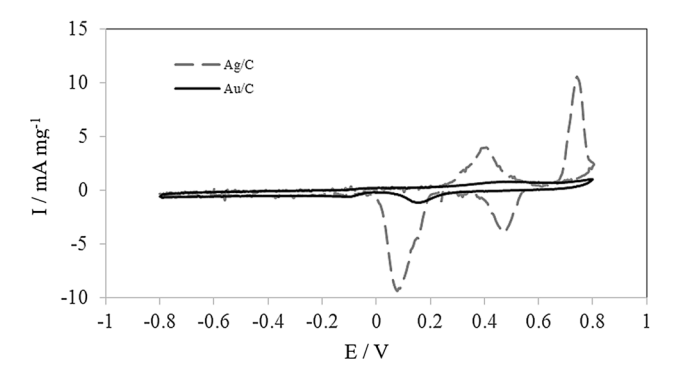


Fig. 5 CVs of Ag/C and Au/C in 0.1 M KOH at scan rate of 20 mV $_{\rm s}^{-1}$

the catalyst, such as 30%AuAg/C, had a low content of Ag. In addition, the onsets of the oxide formation and reduction peaks of all the AuAg/C catalysts, except for 30%AuAg/C, were similar to those of Ag/C. For 30%AuAg/C, the anodic shift was observed with all the peaks, indicating higher stability for the metal oxide.

Both Ag/C and Au/C were active for glycerol electrooxidation under the condition of the experiment, as shown in Fig. 7. By comparing the CVs of the Ag/C catalyst in Figs. 5 and 7, the glycerol electrooxidation peak occurs at 0.2 V, which is more positive than the first peak of AgO formation. It is anticipated that the alcohol electrooxidation on Ag takes place on its oxide surface, which is different from other metals, such as Au and Pt [25]. The glycerol electrooxidation peak appeared after the first AgO formation peak. This catalytic active surface was not recovered by the cycling of the potential, since the activity gradually declined as the number of cycles increased.

For Au/C, the glycerol electrooxidation took place on the bare Au surface and was inhibited by the surface oxide formation. The onset of the reaction was observed at about

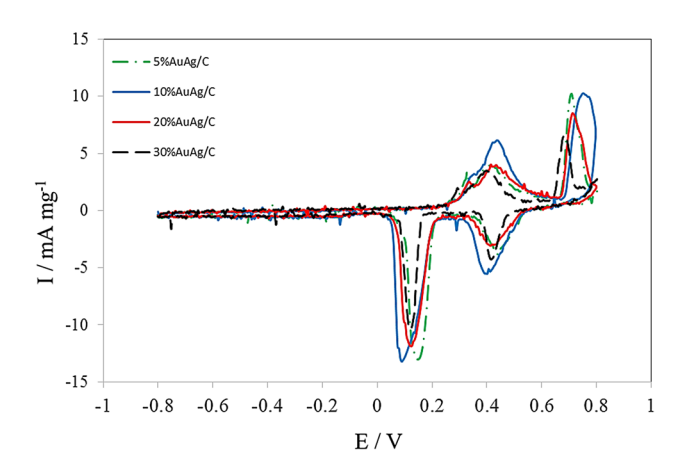


Fig. 6 CVs of AuAg/C catalysts in 0.1 M KOH at scan rate of 20 mV s^{-1} . (Color figure online)



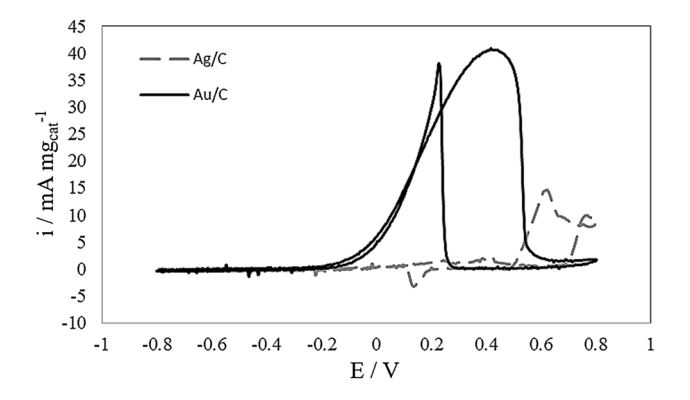
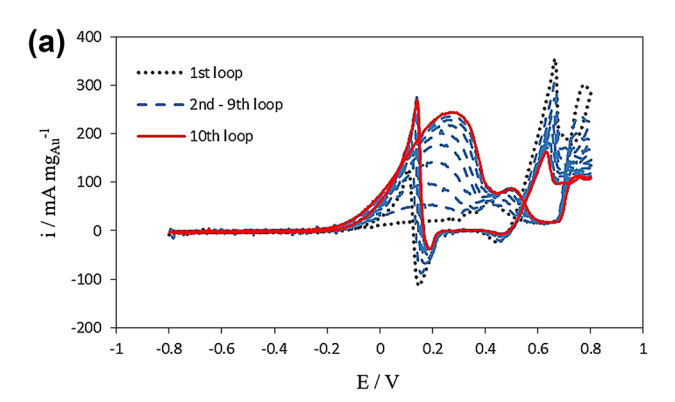


Fig. 7 CVs of Ag/C and Au/C in 0.1 M glycerol and 0.1 M KOH at scan rate of 20 mV $\rm s^{-1}$



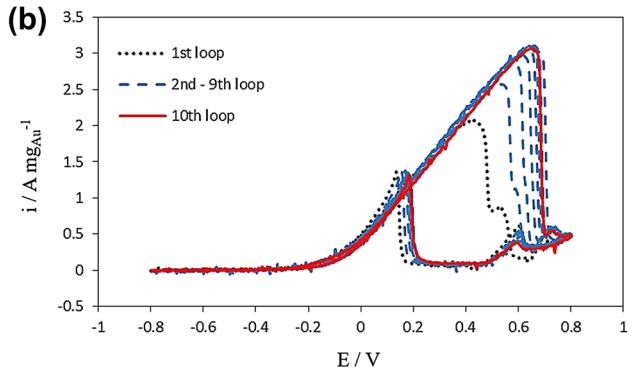


Fig. 8 Au mass normalized CVs of 10%AuAg/C catalysts in **a** 0.1 M glycerol and 0.1 M KOH, and **b** 1 M glycerol and 2 M KOH at scan rate of 20 mV s⁻¹

-0.2 V. The current density rapidly increased and reached the maximum current density at 0.4 V. After this point, the surface oxide formed and the reaction was inhibited. In the reverse scan, the oxide was removed from the Au surface at 0.25 V and the catalyst activity was recovered, resulting once again in the oxidative current of glycerol electrooxidation.

3.2.1 Surface activation of AuAg/C catalyst

Figure 8a and b displays the CVs of the 10%AuAg/C catalyst for glycerol electrooxidation at two electrolyte concentrations. It was noticed that the peak characteristics and the current densities of the CVs changed as the number of cycles increased, indicating that the structure of the AuAg/C catalyst had changed as the reaction proceeded. In the first loop (Fig. 8a), the CVs of the 10%AuAg/C in a solution of 0.1 M glycerol and 0.1 M KOH were quite similar to that of the Ag/C in 0.1 M KOH, except that the sharp peak of glycerol electrooxidation on the recovered gold surface appeared in the reverse scan. In addition, the oxidation peaks of glycerol on Au (from -0.2 to 0.6 V) were very low while the dominant oxidation peak belonged to the glycerol electrooxidation on AgO (from 0.7 V onward). As the number of cycles increased, the peak of the glycerol electrooxidation on Au was enhanced, whereas that on AgO was reduced. The Au catalyst activity improved as the number of cycles increased and became steady at the ninth loop, at which the glycerol electrooxidation on Au was more pronounced than that on AgO. The potential at the maximum current density and the onset of AuO reduction had also shifted closer to those of the Au/C catalyst. The activation of the catalyst surface was also accelerated by the glycerol concentration. At higher glycerol concentration, the activation proceeded much faster, as shown in Fig. 8b. The glycerol electrooxidation on the Au catalyst was clearly observed and became the main oxidation peak starting from the first scan. A steady CV was achieved after the sixth loop.

The surface compositions of the as-prepared 10%AuAg/C and the catalyst activated by glycerol electrooxidation at a low EDX potential were compared. Au and Ag on all the catalysts were non-uniformly distributed all over the nanoparticles. The Au:Ag ratios of the prepared catalyst and the catalyst cycled in the KOH electrolyte were similar at 0.145 ± 0.017 and 0.142 ± 0.066 , respectively. However, the catalyst surface became an Au-rich surface after scanning in 1 M glycerol electrolyte, since the Au: Ag ratio increases to 0.366 ± 0.050 , providing evidence of the adsorbate-induced surface segregation of the AuAg surface. The surface segregation of a more reactive component to the adsorbate on the surface of the alloy was well described [26]. Prior to the glycerol electrooxidation test, the working electrode was cleaned by performing a cyclic scan in a KOH solution at the same concentration. This step may bring the Ag atom to the nanoparticle surface, since Ag exhibits a higher affinity for adsorbing the oxygenated species than does the Au atom [27]. The catalyst showed a low glycerol electrooxidation activity in this state, since Ag was inactive for glycerol electrooxidation at low potentials. However, the surface of the AuAg nanoparticles was reconstructed and became highly active after interacting with glycerol. The activation



process proceeded much faster at high glycerol concentration. Hence, the surface segregation may have been led by a strong interaction between either the surface or underlying Au atoms and the glycerol, which induced the Au atoms to rise to the nanoparticle surface, since Au is better than Ag at adsorbing alcohol [13]. In other words, the deactivation of the catalyst surface is reversible depending on the electrolyte deployed. The catalyst was easily deactivated by the interaction between Ag and hydroxide ions. The fully activated catalyst was reversed to its inactive form after cycling the potential in the KOH electrolyte. To regain its activity, this deactivated catalyst must be reactivated by cycling the potential in the electrolyte containing the glycerol. Hence, the surface of AuAg may constantly be changing as the reaction proceeds in the electrolyte containing both glycerol and OH-.

The displacement method yielded a catalyst in the form of an Au-rich shell at the beginning of the preparation step. Therefore, the surface reconstruction of this catalyst was possible, since most of the Au atoms were either at or near the surface. In contrast, this process may not have been possible in the case of the Ag-rich shell because the interaction between the surface and deeper underlying Au may not have been strong enough at low glycerol concentrations. This may be the main difference between the catalysts prepared by the co-reduction method of AgNO₃ and AuCl₃, and the catalysts fabricated by the galvanic displacement method.

The catalysts containing different Au content exhibited dissimilar behaviors during the activation process. As shown in Fig. 9, two distinct behaviors were observed according to the Au content. The current density obtained from the low Au content catalysts, 5 and 10%AuAg/C, firstly decreased according to the decrease in the double layer charging current. Later, the current density gradually increased and became rather steady after about 5 min. The stable increase in the current density indicates that the continuation of the

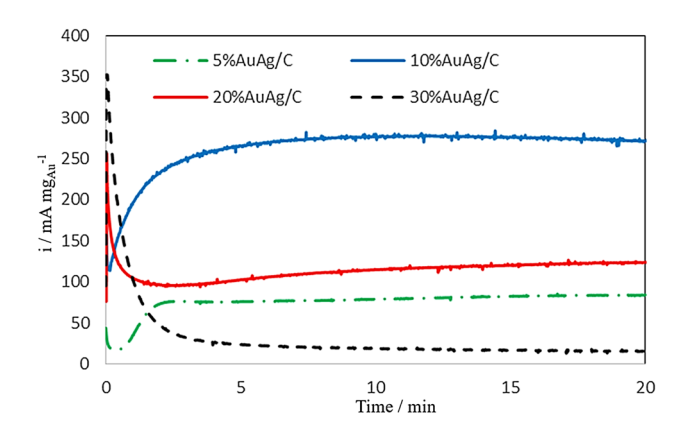
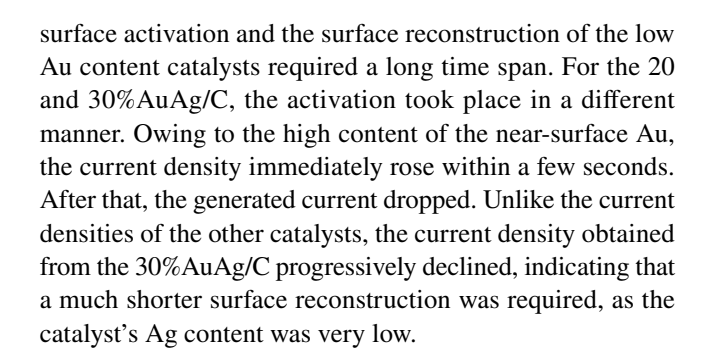


Fig. 9 CAs of AuAg/C catalysts in 1 M glycerol and 2 M KOH at 0.25 V after 10 cycles of activation in 2 M KOH. (Color figure online)



3.2.2 Catalyst activity test

Figure 10 shows the steady and fully activated CVs of AuAg/C in a solution of 0.1 M glycerol and 0.1 M KOH. The glycerol electrooxidation characteristics and activities of the synthesized AuAg/C catalysts depended strongly on the Au:Ag ratio. For the catalysts with low Au:Ag ratios, e.g., 5 and 10%AuAg/C, the promotional roles of Ag, such as the negative shifts of both the onset potential and the potential at the maximum current density, were clearly observed. The lower onset potential was caused by the reduction of the 5d band density of Au, which altered the adsorption capability of the Au surface [11]. The addition of Ag would also result in faster self-poisoning by oxide formation. The potentials at the maximum current density of both 5 and 10%AuAg/C were at about 0.29 V.

At high Au content, e.g., 20 and 30%AuAg/C, the promotion effects of Ag almost vanished. The main glycerol electrooxidation peaks on these two catalysts were similar to that of Au/C. However, the small oxidation peak related to the glycerol electrooxidation on the Ag surface and the higher stability of the oxide reduction were still observed.

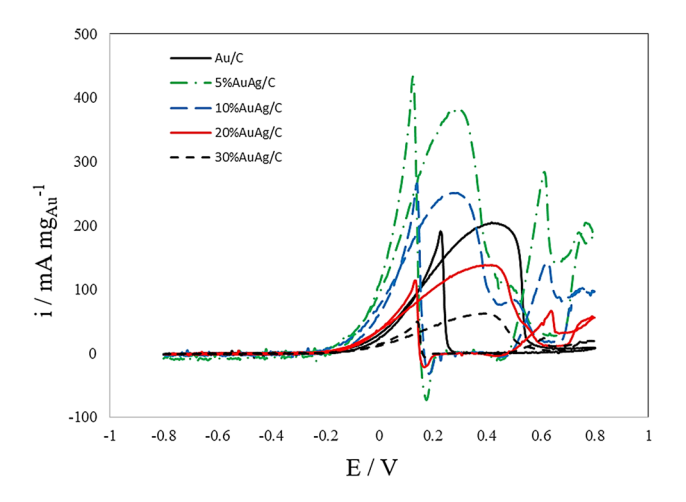


Fig. 10 Au mass normalized CVs of Au/C and AuAg/C catalysts in 0.1 M glycerol and 0.1 M KOH at scan rate of 20 mV s⁻¹. (Color figure online)



Apparently, the peak potential was affected by the Au loading [28, 29]. The drop-off potential generally increased with increased Au loading. However, the results shown here did not follow the regular trend. Thus, it was possible that the effects of Ag on the glycerol electrooxidation had prevailed over the effects of the support [28] or the accumulation of the oxidative species within the catalyst layer [29].

For the electrolyte containing 0.1 M glycerol and 0.1 M KOH, the most active catalyst was the 5%AuAg/C, which provided a mass normalized current density at about 382 mA mg_{Au}⁻¹ almost twice as high as that of Au/C at 203 mA mg_{Au}⁻¹. This result contradicted that of the Ag-rich shell AuAg/C catalyst prepared by the co-reduction method, which was quite inactive in the low glycerol concentration electrolyte [11]. Despite their large particle sizes, both the 5 and 10%AuAg/C catalysts benefited by the promotion effect of Ag and the activation of the AuAg nanoparticles. The formation of an Au-rich shell may compensate for the low surface area of the large particles. For the high Au loading catalysts, however, this promotional effect of Ag was diminished according to the lower content of Ag, so the particle size played an important role instead.

Figure 11 depicts the CVs of all the AuAg/C and Au/C catalysts in high concentrations of glycerol and electrolyte, i.e., 1 M glycerol and 2 M KOH, respectively. The electrooxidation characteristic of Au was obviously dominant in this condition while the reaction on Ag was diminished. The synergistic effect between Au and Ag was still observed under this condition, i.e., the negative onset potential shifts for the 5 and 10%AuAg/C catalysts were the same as in the low glycerol and electrolyte concentrations. However, no clear trend on the potential at maximum current density could be concluded, although this potential was related to the stability of the surface oxide. The AuAg/C catalyst with faster oxide reduction in the reverse scan was less deactivated by the oxide formation and tended to oxidize glycerol at higher potentials.

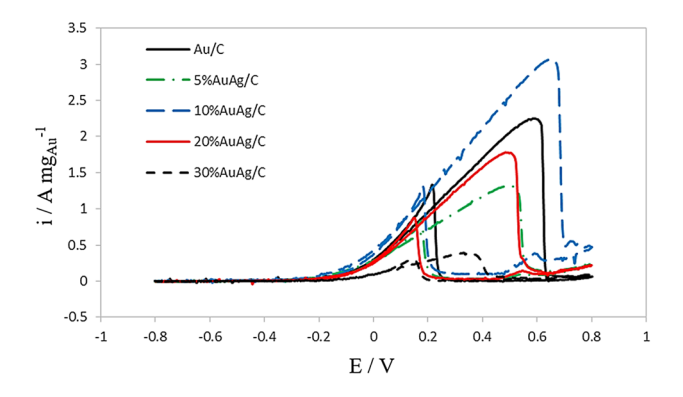


Fig. 11 Au mass normalized CVs of Au/C and AuAg/C catalysts in 1 M glycerol and 2 M KOH at scan rate of 20 mV s⁻¹. (Color figure online)

Figure 11 shows that 10%AuAg/C was the most active catalyst, yielding 3.04 A mg_{Au}⁻¹ while the Au/C catalyst provided only 2.22 A mg_{Au}⁻¹. The activities of 20% and 30%AuAg/C were still low under this condition.

3.2.3 Catalytic stability test

To measure the stability of the AuAg/C catalysts at their fully activated states, the CA experiments were conducted after the catalysts had been activated by 10 cycles of CV scans in their respective electrolytes. The resulting CA in the low and high glycerol concentration electrolytes are displayed in Fig. 12a and b, respectively. After being activated by the glycerol, the typical CA shape of AuAg/C was similar to that of Au/C.

In the low glycerol concentration electrolyte, as shown in Fig. 12a, most of the AuAg/C catalysts exhibited a slower decay in their current densities than did Au/C, except for 30%AuAg/C, during the initial stage. Unfortunately, the final current densities of all the AuAg/C catalysts, except for 5%AuAg/C, were lower than that of Au/C. The final current density at the 60th minute of 5%AuAg/C was close to that of Au/C. Moreover, the average current densities decaying from the 20th to 60th min of 5%AuAg/C and 10%AuAg/C (0.30 and 0.19 mA mg_{Au}⁻¹ min⁻¹, respectively) were close to or lower than that of Au/C at 0.28 mA mg_{Au}⁻¹ min⁻¹. This result indicated that all the AuAg/C catalysts had been subjected to surface deactivation by a cause other than poisoning by the reaction intermediates, which was proposed here as the Ag segregation previously mentioned in Sect. 3.2.1.

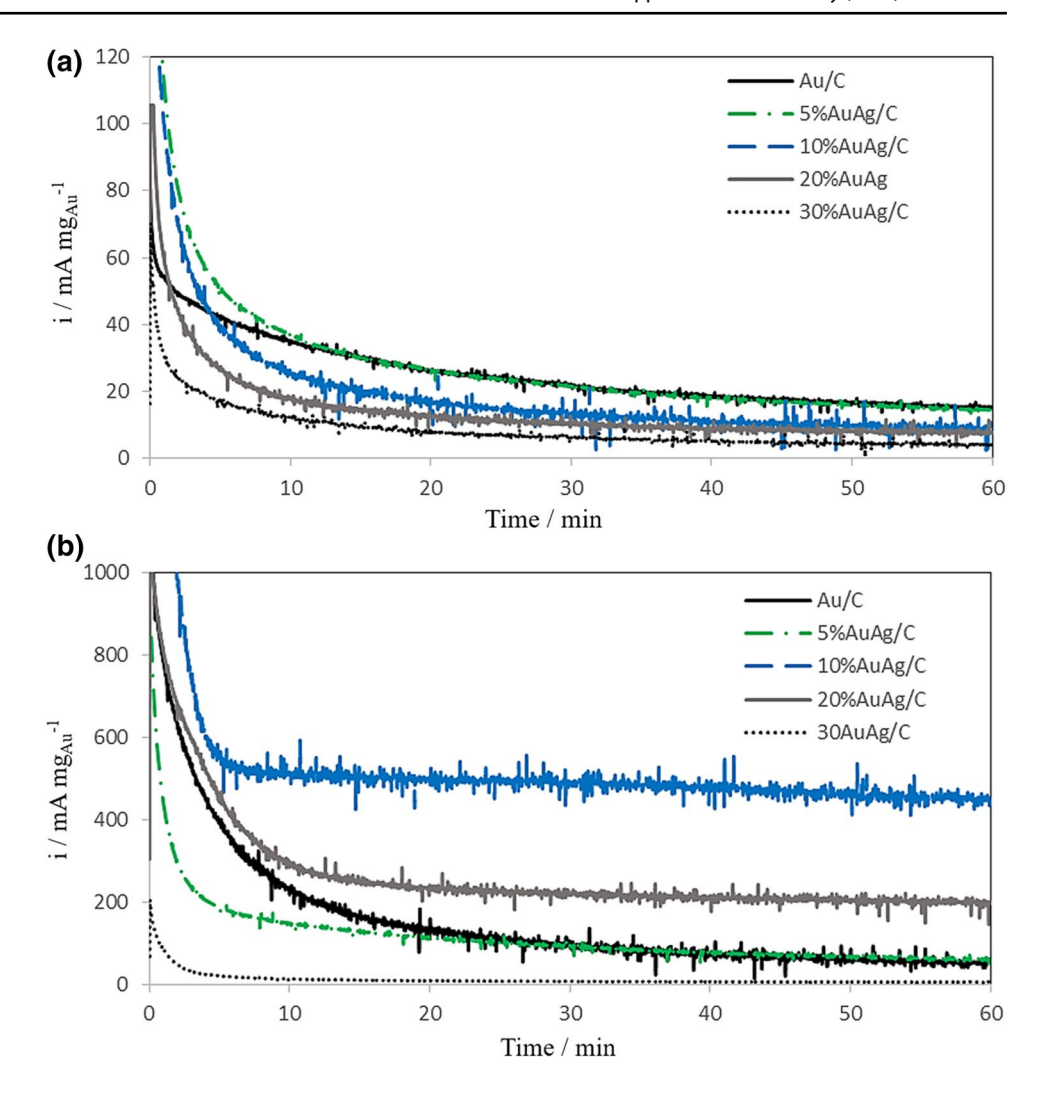
The use of higher glycerol concentrations in the electrolytes gave different results. In Fig. 12b, the current density trend of the CA is similar to that of the CV. The 10%AuAg/C catalyst was the most active catalyst and more stable than Au/C. The average current decay rates of the highly active AuAg/C, such as 10%AgAu/C and 20%AuAg/C (1.24 and 0.82 mA mg_{Au}^{-1} min $^{-1}$, respectively), were much lower than that of Au/C (1.94 mA mg_{Au}^{-1} min $^{-1}$).

The electrooxidation of glycerol and removal of the reaction intermediates on the Au surface required the formation of the oxygenated species on the catalyst surface. With Ag, the rates of hydroxide adsorption and oxidation on the nanoparticle surface were accelerated around the glycerol electrooxidation potential, as was observed from the Ag₂O formation starting at 0.25 V in Figs. 5 and 6. As a result, the catalyst surface was enriched with the oxygenated species forming on the remaining Ag atoms on the surface. This extra oxygenated species was supplied to the Au atoms for the glycerol electrooxidation and removal of the reaction intermediates, thereby lowering the decay rates of the AuAg catalysts.

These results suggest that activation by glycerol is an essential step for preparing the AuAg/C catalysts by the



Fig. 12 CAs of AuAg/C catalysts in a 0.1 M glycerol and 0.1 M KOH at 0.25 V after 10 cycles of CV activation in 0.1 M glycerol and 0.1 M KOH, and b 1 M glycerol and 2 M KOH at 0.25 V after 10 cycles of CV in 1 M glycerol and 2 M KOH. (Color figure online)



galvanic displacement method, and that a certain glycerol concentration would be required to maintain catalyst activity and stability during the glycerol electrooxidation reaction, since the interaction between glycerol and Au would be needed to keep Au on the catalyst's surface. The remaining Ag could supply the oxygenated species to the Au atoms on the surface for the glycerol electrooxidation reaction, thereby improving the stability of the Au catalyst.

The catalytic properties of the Au-based catalysts were influenced by the sizes of the Au nanoparticles [30]. Small Au particles show higher activity and lower onset potential than do the large particles on a mass basis. However, on a real surface area basis, the specific activity increases as particle size increases because of the higher portion of the Au(111) surface appearing in the larger particles. In our present work, although particle size may play some role in the activities of the catalysts, the results prove that the AuAg catalyst is highly active in an alloy form. New strategies, such as the PVP-protected AuAg alloy preparation method [31, 32] or heat treatment to induce alloy

formation, to prepare small AuAg alloy particles will be adopted in future works.

4 Conclusions

A series of AuAg/C catalysts were prepared by the galvanic displacement of Ag on carbon with Au³⁺. The sizes and shapes of the AuAg nanoparticles deposited on carbon varied with the Au loading. The sizes of the AuAg nanoparticles were much larger than those of Au/C prepared by the PVA protection method. However, with the electronic modification of an AuAg alloy and the presence of Ag on the nanoparticle surface, the AuAg/C catalysts became more active than did Au/C at low Au loading. 5%AuAg/C and 10%AuAg/C were the most active catalysts in the electrolytes of 0.1 and 1 M glycerol, respectively.

The catalytic performances of the AuAg/C catalysts greatly depended on the glycerol concentration and their activities improved after activation with glycerol. In this



active form, a negative shift of the glycerol electrooxidation peak was observed. The oxide formation on AuAg/C also occurred at a lower potential than did Au/C, because Ag induced the hydroxide species to adsorb on the metal surface. This mechanism improved the stability of the AuAg/C catalyst in the high glycerol concentration electrolyte.

Acknowledgements This work was supported by the Thailand Research Fund (TRF) and King Mongkut's University of Technology Thonburi (KMUTT) under Grant No. TRG5880131, KMUTT through the "KMUTT 55th Anniversary Commemoration Fund" and by the National Research University (NRU) Project of Thailand, Office of the Higher Education Commission.

References

- Kwon Y, Lai SCS, Rodriguez P, Koper MTM (2011) Electrocatalytic oxidation of alcohols on gold in alkaline media: base or gold catalysis? J Am Chem Soc 133:6914–6917
- Zhang JH, Liang YJ, Li N, Li XY, Xu CW, Jiang SP (2012) A remark activity of glycerol electrooxidation on gold in alkaline medium. Electrochim Acta 59:156–159
- Yongprapat S, Therdthianwong A, Therdthianwong S (2012) Au/C catalyst prepared by polyvinyl alcohol protection method for direct alcohol alkaline exchange membrane fuel cell application. J Appl Electrochem 42:483–490
- Kannan R, Kim AR, Yoo DJ, (2014) Enhanced electrooxidation of methanol, ethylene glycol, glycerol, and xylitol over a polypyrrole/manganese oxyhydroxide/palladium nanocomposite electrode. J Appl Electrochem 44:893–902
- Kannan R, Kim AR, Nahm KS, Lee HK, Yoo DJ (2014) Synchronized synthesis of Pd@C-RGO carbocatalyst for improved anode and cathode performance for direct ethylene glycol fuel cell. Chem Commun 50:14623–14626
- Kannan R, Kim AR, Nahm KS, Yoo DJ (2016) Manganesetitanium-oxide-hydroxide-supported palladium nanostructures: a facile electrocatalysts for the methanol, ethylene glycol and xylitol electrooxidation. Int J Hydrog Energy 41:6787–6797
- Gholami Z, Abdullah AZ, Lee KT (2014) Dealing with the surplus glycerol production from biodiesel industry through catalytic upgrading to polyglycerols and other value-added products. Renew Sust Energ Rev 39:327–341
- Yongprapat S, Therdthianwong A, Therdthianwong S (2013) Au/C catalysts promoted with metal oxides for ethylene glycol electro-oxidation in alkaline solution. J Electroanal Chem 697:46–52
- Yongprapat S, Therdthianwong S, Therdthianwong A (2012) RuO₂ promoted Au/C catalysts for alkaline direct alcohol fuel cells. Electrochim Acta 83:87–93
- Padayachee D, Golovko V, Marshall AT (2013) The effect of MnO₂ loading on the glycerol electrooxidation activity of Au/ MnO₃/C catalysts. Electrochim Acta 98:208–217
- Garcia AG, Lopes PP, Gomes JH, Pires C, Ferreira EB, Lucena RGM, Gasparotto LHS, Tremiliosi-Filho G (2014) Eco-friendly synthesis of bimetallic AuAg nanoparticles. New J Chem 38:2865–2873
- Garcia AG, Caliman J, Ferreiara EB, Tremiliosi-Filho G, Linares JJ (2015) Promotional effect of Ag on the catalytic activity of Au for glycerol electrooxidation in alkaline medium. ChemElectroChem 2:1036–1041
- 13. Gomes JF, Garcia AC, Gasparotto LHS, de Souza NE, Ferreira EB, Pires C (2014) Influence of silver on the glycerol

- electro-oxidation over AuAg/C catalysts in alkaline medium: a cyclic voltammetry and in situ FTIR spectroscopy study. Electrochim Acta 144:361–368
- Liu Z, Huang L, Zhang L, Ma H, Ding Y (2009) Electrocatalytic oxidation of d-glucose at nanoporous Au and Au-Ag alloy electrodes in alkaline aqueous solutions. Electrochim Acta 54:7286–7293
- Toninaga M, Shimazoe T, Nagashima M, Kusuda H, Kubo A, Kuwahara Y, Taniguchi I (2006) Electrocatalytic oxidation of glucose at gold-silver alloy, silver and gold nanoparticles in an alkaline solution. J Electroanal Chem 590:37–46
- Cuevas-Muniz FM, Guerra-Balcazar M, Castaneda F, Ledesma-Garcia J, Arriaga LG (2011) Performance of Au and AuAg nanoparticles supported on Vulcan in a glucose laminar membraneless microfuel cell. J Power Sources 14:5853–5857
- Aoun SB, Dursun Z, Koga T, Bang GS, Sotomura T, Taniguchi I (2004) Effect of metal ad-layers on Au(111) electrodes on electrocatalytic oxidation of glucose in an alkaline solution. J Electroanal Chem 567:175–183
- Aoun SM, Bang GS, Koya T, Nonaka Y, Sotomura T, Taniguchi I (2003) Electrocatalytic oxidation of sugars on silver-UPD single crystal gold electrodes in alkaline solutions. Electrochem Comm 5:317–320
- Sun Y, Xia Y (2004) Mechanistic study on the replacement reaction between silver nanostructures and chloroauric acid in aqueous medium. J Am Chem Soc 126:3892–3901
- Lee KJ, Lee YI, Lee J, Myung NV, Choa YH (2012) Structural evolution of Ag-Au nanoplates by pH controlled galvanic displacement. Curr Appl Phys 12:S53–S58
- Obliosca JM, Wu YS, Hsieh HY, Chang CJ, Wang PC, Tseng FG (2012) Synthesis and optical properties of gold/silver nanocomposites prepared on multiwalled carbon nanotubes via galvanic replacement of silver. J Nanopart Res 14:834
- Jiménez JA, Liu H, Fachini E (2010) X-ray photoelectron spectroscopy of silver nanoparticles in phosphate glass. Mater Lett 64:2046–2048
- Mayer ST, Muller RH (1988) Nucleation of silver (I) oxide investigated by spectroscopic ellipsometry. J Electrochem Soc 135(9):2133–2142
- 24. Hecht D, Frahm R, Strehblow HH (1996) Quick-scanning EXAFS in the reflection mode as a probe for structural information of electrode surfaces with time resolution: an in situ study of anodic silver oxide. J Phys Chem 100:10831–10833
- Avramov-Ivić M, Jovanović V, Vlajnić G, Popić J (1997) The electrocatalytic properties of the oxides of noble metals in the electro-oxidation of some organic molecules. J Electroanal Chem 423:119–124
- Liao H, Fisher A, Xu ZJ (2015) surface segregation in bimetallic nanoparticles: a critical issue in electrocatalyst engineering. Small 11(27):3221
- Yang C, Huang B, Xiao L, Ren Z, Liu Z, Lu J (2013) Activating Ag by even more inert Au: a pericular effect on electrocatalysis toward oxygen reduction in alkaline media. Chem Commun 49:11023–11025
- Gomes JF, Gasparotto LMS, Tremiliosi-Filho G (2013) Glycerol Electro-oxidation over glassy-carbon-supported Au nanoparticles: direct influence of the carbon support on the electrode catalytic activity. Phys Chem Chem Phys 15:10339–10349
- Marshall AT, Golovko V, Padayachee D (2015) Influence of gold nanoparticle loading in Au/C on the activity towards electrocatalytic glycerol oxidation. Electrochim Acta 153:370–378
- Padayachee D, Golovko V, Ingham B, Marshall AT (2014) Influence of particle size on the catalytic oxidation of glycerol over carbon-supported gold nanoparticles. Electrochim Acta 120:398–407



- 31. Zhang H, Okuni J, Toshima N (2011) One-pot synthesis of Ag-Au bimetallic nanoparticles with Au shell and their high catalytic activity for aerobic glucose oxidation. J Colloid Interface Sci 354:131–138
- 32. Zhang H, Toshima N, Takasaki K, Okumura M (2014) Preparation of Ag_{core}/Au_{shell} bimetallic nanoparticles from physical mixture

of Au clusters and Ag ions under dark conditions and their catalytic activity for aerobic glucose oxidation. J Alloys Compd 586:462-468

Affiliations

S. Yongprapat 10 · A. Therdthianwong 1 · S. Therdthianwong 2

- Fuel Cells and Hydrogen Research and Engineering Center, Pilot Plant, Development and Training Institute (PDTI), King Mongkut's University of Technology Thonburi (KMUTT), 126 Pracha-Uthit Rd., Bang Mod, Thung Khru, Bangkok 10140, Thailand
- Department of Chemical Engineering, Faculty of Engineering, King Mongkut's University of Technology Thonburi (KMUTT), 126 Pracha-Uthit Rd., Bang Mod, Thung Khru, Bangkok 10140, Thailand



The activity of AuAg/C prepared by galvanic displacement of Ag on carbon by Au³⁺ towards alcohol electrooxidation

Sarayut Yongprapat^{1,*}, Apichai therdthianwong¹, Supaporn Therdthianwong²

Abstract:

The AuAg/C catalysts were prepared by using the galvanic displacement of Ag/C by Au³⁺. The shape and distribution of AuAg nanoparticles depended on the displaced degree yielding a large porous for 10AuAg/C or smaller fragments for 30AuAg/C. The activity of AuAg/C catalysts required an activation from alcohol electrooxidation. The activity was improved as the number of cyclic voltammogram increased. The catalyst activation depended on type and concentration of alcohol used. The higher molecular weight alcohol molecule tends to be a better activator. Glycerol was the only alcohol used in this study that active was at 0.1 M concentration, while ethylene glycol was active at higher concentrations. For ethanol, even though active on Au/C, it was not oxidized on AuAg/C catalysts. The activation process was the reversible process, controlled by the electrolyte, which pull Au or Ag towards the nanoparticle surface by the interaction with alcohol or hydroxide. For the oxidizeable alcohols, the promotion effects of Ag was observed. The onset potential and the potential at maximum current density was shifted to more anodic. The 10AuAg/C catalyst was more active than Au/C for glycerol electrooxidation.

Keywords: AuAg/C catalyst; Alcohol electrooxidation; Electrocatalysts; Fuel cell; Galvanic displacement.

*Corresponding author. Tel.: +02-470-9612, Fax: +02-470-9325 E-mail address:sarayut.yon@kmutt.ac.th

1. Introduction

Au-based catalysts were excellent for glycerol electrooxidation in an alkaline medium. This makes them capable as an anode catalyst in direct glycerol anion exchange membrane fuel cell. Ag was found to further improve the catalytic properties of Au by lowering the onset potential of the reaction, but, with lower activity because of the segregation of Ag on catalyst surface (Garcia et al., 2014). This work aims to elaborate the effects of Ag on the electrooxidation properties of AuAg/C on alcohols by using the voltammetric method. The AuAg/C catalysts were prepared by galvanic displacement of Ag by Au³⁺ according to the reaction:

$$Au^{3+} + 3Ag \rightarrow Au + Ag^{3+}$$
 (1).

3 moles of Ag were replaced by one mole of Au which lower the volume of metal nanoparticles and produces an Alloy AuAg nanoparticles in the process (Sun and Xia, 2004). The result was compared with the Au/C prepared by PVA method (Yongprapat et al., 2012).

2. Materials and methods

The 60% Ag/C was first prepared by using the citrate reduction in alkaline. AgNO₃ and potassium citrate were dissolved in a dispersed mixture of Vulcan XC-72 in deionized water. The reduction reaction was initiated by addition of KOH solution. The obtained Ag/C was filtered, washed and dried. This formed Ag nanoparticles on carbon was then used as a sacrifice material to deposit Au³⁺ onto Ag/C by the galvanic displacement reaction. To prepare the AuAg/C, the calculated amount of Au³⁺ was added into the dispersed 60% Ag/C in deionized water. The AuAg nanoparticles were formed as Ag oxidized to Ag⁺ and formed AgCl in the mixture. Finally, the AuAg/C was filtered, washed and dried. Two AuAg/C catalysts at 10 and 30 %wt Au loading were used in this study namely 10AuAg/C and 30AuAg/C, respectively. The intended ratios of Au:Ag in 10AuAg/C and 30AuAg/C were at 0.23 and 2.81. The Au/C was prepared by the PVA method described elsewhere

¹ Fuel Cells and Hydrogen Research and Engineering Center, Pilot Plant, Development and Training Institute (PDTI), King Mongkut's University of Technology Thonburi (KMUTT), Bangkok, Thailand

² Department of Chemical Engineering, Faculty of Engineering, King Mongkut's University of Technology Thonburi (KMUTT), Bangkok, Thailand

(Yongprapat et al., 2012). These catalysts were used to form the working electrode by dropping the well mixed catalyst ink onto a glassy carbon electrode. The cyclicvoltammetry was performed by using the Bipotentiostat AFCBP1 (Pine Research Instrument).

3. Results and discussion

Fig.1 shows the TEM image of 60% Ag/C, 10AuAg/C and 30AuAg/C. The large particles of Ag was observed in Fig. 1(a) with the wide particle size of 100-300 nm. After the displacement reaction, the Ag nanoparticles were corroded and produced a porous or a small AuAg fragment. The average size of the AuAg nanoparticles of 10% AuAg/C and 30% AuAg/C catalysts was around 20 nm which was larger than the Au nanoparticles on Au/C with the average size of 3.69 nm (Yongprapat et al., 2012).

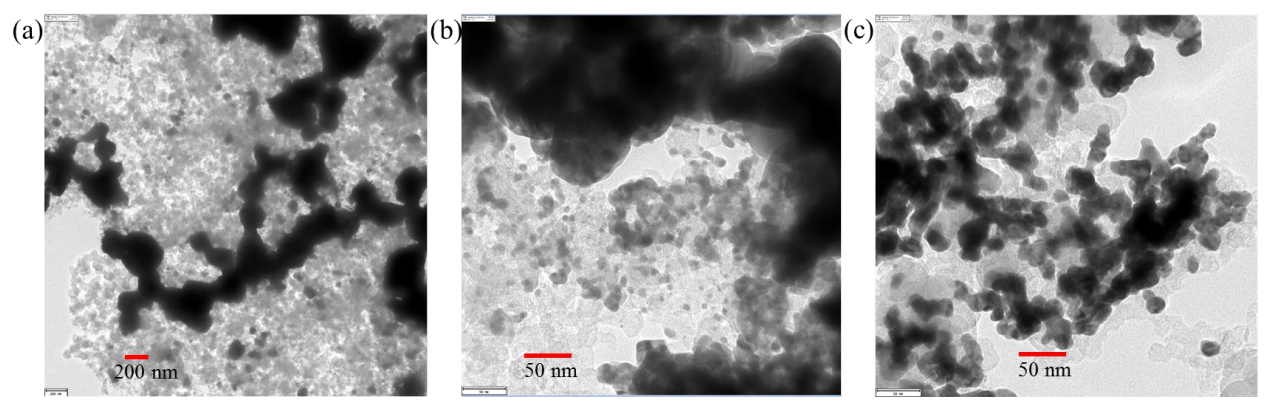


Fig. 1 TEM images of (a) Ag/C, (b) 10AuAg/C and (c) 30AuAg/C.

The activity of AuAg/C catalysts depends on type and concentration of the alcohol solutions. All the alcohols used in this study which are ethanol, ethylene glycol and glycerol were active on Au/C catalyst. However, the AuAg/C catalysts were not active for ethanol electrooxidation even in 1 M ethanol electrolyte (results not shown). This result was quite astonishing since the AuAg particle of 30AuAg/C was comprised mainly by Au atoms.

Figs. 2 and 3 show the cyclic voltammograms of ethylene glycol electrooxidation on 10AuAg/C and 30AuAg/C in 0.1 M and 1 M ethylene glycol electrolyte in comparison with those of Au/C. At 0.1 M ethylene glycol, only 30AuAg/C shows low alcohol electrooxidation activity in Au region (around -0.1-0.4 V) while 10AuAg/C was inactive. The 30AuAg/C was inactive in the first scan but the activity was gradually increased after the number of scan increased.

The ethylene glycol activity on both AuAg/C catalysts was clearly observed in 1 M ethylene glycol electrolyte as shown in Fig. 3. Ethylene glycol electrooxidation occurred in 2 regions. The first one was on the active Au surface in the potential range of -0.2-0.4V. The potential at the maximum current density of AuAg/C was around 0.3 V compared with that at 0.5 V on Au/C. At 0.3 V, the metal oxide formation began which prevents alcohol adsorption on the metal surface. The current density in this range was very low in the first scan and then increased as the course of scan progress. The second region was on the active Ag surface which displays as a sharp peak in the potential range of 0.4-0.6 V. The current density trend was reverse with that on the active Au region.

The activation of AuAg surface differ by the Au:Ag ratio. 30AuAg/C was faster activated than 10AuAg/C. The current density in Au region reaches half of the maximum current density in the 2^{nd} loop while that on 10AuAg/C was on the 5^{th} loop.

The activation process became faster with glycerol, as shown in Fig. 4(a). 30AuAg/C was almost inactive in the first cycle. After that, the current density increased drastically up to around 75% of the maximum current density in the 2nd scan and became stable from the 3rd scan onward.

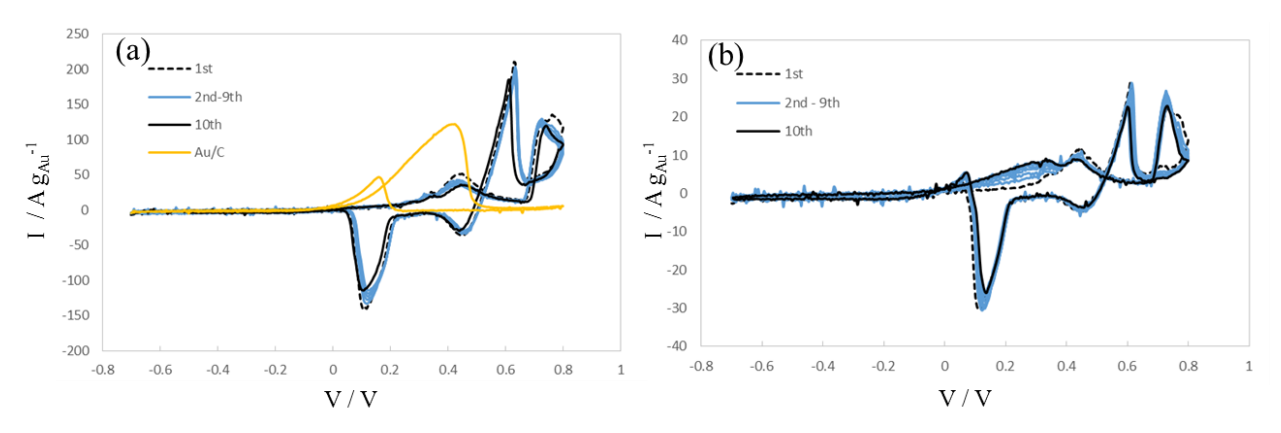


Fig. 2 CVs of (a) 10AuAg/C and Au/C, and (b) 30AuAg/C in 0.1 M ethylene glycol and 0.1 M KOH at a scan rate of 20mV s⁻¹.

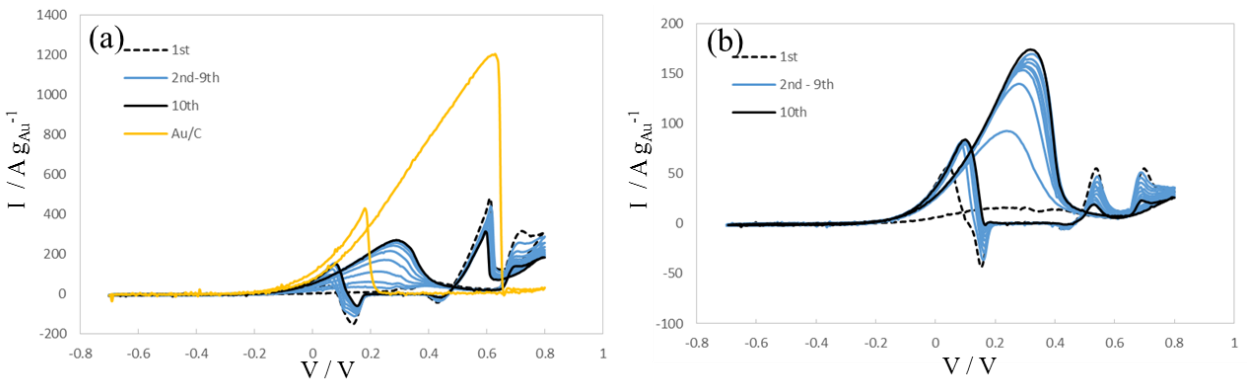


Fig. 3 CVs of (a) 10AuAg/C and Au/C, and (b) 30AuAg/C in 1 M ethylene glycol and 1 M KOH at a scan rate of 20mV s⁻¹.

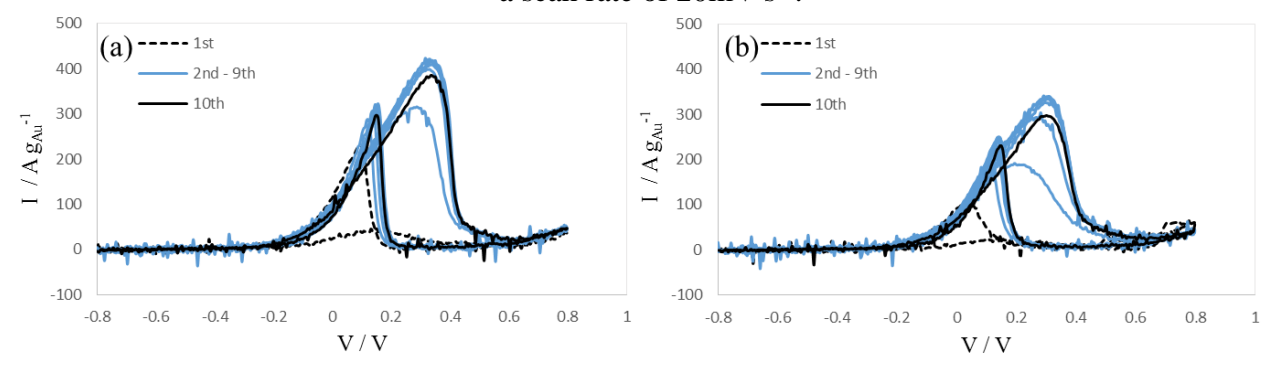


Fig. 4 CVs of 30% AuAg/C in 1 M glycerol and 2 M KOH (a) fresh catalyst and (b) the same electrode after deactivated in 2 M KOH at a scan rate of 20mV s⁻¹.

Fig. 4(b) shows the results of the electrode as shown in Fig. 4(a) after cycle in 2 M KOH. Even though this electrode was fully activated in the first experiment, the electrode was deactivated by KOH and was inactive. Then, after subjected to the electrolyte with glycerol the AuAg surface was reactivated and the current density raised again.

These results suggested that the surface activation was reversible when the electrolyte was changed. This indicates that the composition of AuAg/C was electrolyte dependent. Ag was the metal with the higher affinity to adsorb the oxygenate species such as hydroxide than Au. However, Ag was inactive toward alcohol electrooxidation in the region of alcohol electrooxidation on Au. As a consequence, Ag atom may be pulled toward the catalyst surface by hydroxide and cover the active Au surface. For Au, however, had better adsorption of alcohol. Since Au was more active for alcohol with high molecular weight, the surface activation which pulls Au atom to the nanoparticle

surface progressed better with high molecular weight alcohol such as glycerol. For low molecular weight alcohol such as ethanol and ethylene glycol, however, the AuAg surface cannot be activated and became inactive. Moreover, the concentration of alcohol and the ratio of Au in nanoparticle also affected the activation process.

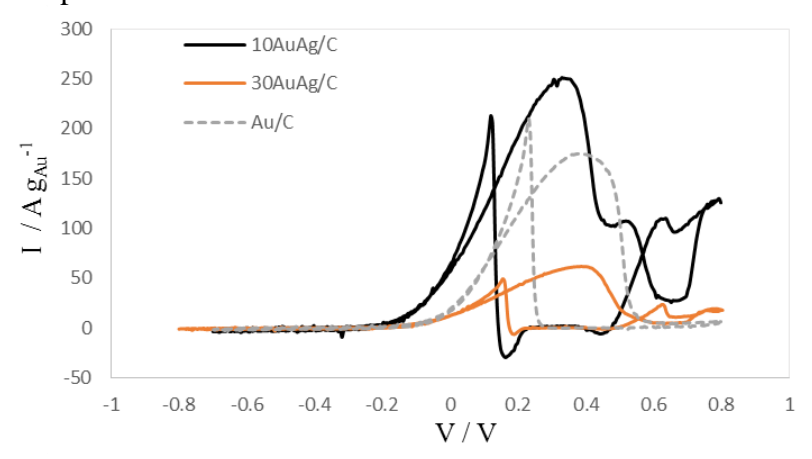


Fig. 5 CVs of fully activated AuAg/C and Au/C catalyst in 0.1 M glycerol and 0.1 M KOH at a scan rate of 20 mV sec⁻¹.

Fig. 5 shows the activity of 10AuAg/C, 30AuAg/C and Au/C in 0.1 M glycerol electrolyte. 10%AuAg/C catalyst was the most active catalyst in this condition. Ag provided several promotion effects on the electrooxidation on AuAg/C. The onset potential and the potential at maximum current density were shifted to more negative potentials. This was due to the higher affinity of hydroxide to Ag over Au which provides hydroxide to Au for the electrooxidation or AuO formation.

4. Conclusion

The activity of electrooxidation on AuAg/C catalysts strongly relates with the molecular weight of alcohol. AuAg/C was inactive without a strong interaction with alcohol because of the overlying Ag atoms on nanoparticle surface. With strong interaction with alcohol, the Au atom was pulled toward the surface and the catalyst was active for the reaction. This process was reversible depending on the electrolyte concentration. The promotion effects of Ag were clearly observed.

Acknowledgements

This work is financial supports from the Thailand Research Fund (TRF) under grant No.TRG5880131 and the National Research University (NRU) project of Thailand's office of the Higher Education Commission.

References

Garcia, A.G., Lopes. P.P., Gomes, J.H., Pires, C., Ferreira, E.B., Lucena, R.G.M., Gasparotto, L.H.S. and Tremiliosi-Filho, G. 2014. Eco-friendly synthesis of bimetallic AuAg nanoparticles. New J. Chem 38: 2865-2873.

Sun, Y. and Xia, Y. 2004. Mechanistic study on the replacement reaction between silver nanostructures and chloroauric acid in aqueous medium. J. Am. Chem. Soc. 126: 3892-3901.

Yongprapat, S., Therdthainwong, A., and Therdthainwong, S. 2012. Au/C catalyst prepared by polyvinyl alcohol protection method for direct alcohol alkaline exchange membrane fuel cell application. J. Appl. Electrochem. 42: 483-490.









Proceedings



ITIChE 2017 TIChE 2017

October 18 - 20, 2017

Shangri-La hotel Bangkok, Thailand The 7th International Thai Institute of Chemical Engineering and Applied Chemistry Conference 2017 (ITIChE 2017) and The 27th National Thai Institute of Chemical Engineering and Applied Chemistry Conference 2017 (TIChE 2017)

Organized by
Department of Chemical Engineering
King Mongkut's University of Technology Thonburi

TIMETABLE FOR ORAL PRESENTATIONS

Friday 20 October 2017:

Ţ				Room			
2	Malaysia I	Malaysia II	Indonesia I	Indonesia II	Brunei I	Brunei II	Myanmar
i i	I-CARE-OP-03:	I-POMA-OP-10:	I-BEFT-OP-01:	I-PDSC-OP-06:	T-PEPT-OP-01:	T-PDSC-OP-01:	I-CEDI-OP-05:
10:35-10:50	N. Ovatnupat	U. Kanta	P. B. Yim	P. Prayoonyong	ฉัตรชัย กันยาวุธ	ธีรพันธ์ ตั้งกิตติมศักดิ์	W. Songmuangkean
	I-CARE-OP-04:	I-POMA-OP-11:	I-BEFT-OP-02:	I-PDSC-OP-07:	T-ESHR-OP-01:	T-PDSC-OP-02:	I-CEDI-OP-06:
10:50-11:05	P. Worawatthananon	T. Noochsuparb	P. Janepinich	W. Wanchan	ศิริพร ศรีพิบูลย์	นิจิต หงส์บิน	M. Siebenhofer
	I-CARE-OP-06:	I-POMA-OP-12:	I-BEFT-OP-03:	I-PDSC-OP-08:	T-POMA-OP-01:	T-SEGE-OP-01:	I-CEDI-OP-07:
11:05-11:20	W. Lamai	J. Singto	V. Thongtus	T. Ruttithiwapanich	ชลิตา นิมนวล	รวมพร นิคม	S. Mekchai
	I-CARE-OP-07:	I-POMA-OP-13:	I-BEFT-OP-04:	I-PDSC-OP-09:	T-POMA-OP-02:	T-SEGE-OP-02:	I-CEDI-OP-08:
11:20-11:35	P. Kerdnoi	C. Wilhelm	N. Chairerk	A. Veerachayaporn	สุพจน์ พลหาญ	ชานนท์ ช้างฉาว	S. Sri-indrangkura
	I-CARE-OP-08:	I-POMA-OP-14:	I-BEFT-OP-05:	I-PDSC-OP-10:	T-POMA-OP-03:	T-SEGE-OP-03:	I-CEDI-OP-09:
11:35-11:50	W. Tongtawee	O. Chailee	T. Wimolsate	K. Wareerat	กนกพร อนันต์ชื่นสุข	อาคเนย์ ประวัติยากูร	T. Phromsatit
	I-CARE-OP-09:	I-POMA-OP-15:	I-BEFT-OP-06:	I-PDSC-OP-11:	T-SEPT-OP-01:	T-SEGE-OP-04:	I-CEDI-OP-10:
11:50-12:05	P. Kaewmaneel	L.M. AUNG	S. Mingphimai	K. Niemthes	ปณิชา ชุติชัยจรัส	วรุฒ ขลุดสกุล	S. Boonyuen
	I-SEGE-OP-10:	I-SEGE-OP-15:	I-SEPT-OP-06:	I-BBBE-OP-01:	T-SEGE-OP-05:		I-CEDI-OP-11:
14:05-14:20	A. Prokaew	N. Wongyao	S. Tantiwisawaruji	N. Weeranoppanant	อิทธิศักดิ์ เภาโพธิ์		P. Luangsriprech
	I-SEGE-OP-11:	I-SEGE-OP-16:	I-SEPT-OP-07:	I-BBBE-OP-02:	T-SEGE-OP-06:		I-CEDI-OP-12:
14:20-14:35	K. Khanthong	N. Chaidach	E. Asnachinda	B. Phonyotin	กิตติพงษ์ เรือนคำ		S. Phromma
	I-SEGE-OP-12:	I-SEGE-OP-17:	I-SEPT-OP-08:	I-BBBE-OP-03:	T-SEGE-OP-07:		I-CEDI-OP-14:
14:35-14:50	P. Suwanpituk	K. Deeying	C. Seedao	R. Lomsri	ณัฐนนท์ ไพบูลย์ศิลป์		J. Pimsamarn
	I-SEGE-OP-13:	I-SEGE-OP-18:	I-SEPT-OP-09:	I-BBBE-OP-04:	T-SEGE-OP-08:		
14:50-15:05	S. Yongprapat	K. Changwichan	N. Weeranoppanant	D. S. Lee	เล็ก วันทา		
7 7 7 7 7 7 7 7 7 7 7 7 7 7 7 7 7 7 7 7	I-SEGE-OP-14:	I-SEGE-OP-19:		I-BBBE-OP-05:			
15:05-15:20	J. Banjong	M.M. Khaing	_	T. Pitukdechatanakit			



ROLES OF ELECTRODEPOSITED Pd ON GLYCEROL ELECTROOXIDATION ACTIVITY OF AuAg/C CATALYST

Sarayut Yongprapat*¹, Apichai Therdthianwong¹, Supaporn Therdthianwong²

¹Fuel Cells and Hydrogen Research and Engineering Center, Pilot Plant, Development and Training Institute (PDTI) ² Department of Chemical Engineering, Faculty of Engineering King Mongkut's University of Technology Thonburi (KMUTT), Bangkok, Thailand 126 Pracha-Uthit Rd., Bang Mod, Thung Khru, Bangkok 10140 Thailand * Sarayut.yon@kmutt.ac.th

Roles of Pd on the electrooxidation activity of galvanic displaced AuAg/C toward glycerol electrooxidation activity were investigated. The AuAg/C catalyst was firstly prepared by using the galvanic displacement reaction between Au³⁺ and Ag on carbon. This type of catalyst was much more active than Au/C catalyst for glycerol electrooxidation in alkaline medium. The presence of Ag also lowered the onset potential and the potential at maximum current density. However, the activity of the AuAg/C catalyst depended on the surface composition of Ag and Au on catalyst surface. The catalyst would be active while the surface was enriched with Au but inactive with Ag. The surface composition was controlled by the composition of the electrolyte. However, the surface composition between Au and Ag may be shifted toward Au with the addition with Pd, since Pd tended to segregate on Ag and formed a stable AuPd alloy. The electrodeposition of Pd was carried out by using cyclic voltammetric method. The deposition of Pd on AuAg/C catalyst was confirmed since the catalyst became Pd-like surface while using 1 mM PdNO₃ in 0.1 M KCl. At a lower Pd concentration (0.01 mM PdNO₃) the catalytic activity of AuAg/C catalysts was changed upon the composition of the electrodeposition bath. The catalytic activity of Pd-AuAg/C electrodeposited by using PdNO₃ in both KNO₃ and KCl electrolytes was higher than that on the base AuAg/C catalyst upon 10 cycles of deposition. The glycerol electrooxidation properties of resulting Pd-AuAg/C catalyst carried out in KCl electrolyte was similar to those of AuAg/C, but with higher activity. However, while KNO3 was used as the supporting electrolyte, the yielding Pd-AuAg/C catalyst tended to be more like Au-rich surface 1. These results showed that the Pd can be used to promote the glycerol electrooxidation activity of AuAg/C. The addition of appropriate amount of Pd resulted in Au-like surface which may cause from the higher concentration of surface Au.

Keywords: AuAg catalyst, Pd promoter, Glycerol electrooxidation, Fuel cell, Electrodeposition.

INTRODUCTION

Glycerol was produced in a very large amount as a coproduct from biodiesel production. With a low consumption, the price of glycerol was lowered for decades and sometimes considered as a waste. Thus, finding the way to utilize glycerol should provide a lot of benefit. Fortunately, glycerol was electro-oxidized rapidly on Au-based catalyst in alkaline, which make glycerol a capable fuel for direct glycerol alkaline type fuel cell. Recent study indicated that the glycerol electrooxidation on Au-based catalyst can be promoted by Ag [1]. The AuAg/C can not only be more active than Au/C but also shift the onset potential and the potential at maximum current density to more anodic potential. However, the activity of AuAg/C greatly depends on the concentration of electrolyte and also requires the activation by the reaction with glycerol. This was due to the surface segregation of both Au and Ag through the reaction with glycerol and OH⁻, respectively. The surface segregation was the process that normally occurred to stabilize the surface energy of the nanoparticles via the interaction between metal and adsorbate [2].

Since this catalyst was only active when the surface was in Au-enriched form, its activity would be further promoted by shifting the surface composition toward higher Au portion. From a systematic search, Pd was proposed in this work to help achieving such a cause by two reasons. First, Pd tends to segregate on Ag in bimetallic PdAg [3]. Second, Pd can form a stable PdAu alloy which is more stable than PdAg alloy [4]. In this work, a small amount of Pd was electrodeposited via potential sweep method onto the prior prepared AuAg/C catalyst. The activity of the obtained Pd-AuAg/C catalyst toward glycerol electrooxidation was studied via cyclic voltammetric method.



EXPERIMENTAL

The detail on preparation of AuAg/C catalyst was described elsewhere [1]. The Ag on carbon (60%wtAg/C) which was used as a secrifice material for Au deposition was prepared by using citrate reduction in alkaline. After that, Au was deposited onto the Ag/C via galvanic displacement reaction between Au³⁺ and Ag/C. The obtained AuAg/C with 10% wt of Au (10AuAg/C) was used as an electrodeposit substrate for Pd. This 10AuAg/C contains the AuAg nanoparticles with the average size of around 20 nm [1]. The electrodeposition of Pd was performed by using a cyclic voltammetric method. First, the 10AuAg/C catalyst ink composed of 10AuAg/C, nafion ionomer and isopropanol was dropped on the glassy carbon electrode to yield a very thin film of 50 ug cm⁻²_{Au}. After dried in ambient air, the electrode was dipped into the electrodeposition bath containing Pd salt and supporting electrolyte. The electrodeposition was performed in the potential window of -0.8 V-0.8 V vs. Mercury/Mercury oxide (MMO) reference electrode. The potential program of deposition and glycerol electrooxidation activity test was controlled by Bipotentiostat AFCBP1 (Pine Research Instrument). The nomenclature of 4 Pd-AuAg/C catalysts presented in this work is shown in Table 1.

Table 1 Nomenclature of Pd-AuAg/C catalysts and their electrodeposition conditions.

Catalyst	Electrodeposition bath Solution	No. of electrodeposition cycle
1Cl-Pd-AuAg/C	$1 \text{ mM PdNO}_3 + 0.1 \text{ M KCl}$	1
10Cl-Pd-AuAg/C	0.01 mM PdNO ₃ + 0.1 M KCl	10
1N-Pd-AuAg/C	0.01 mM PdNO ₃ + 0.1 M KNO ₃	1
5N-Pd-AuAg/C	0.01 mM PdNO ₃ + 0.1 M KNO ₃	5

RESULTS AND DISCUSSION

Fig.1 shows the glycerol electrooxidation of the AuAg/C and Pd-AuAg/C catalysts prepared via Pd electrodeposition in KCl electrolyte containing 0.01 mM and 1 mM PdNO₃. The glycerol electrooxidation activity of all the catalysts in this work required several cycles of reaction with glycerol to activate them from their inactive state, as described elsewhere [1]. The CVs shown in this work were the CV at the steady states, while the surfaces of electrocatalysts reach their equilibrium states with the glycerol electrolyte used. The CV displayed in the Pd electrodeposition was showed in the insert of Fig. 1. The CV of Pd deposition in KCl electrolyte contains only one pair of sharp peak associated with AgCl formation and reduction. The CVs of AuAg/C catalyst with and without PdNO₃ in KCl electrolyte were the same. Then, there was no peak related with the Pd deposition appeared in this condition. However, the deposition of Pd was confirmed as the 1Cl-Pd-AuAg/C became a Pd-like surface since the glycerol electrooxidation on Pd took place at more anodic potential than on Au-based catalyst, as shown in Fig. 1. The glycerol electrooxidation on Pd surface starts at -0.4 V. After that, the current density sharply increases and then declines in a narrow potential window.

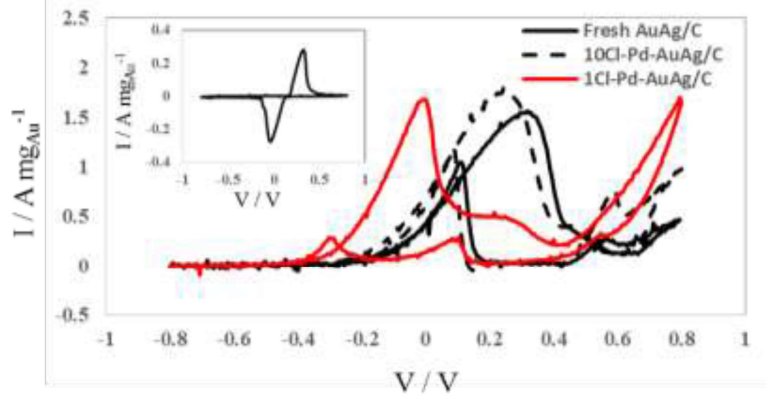


Figure 1. CVs of glycerol electrooxidation in 1 M Glycerol and 2 M KOH of fresh AuAg, 1Cl-Pd-AuAg/C, and 10Cl-Pd-AuAg/C at a scan rate of 20 mV sec⁻¹. Insert: CV of AuAg/C in 0.01 M PdNO₃ and 0.1 M KCl.



The glycerol electrooxidation on AuAg/C begins around -0.3 V where glycerol begins to adsorb on the metal surface. This potential was more anodic than that on Au/C indicating the promotional effect from Ag [1]. After that, the current density increases until it reaches the maximum current density at around 0.31 V. At this potential, oxide formation on metal surface occurred which prevented further glycerol adsorption. Hence, the current density was lowered and normally diminished on Au-based catalysts as the entire metal surface was covered by the oxide. The two consecutive peaks from 0.45 V onward are corresponding to glycerol electrooxidation on Ag oxide. In the reversed scan, the catalytic activity of the catalyst was regained as a very sharp oxidation peak after the surface metal oxide was reduced at 0.2 V.

For the 10Cl-Pd-AuAg/C, the onset of the glycerol electrooxidation was close to that of the AuAg/C catalyst. However, the potential at maximum current density was shifted to a lower potential. In the reversed scan, the small oxide reduction peak can also be observed at 0.2 V prior to the sharp glycerol electrooxidation peak. These two occurrences indicate that the oxide formation and reduction on this catalyst takes place at lower potentials than that on AuAg/C catalyst. The maximum current density, as shown in Table 2, was higher than that on the AuAg/C catalyst.

The change in catalytic activity of this catalyst could be raised from 2 possibilities: the surface modification via the AgCl formation in the electrodeposition process and the deposited Pd. However, the CVs of glycerol electrooxidation on the AuAg/C catalyst preconditioned by using on only KCl electrolyte (without PdNO₃) was similar to that on fresh AuAg/C catalyst (result not shown). This means that the modification of the catalytic properties was from the deposited Pd.

Table 2 Potential and current density at maximum current density.

Catalyst	Potential (V)	Current density (A mg _{Au} ⁻¹)
AuAg/C	0.31	1.52
1Cl-Pd-AuAg/C	0.00	1.62
10Cl-Pd-AuAg/C	0.26	1.74
1N-Pd-AuAg/C	1.71	0.34
5N-Pd-AuAg/C	0.66	2.83

The CVs of glycerol electrooxidation on 1N-Pd-AuAg/C and 5N-Pd-AuAg/C are shown in Fig. 2. In KNO_3 electrolyte, the main peaks occurred are corresponding to the oxide formation on the Au and Ag surface. The current densities of these peaks were lowered as the number of deposition cycle increased indicating the deposition of Pd on the AuAg surface.

The CVs of both 1N-Pd-AuAg/C and 5N-Pd-AuAg/C catalysts resembled the typical CV of Au/C more than than that of AuAg/C [1]. The potential at maximum current density was shifted toward higher potential, as shown in Table 2, as well as the oxide reduction potential in the reversed scan. This potential shift was larger as the number of electrodeposition cycle increased. Moreover, the peak related to Ag was almost disappeared in both catalysts. Despite all these changes, the onset potential was still close to that on the AuAg/C catalyst. This indicated that the synergistic effect of Ag on Au remained.

The maximum current density of both 1N- and 5N-Pd-AuAg/C was increased as the number of electrodeposition cycle increased, as shown in Table 2. The glycerol electrooxidation on 5N-Pd-AuAg/C yielded almost 2-fold higher than that on AuAg/C. The higher activity of these two catalysts may be grounded from the promotional effects of Pd which increased the portion of Au on the electrocatalyst surface via a stable PdAu alloy. Theoretically, the PdAu alloy was formed to lower the overall surface energy of the Pd-AuAg nanoparticles since PdAu was more stable at the surface than PdAg and the separated Pd-Au form. As a consequence, the surface of AuAg nanoparticles become an Au-rich surface. Thus, the CVs of these catalysts were shift toward Au/C pattern with a high current density while still keeping the synergistic of Ag from the underlying Ag core.



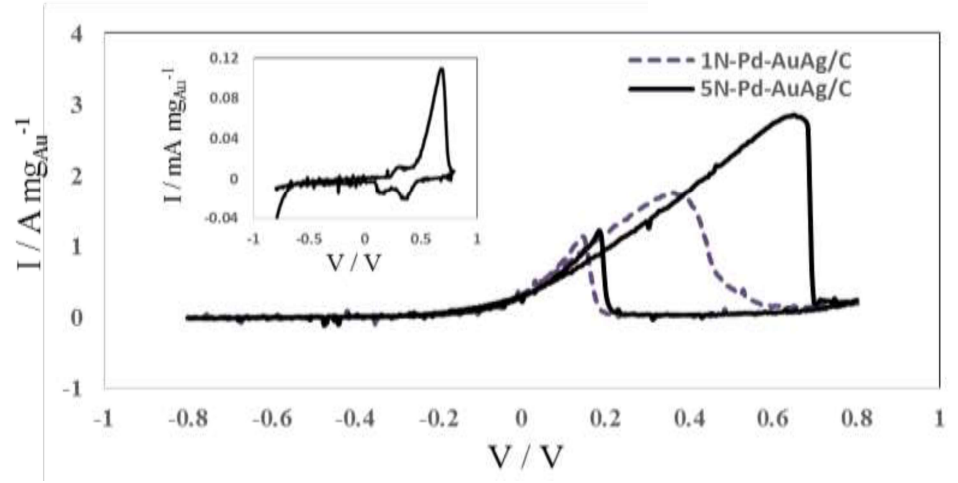


Figure 2 CVs of glycerol electrooxidation in 1 M Glycerol and 2 M KOH at a scan rate of 20 mV sec⁻¹ of 1N-Pd-AuAg/C and 5N-Pd-AuAg/C catalysts.

The role of supporting electrolyte on the catalytic activity of the electrodeposited Pd-AuAg/C was large. The properties of Pd-AuAg/C prepared by using KNO₃ as a supporting electrolyte was much different with those using KCl. While KCl was used, the surface of the metal oxide was changed to AgCl which is a stable salt. This AgCl-covered surface may make the AuAg surface less active for Pd deposition. Then, only small amount of Pd was deposited on the catalyst surface or Pd may only deposited on the site that was not entirely covered with AgCl, eg. Au-rich area. However, NO₃⁻¹ ion cannot form a stable species on AuAg surface. As a consequence, the AuAg surface was more active in KNO₃ than in KCl electrolyte. Larger amount of Pd may possibly deposit on AuAg surface and then make a greater change on the catalytic activity of the catalyst.

CONCLUSIONS

The Pd-AuAg/C catalysts were prepared via electrodeposition of Pd on the AuAg/C substrate. The properties of Pd-AuAg/C catalysts depend on the type and the concentration of electrodeposition bath. All the Pd-AuAg/C catalysts were more active than AuAg/C, however, with a different promotional effect. The electrodeposition in KCl electrolyte yield the catalyst with the properties quite similar to those of AuAg/C with an anodic shift in peak potential and higher current density. However, while KNO₃ electrolyte was used, the change in the catalytic activity from the AuAg/C was more pronounced than KCl. The CVs of 1N-Pd-AuAg/C and 5N-Pd-AuAg/C were quite similar to that of the Au/C. The surface of these catalysts become Au-rich surface. The proposed Pd role in this case was to increase the surface Au portion via the stable PdAu alloy. The 5N-Pd-AuAg/C catalyst provides around two fold higher current density than the AuAg/C.

ACKNOWLEDGMENTS

This work was supported by the Thailand Research Fund (TRF) under grant No.TRG5880131, King Mongkut's University of Technology Thonburi (KMUTT) through the "KMUTT 55th Anniversary Commemorative Fund".

REFERENCES

- [1] S. Yongprapat, A. Therdthianwong, S. Therdthianwong, SEE 2016 on "Energy & Environment Change: Innovating for a Sustainable Future, Bangkok, 28-30 Nov. 2016, paper No. 1A-028.
- [2] H. Liao, A. Fisher, Z.J. Xu, Small, 11 (27) (2015) 3221.
- [3] L. Wang and D.D. Johnson, J. Am. Chem. Soc., 131 (2009) 14023.
- [4] S. Takizawa, K. Terakura, Phys. Rev. B, 39 (9) (1989) 5792.